CLAY MINERALOGY AND CHEMICAL VARIATION IN URANIUM ROLL-FRONT DEPOSITS IN THE GAS HILLS URANIUM DISTRICT, WYOMING

by

Alexander Jay Moyes

A thesis submitted to the faculty of
The University of Utah
in partial fulfillment of the requirements for the degree of

Master of Science

in

Geology

Department of Geology and Geophysics

University of Utah

August 2013

The University of Utah Graduate School

STATEMENT OF THESIS APPROVAL

The thesis of **Alexander Jay Moyes**

has been approved by the following supervisory committee members:

Erich Petersen	, Chair	**05/02/13**
		Date Approved
Richard Jarrard	, Member	**05/01/13**
		Date Approved
Paul Jewell	, Member	**05/02/13**
		Date Approved

and by **D. Kip Solomon**, Chair of

the Department of **Geology and Geophysics**

and by Donna M. White, Interim Dean of The Graduate School.

ABSTRACT

In the Gas Hills District, located near Riverton, Wyoming, a clay mineral assemblage was identified within and around the ore bodies, which includes 5 to 11 percent kaolinite, with the highest amount in the ore body, 4 to 7 percent smectite, with the highest amount being in the reduced sandstone, and 5 to 8 percent illite, with the highest amount in the oxidized sandstone. This assemblage can be classified as argillic alteration.

Three different habits associated with the clays were identified that change systematically from the reduced sandstone to the oxidized sandstone. These textural differences are a result of changes in fluid composition over time. The disseminated habit in the reduced sandstone is likely formed during diagenesis. The clot-like habit in the oxidized sandstone was created at the onset of oxidation and near surface weathering. The grain replacement habit seen in the ore body is a result of alteration during mineralization.

Porosity changes considerably, from an average of 5 percent in the reduced sandstone to 23 percent in the oxidized sandstone. The controls on porosity include the distribution of clays, the habit of the clay, and the presence of authigenic quartz in the ore body.

K, P, Tl, As, Rb, and Zr are correlated with uranium and have increased concentrations in the ore zone. Cu, Ti, Mg, Zn, Ni, and Cr are most concentrated in the unaltered, reduced sandstone. K and Rb are the only elements that increased in concentration in the distal oxidized sandstone. In the mineralized sandstone, U correlates strongly with Zn, Co, Mg, and has a negative correlation with V. This is due to differences in solubility. In the reduced sandstone, U correlates with Mo and Tl. In the oxidized sandstone, U strongly correlates with As, Fe, and Co.

Rare earth elements in the mineralized sandstone increase as compared to the reduced sandstone by a factor of five. The LREE move separately from the HREE. The LREE vary in concentration within the oxidized, reduced, and mineralized sandstones.

TABLE OF CONTENTS

LIST OF FIGURES

LIST OF TABLES

ACKNOWLEDGEMENTS

David Miller, CEO at Strathmore Minerals, donated the core for this project. David Miller, Terrance Osier, Jim Crouch, David Frank, and Mark Travis were instrumental in providing access to data and property, as well as giving generously of their time and expertise. Thanks to Erich Petersen, whose experience helped guide this project.

This research was funded by Strathmore Minerals, the McKinstry grant from the Society of Economic Geologists, and through a teaching assistantship from the Department of Geology and Geophysics.

Many thanks are due to my family who supported me and kept me motivated even when the end looked far. Also, thanks to my fellow class mates; they were as much a part of my learning as anything.

CHAPTER 1

INTRODUCTION

The Gas Hills District is located on the southern border of the Wind River Basin near the geographic center of Wyoming. It lies between the Granite Mountains to the south and to the northwest is the Wind River Mountains (Fig. 1). The deposits are located 40 miles southeast of Riverton, Wyoming and are currently owned and operated by Strathmore Minerals Company.

History of the Gas Hills District

Uranium was first discovered in the Gas Hills area in September, 1953 by Neil E. McNeice (Armstrong, 1970). Mining began within a year. For approximately thirty years, successful exploration programs led to numerous open pit mines and three mills. After closure of the district in the early 1980s, multiple operators began to acquire existing deposits and explore for new ones. The district has produced over 100,000,000 pounds of uranium (from 1953 – 1984) (Armstong, 1970).

Low uranium prices over the last several decades have resulted in a paucity of studies on roll-front deposits (Zeller, 1957; Austin and King, 1966, Armstrong, 1970, Granger and Warren, 1978; Snow, 1978, Harshman and Adams, 1980, Dahlkamp, 1991).

Fig. 1. Map of the state of Wyoming showing locations of the Gas Hills District, the Granite Mountains, the city of Riverton, and the Wind River Mountain Range.

Recent interest in nonhydrocarbon energy resources and increased uranium prices are driving an interest in the search for and re-evaluation of numerous uranium districts. The Gas Hills district of Wyoming is the second largest uranium district in the United States and is poised to become the largest district (Strathmore, 2009). Hence, a better understanding of the hydrological setting and the mineralization characteristics of the roll-front deposits in the district is a prerequisite to an increase in productivity and future exploration.

Background

Over that last three decades, new analytical techniques have become available which can be used to describe ore bodies more precisely. The Gas Hills was an ideal location to pursue modern mineralogical and geochemical studies because suitable core was available and with current operational activity in the district, the study was timely.

This project is intended to better define the alteration and chemical variation associated with uranium mineralization in the Loco Lee and George Ver deposits in the Gas Hills District (Fig. 2). The goal is to add to the description of this important deposit type and provide new information on the clays present in the system. This is important to gain a better understanding of fluid-induced mineralogical and geochemical changes in the host sandstone due to alteration connected with roll-front deposits. These alteration zones may be significantly larger in size and easier to find than the deposits themselves. Data have been collected to document mineralogical and geochemical changes in the host rock and how they are connected to the migration of uranium-

Fig. 2. Location map of George Ver and Loco Lee deposits relative to the district.

bearing solutions and the development of roll-front deposits in the Gas Hills.

Traditional exploration methods for roll-front uranium deposits largely focused on defining the geometry of the host sandstone through detailed sedimentological and stratigraphic analysis and using these data to identify likely zones of metal precipitation. Exploration for these deposits was also strongly guided by the search for anomalously colored rocks (Austin and King, 1966).

Alteration associated with the oxidized zone is usually light grey to white, whereas unaltered sandstone is greenish to grey and shows little evidence that water flowed through it (This Study). This change in rock color results from a change in oxidation/reduction conditions across the roll-front and is important because it can be recognized in the field.

The use of sandstone color as an alteration vector to mineralization has limitations. It is restricted to areas with reasonable surface exposure. In addition, sandstone discoloration does not necessarily indicate closeness to an ore body. Strong oxidation involving the formation of hematite can be found at considerable distance from the roll-front (Davis, 1969). In some cases, sandstone discoloration may be unrelated to ore formation. Additional issues can arise if the host sandstone has experienced a re-reduction following the movement of the oxidation front. Under such conditions, sandstone color does not provide a reliable alteration gauge to identify productive host rocks from nonproductive.

Early workers (Austin and King, 1966; Armstrong, 1970; Granger and Warren, 1978; and others) have generally characterized the alteration as oxidized, hematic, or

kaolinitic for the district as a whole. However, there has been no description of the clays associated with the alteration. Warren and Granger (1978) describe the oxidized sandstone in the Gas Hills as typically containing ferric iron in the form of hematite, goethite, or hydrous iron oxides and as a constituent of clays. In the reduced zone, Granger and Warren (1978) note that the sulfide minerals consist almost entirely of pyrite, as is confirmed in this study. Earlier workers note uranium occurs as uraninite (UO_2) or coffinite ($U(SiO_4)_{1-x}(OH)_{4x}$), or both. Vanadium, if present, occurs at the roll-front as montroseite ((VFe)O(OH)) but is generally partly weathered to paramontroseite (VO_2) or some other hydrated vanadium oxide such as doloresite ($V_3O_4(OH)_4$). Molybdenum occurs in some deposits as a black, amorphous material that is thought to be jordisite (MoS_2).

Roll-type uranium deposits are ordinarily found in gently dipping fluvial or marginal-marine aquifer sandstones that are both underlain and overlain by less permeable beds. In vertical section, an altered tongue-shaped zone (a meter thick to over 30 meters thick) projects into the unaltered, reduced rocks. These reduced rocks ordinarily contain disseminated authigenic pyrite and scattered coaly fossil plant remains (Harshman, 1974). Epigenetic accumulations of uranium, selenium, molybdenum, and other elements commonly occur in the ore zone, largely in reduced rocks, adjacent to or near the borders of the oxidized tongue. To date, the most extensive geochemical zoning work indicates that selenium, vanadium, and arsenic are greater in altered sandstones whereas iron and molybdenum are higher in unaltered, reduced sandstone. This was confirmed by this study. In plan, most oxidized tongues

associated with economic ores extend over several tens of square kilometers and have a highly irregular, sinuous outline (Warren and Granger, 1978).

Approach

This project focuses on a quantitative mineralogical description of the host rocks as well as a first order approximation of porosity. The methods used included mineralogical, clay, and geochemical analyses. The tools include x-ray diffraction (XRD), quantitative evaluation of minerals by scanning electron microscopy (QEMSCAN), very near infrared (VNIR) spectrometry, and inductively coupled plasma mass spectrometry (ICP-MS) whole rock analysis.

Bulk rock geochemical analysis was used to determine the concentrations of fifty-five elements in the altered and unaltered sandstone. Particular emphasis was placed on trace elements that were expected to be highly mobile in the roll-front environment as well as the rare earth elements that had not been previously analyzed.

First order porosity determination and high-resolution petrography were carried out by QEMSCAN, and supplemented by transmitted and reflected-light microscopy.

The samples were analyzed by VNIR to evaluate the utility of this tool in "mapping" alteration in the field and in core samples. This method is used commonly to characterize the hydrous silicates.

The samples collected for the analysis were limited to near orebody, approximately 100 meters on either side of the front. Extreme distal end members in the reduced sandstone and in the oxidized sandstone were not analyzed.

CHAPTER 2

GEOLOGIC SETTING

Regional Tectonics

The Wind River Formation is an intermontane, orogenic deposit that can be as thick as 900 feet in the Gas Hills District; therefore, mountain building and basin subsidence were likely necessary to provide space for sediment accumulation (Seeland, 1978).

The first marginal uplift formed during late Cretaceous time in areas that are now the Granite Mountains. Subsidence began concurrently in the northeast portion of the basin. Uplift of the Wind River Range began in early Paleocene time and antiformal folding developed on the margins of the basin. In earliest Eocene time, the rate of erosion had increased, which is recorded by the Indian Meadows Formation, deposited along the margins of the basin. Stream drainage out of the eastern part of the basin was temporarily blocked due to reverse faulting along Casper Arch, southern Big Horn Mountains, and the Owl Creek Mountains. External drainage was reestablished during early Eocene Wind River time (Fig. 3) and erosion from the mountains surrounding the basin resulted in the deposition of thousands of feet of Wind River Formation regionally. The Casper Arch was covered by fluvial sands and silts carried by stream systems flowing

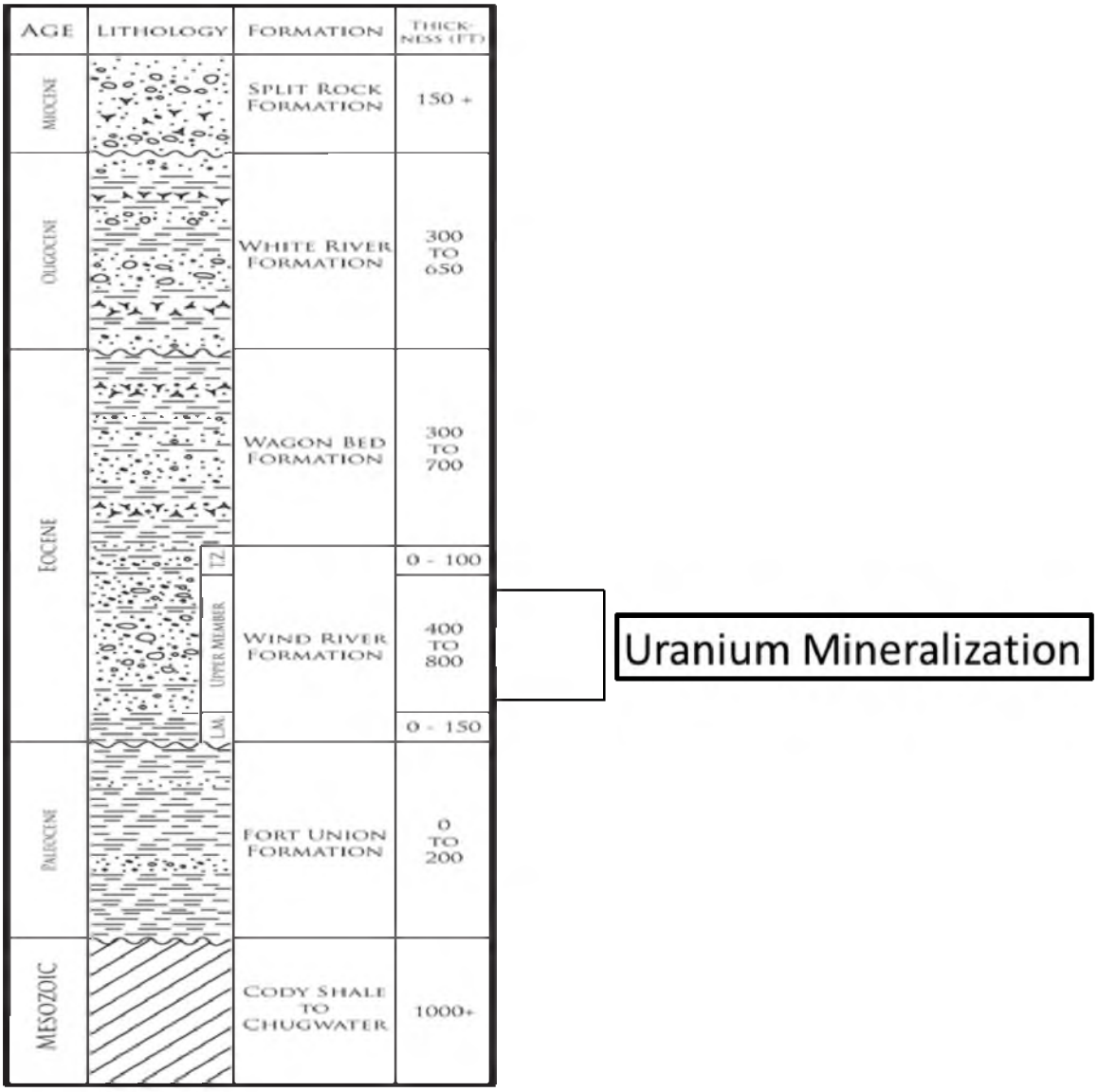

Fig. 3. Idealized stratigraphic column of Gas Hills District strata (modified from Strathmore, 2009). The uranium mineralization is confined to the Upper Member of the Wind River Formation.

eastward into the Powder River Basin (Seeland, 1978).

By the end of the early Eocene, both subsidence and uplift had ceased. The only major structural event in the late Tertiary was normal faulting associated with the breakdown of the Granite Mountains. Deposition of volcanic ash took place during the Oligocene, Miocene, and Pliocene and blanketed the ranges in this area.

Host Rock Sedimentology

The host rock for the Gas Hills uranium deposits is the fluvial, early Eocene Wind River Formation. These lower Tertiary rocks lie unconformably over folded and faulted Mesozoic and older rocks. The Eocene Wagon Bed Formation conformably overlies the Wind River, which is 285 to 660 feet thick (95 to 220 meters). The Oligocene White River Formation is approximately 450 feet thick (150 meters) and lies unconformably over the Wagon Bed Formation (Fig. 3).

The Wind River has been subdivided into three primary units; a lower fine-grained member, the Puddle Springs Arkose Member, and the upper transition zone. The lower fine-grained member is primarily mudstone and can range from being completely absent to over 40 meters thick. This member does not host uranium mineralization, primarily due to its low permeability. The Puddle Springs Arkose Member is the host for uranium mineralization and is made up of poorly consolidated, arkosic, coarse-grained sandstone with inter-beds of shaley sandstone and mudstone. This member can range in thickness between 375 and 750 feet (125 and 250 meters). The upper transition zone can be as thick as 120 feet (40 meters) in parts of the Wind

River Formation, but in the Gas Hills, this member is usually not present and where it is, is included in the Puddle Springs Member. The upper transition zone is primarily unconsolidated sandstone (Armstrong, 1970).

Following uplift of the Granite Mountains and subsequent exposure of their granitic core, the Puddle Springs Arkose Member was deposited on these older rocks. The deposition took place as part of at least two large, coalescing alluvial fans whose positions were controlled by stream systems flowing northward from the Granite Mountains into the Wind River Basin. Basin-ward, sediments were deposited in stream channels, flood plains, lakes, and swamps. Topographic irregularities had considerable influence on the distribution and character of favorable host rocks (Seeland, 1978).

In the northern portion of the basin, the depositional environment transitions from alluvial fan to flood plain deposits. These flood plain sediments are the most typical depositional environment for the Wind River Formation and are characterized by alternating red and gray-green siltstones to claystones and light brown sandstones. These fine clastics are low-energy, overbank deposits and represent deposition of suspended sediment from flood waters. Conglomerates can also be present as channel-lag deposits. The Wind River conglomerates contain abundant Precambrian rock fragments that record exposure of the igneous and metamorphic cores of the granitic ranges bordering the basin (Seeland, 1978).

The favorable facies for hosting mineralization can be linked to the permeability of the host sandstone. Fine-grained, only slightly permeable rocks are unfavorable hosts. Openwork conglomerate, at the other end of the spectrum, appears to be too

permeable to be a good host rock. Well sorted, medium to coarse-grained arkosic sandstone tend to be the preferred facies (Armstrong, 1972).

Ore Bodies and Development

Uranium roll-front deposits are recognized as having a crescent shape in vertical cross section normal to the flow direction (Fig. 4). In the body of the crescent, rolls range from tens of centimeters to many tens of meters in thickness. The average thickness of an ore body is usually 3 – 5 meters. The upper and lower limbs of the crescent thin away from the body of the crescent. In the Gas Hills, the lower limb is normally greatly extended and thins gradually, whereas the upper limb is shorter and tends to thin abruptly, although not always (Armstrong, 1970).

Roll-type deposits typically occur in porous, permeable, fluvial sandstone units containing a small amount of disseminated pyrite before the ore-forming process commenced. Ground water flowing through the host rock contained enough dissolved oxygen to initiate oxidation of this pyrite. The Gas Hills Deposits are based on a non-biogenic system as a form of catalyst in the reduction process (Granger and Warren, 1969). In the formation of the roll-type deposits, the oxygenated ground water flowed down the slight dip of the host rock, which is confined above and below by less permeable mudstone beds (Harshman and Adams, 1980). In these oxygen rich conditions, uranium is oxidized from the insoluble reduced form U^{4+} to the U^{6+} oxidation state. Uranium can be precipitated by lowering the Eh of the fluid to form a uranous oxide, in the form of either uraninite or pitchblende (Robb, 2005).

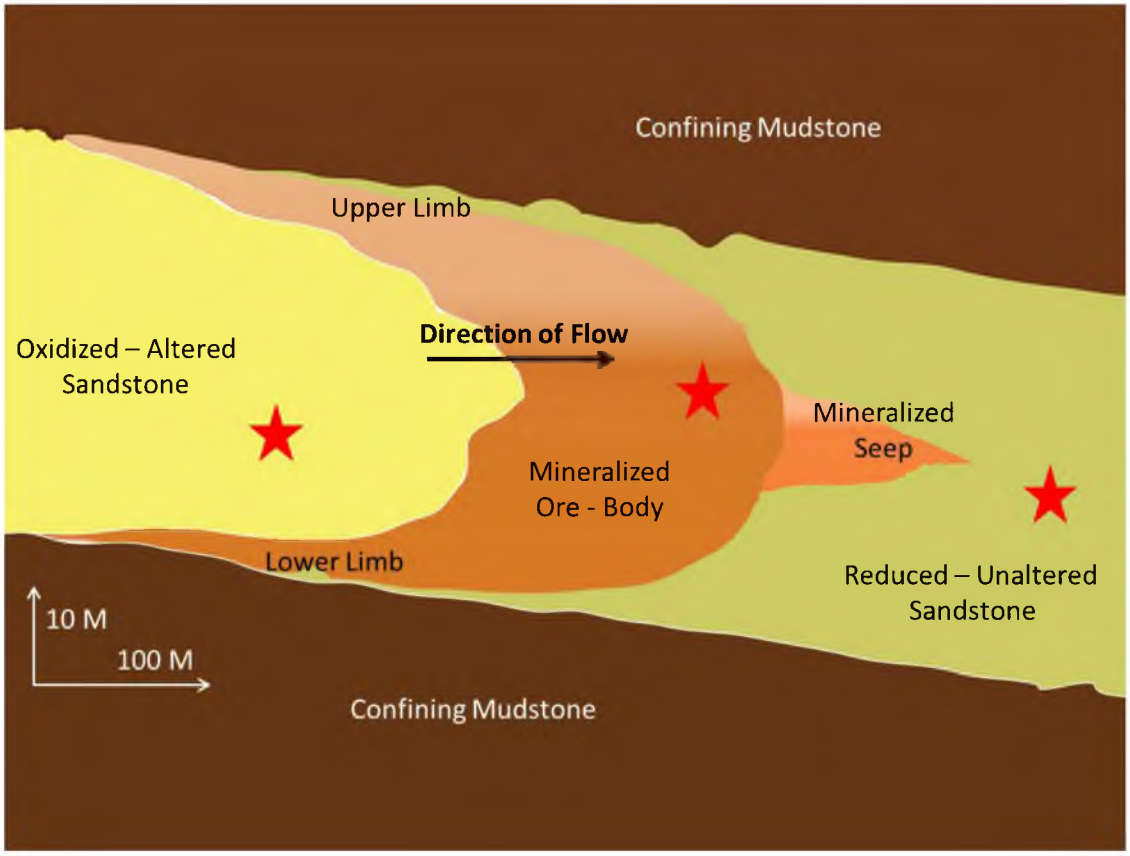

Fig. 4. Schematic cross section of a Gas Hills District roll-front deposit. Stars represent relative sample locations (After Bailey, 1965).

Potential Sources of Uranium

There are two principle ideas regarding the source of uranium in the Gas Hills District. The first source is from uraniferous granitic rocks of Lower Proterozoic to Archean age that crop out in the ranges surrounding the district (Rosholt et al., 1973). The second source is the uraniferous tuffs and bentonitic volcaniclastic sediments of Eocene and younger age that overlie or once overlaid the Wind River Formation (Zielinski, 1980).

The Granitic Mountains of the Sweetwater Uplift that surround the Wind River Basin (see Fig. 1) are the likely source of the arkosic host sediment in the Gas Hills. These granites contain as high as 30 ppm uranium. These granites lost an estimated 75 percent of their original uranium over the past 40 million years as shown by the existing radiogenic lead amounts (Rosholt, 1973).

The tuffaceous sediments also contain anomalous amounts of uranium, up to 250 ppm locally. These sediments are approximately 32.4 million years old. Uranium was leached from ash and carried by groundwater at the times these deposits were thought to have formed (Zielinski, 1980).

Ore Mineralogy

The principal ore minerals are uraninite and coffinite (Harshman, 1970). Mineralization occurs as coatings on sand grains, as void fillings in the sandstones, and as replacements of organic matter (Stewart, 2002). Uranium is accompanied by a

number of elements deposited in or adjacent to the altered tongues forming the roll-front.

CHAPTER 3

METHODS

Sample Selection

Representative samples were collected from sections of the mineralized portion of two roll-front deposits as well as from oxidized sandstone upstream of the deposits and reduced sandstone downstream of the deposits. The extent of reduced sandstone and oxidized sandstone is confined within 100 meters of the ore bodies; extreme end members were not sampled. Core was available from three boreholes in the George Ver deposit and two boreholes from the Loco Lee deposit (see Fig. 2). Because core was limited, variations in lithology do occur from sample to sample, but all samples are representative of their respective zones. Once the wells were completed, a standard well logging instrument was used to collect gamma ray, temperature, and spontaneous potential data. The well logs were inspected and used to locate the various sections of representative core (Fig. 5). Each segment of the roll-front deposit has a unique gamma ray signature that can assist in identifying the specific section of the deposit (Rubin, 1970) (Fig. 6). There are no anomalous gamma spikes in the reduced sandstone. The seepage zone is similar to the reduced sandstone and only produces a small kick on the gamma ray. In the mineralized zone and the high-grade ore, the gamma log anomaly is

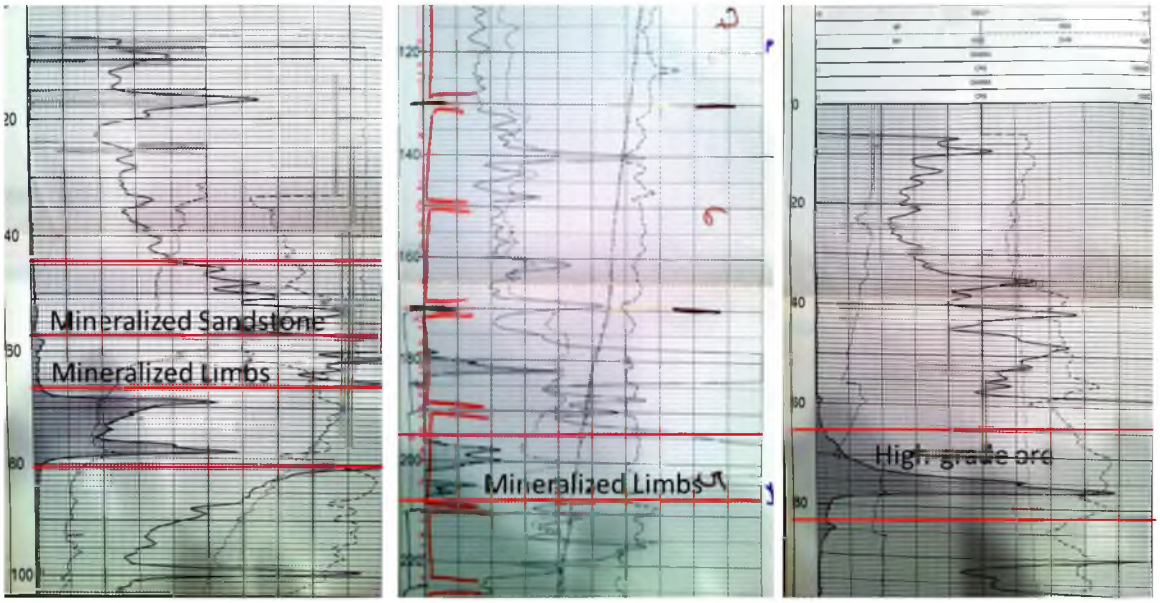

Fig. 5. Representative zones of interest were identified on a well log using the method defined by Rubin (1970). The numbers to the left are depth in feet, the solid line is gamma ray in counts per second, the dotted line below the gamma ray is the spontaneous potential measured in millivolts, and the dashed line to the right of gamma ray is resistivity measured in ohms A) Log of borehole LLS-03 B) log of borehole GVS-S8-08 C) log of borehole LLS-02.

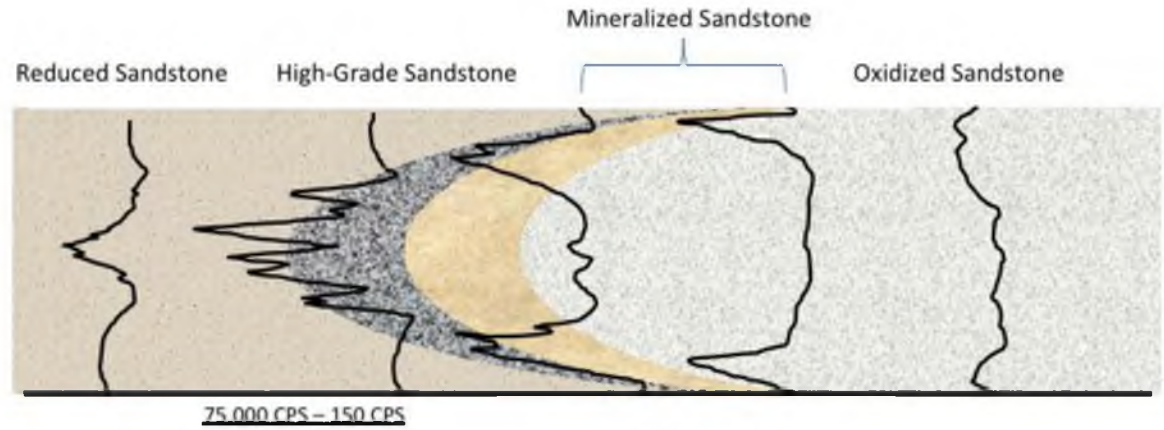

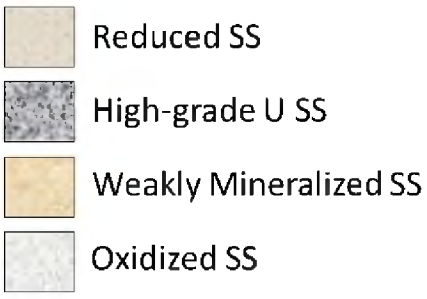

Fig. 6. Idealized gamma ray response signatures in counts per second (CPS) through a cross-section of a uranium roll-front deposit as seen on the gamma ray log. The higher the counts, the more uranium that is present. This is the well log gamma ray response that would be expected in each section of the roll-front.

quite strong and unbroken, producing one large kick. The interface zone between the upper and lower limb usually shows at least two kicks, sometimes three representing the limbs and a portion of the mineralized zone. In the barren, altered sandstone, there is no gamma ray kick as there is no mineralization (Rubin, 1970).

Petrography

Standard Petrographic prepared thirty-seven standard polished thin sections. The samples were selected to represent each distinct zone of interest based on the gamma ray selection method. Using a standard petrographic microscope, each slide was examined using reflected light, transmitted light, and polarized filters. Bulk mineralogy was examined as well as grain size and grain sorting.

Very Near Infrared Spectrometry (ASD)

A FieldSpec 3 portable spectrometer using the modular Goetz spectrometer engine, with a spectral range of 350 – 2500 nm, was used to obtain VNIR spectra. The ASD spectrometer was run for two seconds on 3 points every foot covering the length of core. The associated intensities were then recorded using the software program SpecMin and compared to the standards in the U.S. Geological Survey's spectral library number 6 (Clark et al., 2007). A portion of the data was used in this report but could also be available for a future study.

X-Ray Diffraction Whole Rock Analysis

Samples were prepared by disaggregating approximately 15 cubic centimeters of material by mild hand grinding using an agate mortar and pestle. Once the material was ground to a fine powder, it was packed into a metal tray for analysis. The tray was scanned over a range of 0 – 50° 2θ, with a scan rate of 2°/min, and a step rate of 0.02°2θ.

The samples were analyzed in a D-Max 2000 X-ray powder diffractometer. The diffractometer used a copper cathode and a nickel filter; operating conditions were 40 KV accelerating potential and a 30 mA current. A plot of intensity (counts) versus 2θ was generated. Peaks were identified using the program JADE and compared to a stored mineral database for mineral identification.

X-Ray Diffraction Clay Analysis

The powder was washed of any salts by adding deionized water and mixing. In order to create a stable suspension, 1% calgon solution was added to the water and mixed into the solution with a blender. Because of the inherent acidity associated with the sample (due to the pyrite in the host rock) household ammonia was used to neutralize the acid, allowing the clay to stay in suspension. In order to separate the clay-sized particles, two centrifuges were used. The first centrifuge was run for five minutes at 1000 rpm to remove clay particles greater than two micrometers. The second centrifuge, which was run for four minutes at 4000 rpm, collected clay particles that are less than 2 micrometers in diameter. Excess liquid was discarded and the remaining clay

was smeared onto a glass slide where it air-dried. Slides were glycolated at 60 °C for 24 hours and re-run.

QEMSCAN

False color mineralogical images were created by collecting 1000-count EDAX spectra on each analysis spot on a portion of the thin section at the rate of 350,000 cps. Spectra were classified with iDiscover 4.3 using the Barrick 710A database to obtain a mineralogical classification. A typical image using 10 micron spacing consists of 3 million measured spectra over a 15 X 20 mm surface area. Each spectra corresponds to a phase that has a predefined composition and when recognized, similar spectra are combined. The final output is an image of the mineralogy, mineral texture, porosity, and spatial associations of the minerals.

Whole Rock Geochemical Analysis

Representative pieces of core from all zones were analyzed for fifty-five elements at the SGS Laboratory in Toronto, Canada. Samples were prepared by fusion involving the complete dissolution of the sample in a molten flux.

Statistical Analysis

The software package SAS was used to identify geochemical correlations based on the Pearson Correlation Method. A confidence interval of 95% or higher was used to indicate statistical viability.

CHAPTER 4

RESULTS

Mineralogy of the Oxidized Sandstone

Petrography

Sample GVS-8C-170-174 is a representative oxidized sandstone sample. It is a light-gray to bleach white, medium grained, well-sorted sandstone with angular to rounded quartz and feldspar.

Most grains were quartz, feldspar, and clays. Little to no iron oxides were identified. The sample also contained calcite as identified with reaction to HCL. No pyrite was identified in the sample (Fig. 7A).

X-ray Diffraction/QEMSCAN

A comparison was made by using X-ray diffraction on whole rock powder samples; QEMSCAN analysis was performed on selected thin sections. Minerals identified include quartz, feldspar, plagioclase, calcite, kaolinite, smectite, and illite. QEMSCAN identified small amounts of gypsum (Table 1).

Table 1: Average abundance, based on QEMSCAN results, in percent of rock forming minerals of each sector of the George Ver and Loco Lee deposits in the Gas Hills District.

Mineral Type	Mineral Formula	Oxidized Sandstone	Oxidized Interior	Upper Limb	Lower Limb	Mineralized Sandstone	High-Grade Ore	Reduced Sandstone
Quartz	SiO_2	29	25	47	35	31	57	31
K Feldspar	$KAlSi_3O_8$	29	30	26	25	32	21	19
Plagioclase	$NaAlSi_3O_8$	24	23	19	24	19	13	25
Kaolinite	$Al_2Si_2O_5(OH)_4$	7	6	2	3	11	3	5
Illite	$(K,H_3O)(Al,Mg,Fe)_2(Si,Al)_4O_{10}[(OH)_2,(H_2O)]$	5	8	4	5	6	3	4
Smectite	$(Na,Ca)_{0.33}(Al,Mg)_2(Si_4O_{10})(OH)_2*4H_2O$	3	3	1	6	1	2	5
Calcite	$CaCO_3$	1	0	0	0	0	0	0
Pyrite	FeS_2	0	3	0	0	0	0	8
Gypsum	$CaSO_4*2H_2O$	0	1	0	0	0	0	0

Mineralogy of the Reduced Sandstone

Petrography

Sample GVS-8C-255-259 is a representative sample of reduced sandstone. It is a gray to gray-green, medium grained, poorly sorted sandstone with sub-angular to sub-rounded quartz and feldspar. Some pyrite and a mixture of clays were identified; no calcite was identified, and no oxides were identified (Fig. 7B).

X-ray Diffraction/QEMSCAN

The minerals identified were quartz, plagioclase (an increase from the oxidized sandstone), some K feldspar (less than the oxidized sandstone), pyrite, kaolinite, smectite, and illite. No calcite was observed (Table 1). Based on QEMSCAN, the grain size was similar to that in the oxidized zone. The majority of grains identified were quartz and feldspar; clay minerals were present as well as extensive pyrite.

Mineralogy of the Mineralized Sandstone

Petrography

Sample GVS-15C-167.9 is a representative sample from mineralized sandstone. It is a dark gray, large-grained, moderately sorted sandstone with sub-angular quartz and feldspar grains.

The most abundant mineral identified in this sample was quartz. Quartz grains were commonly corroded and authigenic quartz overgrowths were identified. The next most abundant mineral was feldspar. Some clay and very small amounts of pyrite were

identified and no calcite was identified (Fig. 7C).

X-ray Diffraction/QEMSCAN

Quartz, plagioclase, feldspar, some pyrite, kaolinite, smectite, and illite were identified. No calcite or sulfates were observed (Table 1). Based on QEMSCAN analysis, in the mineralized zone, the grains were larger than the oxidized zone, more angular, with the majority of the grains being quartz and feldspar. Clay minerals were extensive and only some pyrite was identified. The uranium roll-front deposits of the Gas Hills District have the mineralogical make up shown in Fig. 8.

Clay Mineralogy of the Reduced Sandstone

QEMSCAN

The reduced sandstone averages 14 percent clays. Kaolinite and smectite are the most abundant at 5 percent each and illite makes up 4 percent of the clay fraction (Fig. 9).

VNIR Spectrometry (ASD)

The results of the VNIR analysis were consistent with the X-ray diffraction clay separate results. The clays were a mixture of kaolinite, smectite, and illite. The spectrometer indicated that the reduced sample was the least reflective when compared to the oxidized and mineralized sandstones. In general, the less altered samples had peaks in the 510-570nm range, indicating (Fig. 10) that the color of the

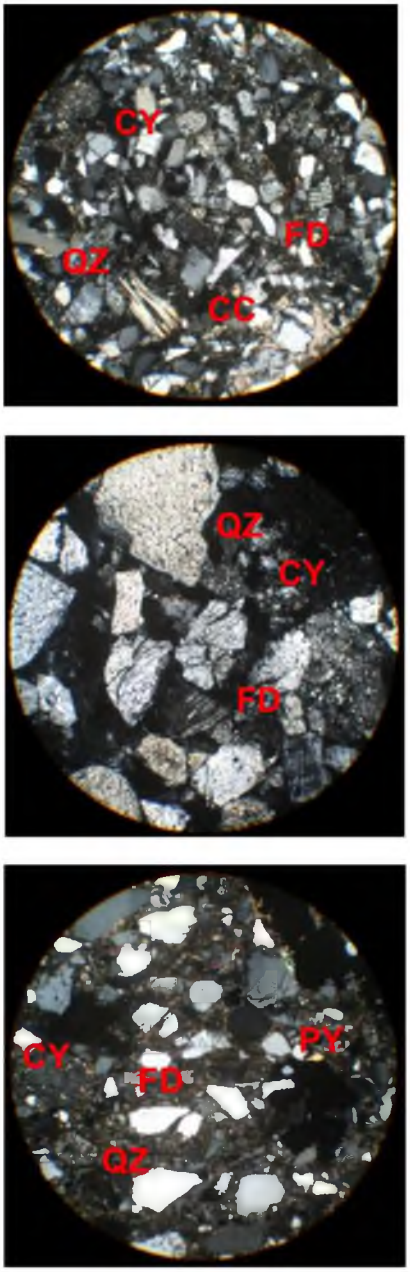

Fig. 7. Transmitted light microscope images of oxidized, reduced, and mineralized sandstones. (A) Oxidized sample GVS-8C-170-174; note the presence of calcite and no pyrite. The sample is finer grained than the reduced sandstone with more angular mineral grains. (B) Reduced sample GVS-8C-255-259. (C) Mineralized sample GVS-15C-167.9. QZ is quartz, FD is feldspar, CY is clay, and CC is calcite.

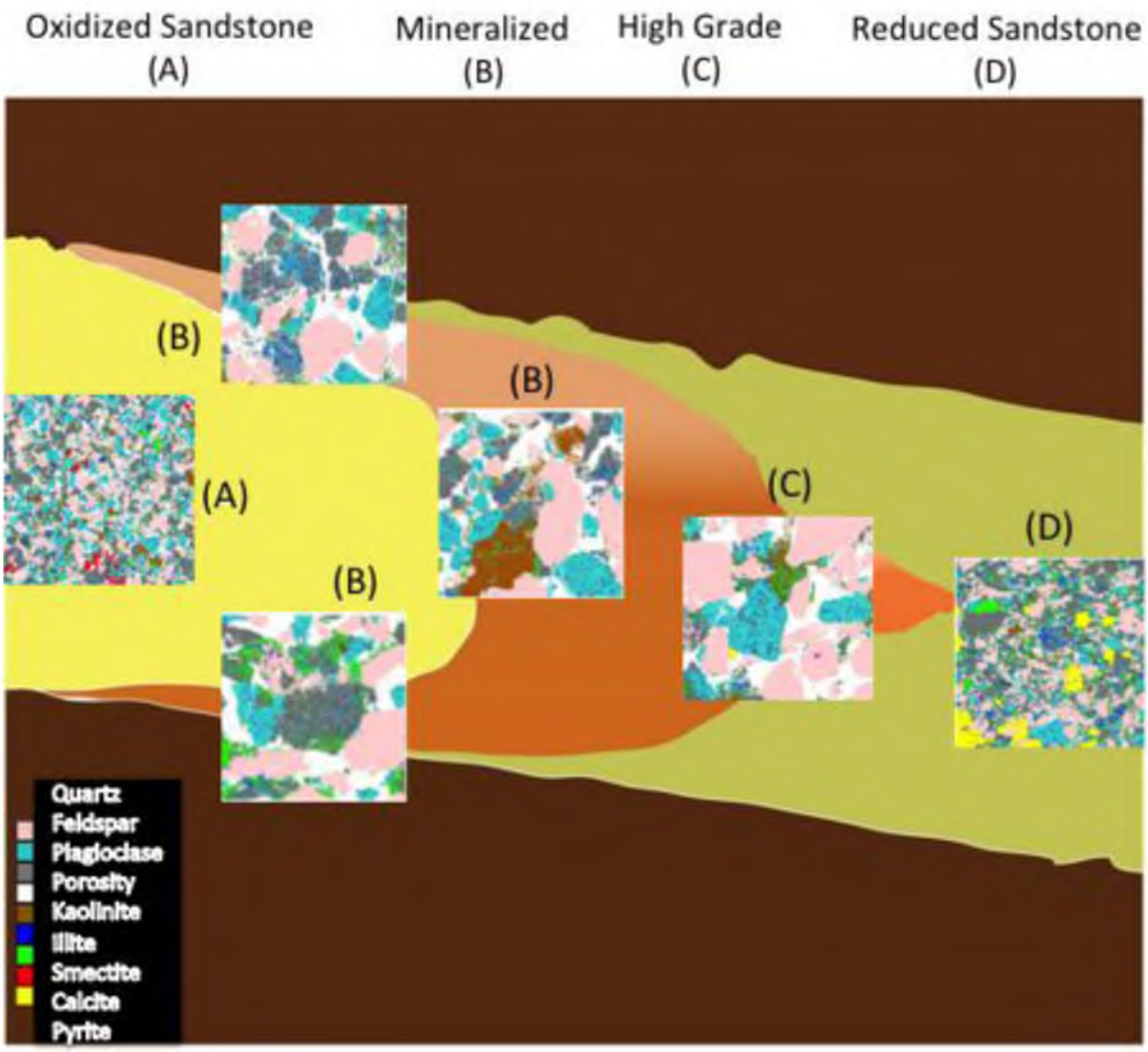

Fig. 8. Mineralogy representative of each "sector" of the uranium roll-front deposit. Mineralogy defined by QEMSCAN (Moyes, 2011). Changes in grain size are a function of lithology and are due to limited sample choices but are still reflective of the indicated zone.

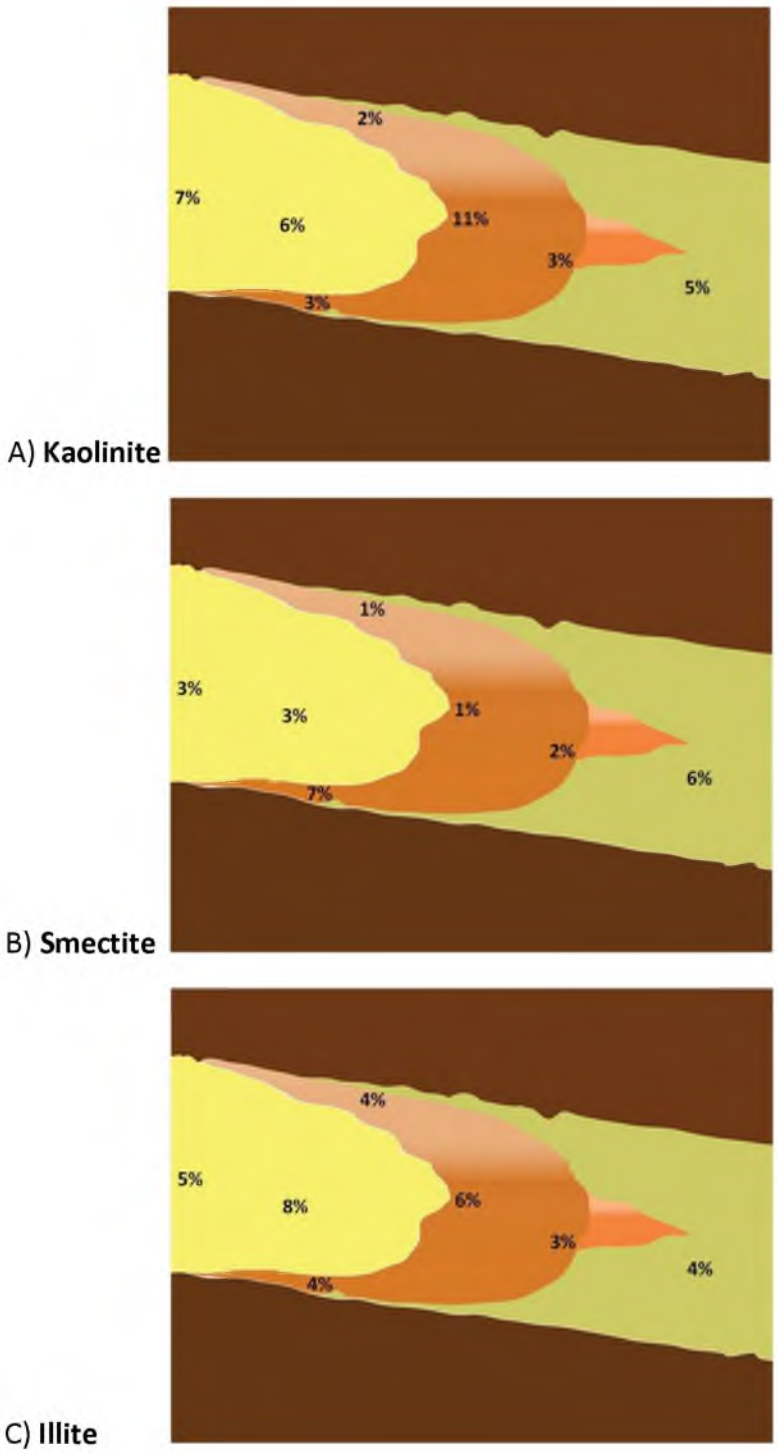

Fig. 9. Clay constituents in the Geroge Ver and Loco Lee deposits based on QEMSCAN results. A) Kaolinite distribution across the roll-front. B) Smectite distribution across the roll-front. C) Illite distribution across the roll-front.

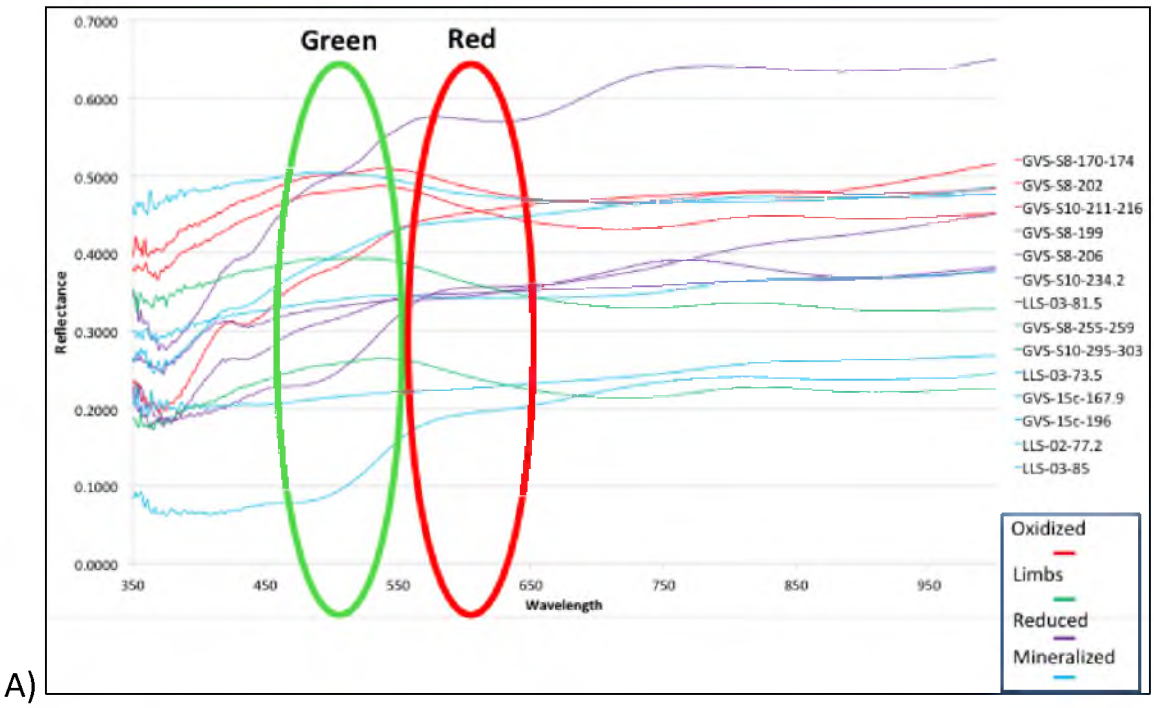

A)

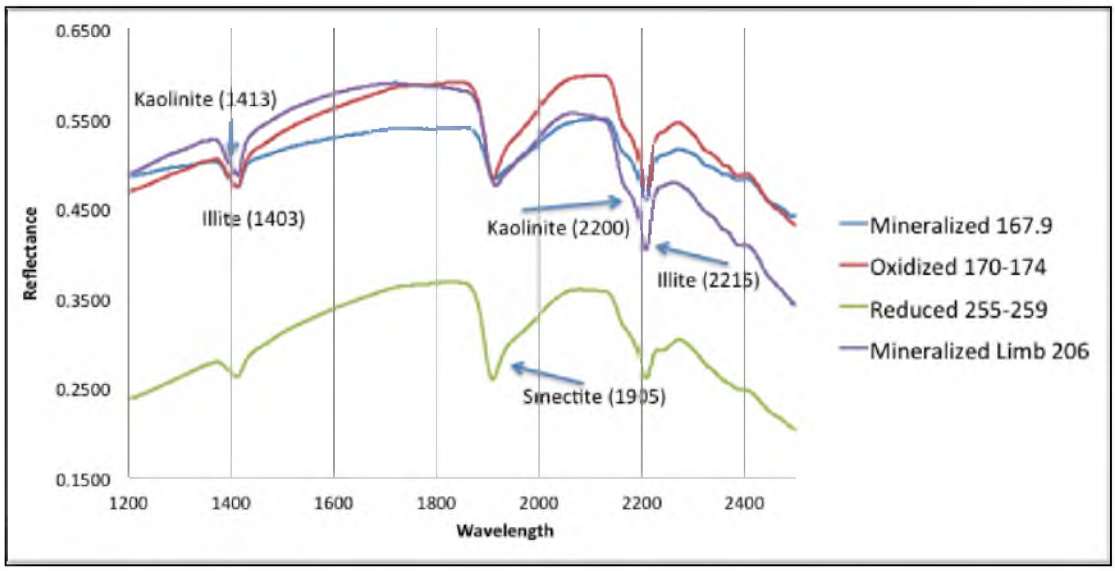

B)

Fig. 10. ASD (VNIR) spectra from various samples of oxidized, reduced and mineralized sandstone. A) Multiple spectra from mineralized, reduced, and oxidized sandstones in the visible spectrum. Peaks in the 510-570 range indicate more green samples while peaks in the 570 to 650 range indicated more red. B) ASD spectrometer comparison of oxidized sample GVS-8C-170-174, reduced sample GVS-8C-255-259, mineralized sample GVS 15C-167.9, and mineralized limb sample GVS-S8-206. Troughs of major clays compared from Clark et al. (2007).

sample is greener when compared to the other samples.

Clay Mineralogy of the Oxidized Sandstone

QEMSCAN

The oxidized sandstone is made up of 15 percent clay. Kaolinite at 7 percent, smectite at 3 percent, and illite at 5 percent constitute the clays in this zone (Fig. 9).

VNIR Spectrometry (ASD)

Based on the VNIR analysis, illite was identified in sample GVS-8C-170-174; kaolinite was also identified. These results are consistent with the X-ray diffraction analysis (Fig. 10). The spectrometer indicated that the oxidized sample was the most reflective when compared to the reduced and mineralized sandstones. In general, the oxidized samples had higher peaks in the 570-650nm range, indicating that the samples are redder compared to the less altered sample.

Clay Mineralogy of the Mineralized Sandstone

QEMSCAN

The ore zone can contain between 8 and 18 percent clay. Locally, kaolinite can be up to 11 percent, smectite at 6 percent, and illite at 6 percent (Fig. 9).

VNIR Spectrometry (ASD)

In the mineralized sandstone, VNIR spectrometry indicates that illite was present

in sample GVS-15C-167.9, seen in Fig. 10. A mixture of kaolinite and smectite was also identified. The spectrometer indicated that the sample was less reflective than the oxidized sandstone, but slightly more reflective than the reduced sandstone. There was a range of color from green to red in the mineralized samples, depending on the degree of alteration of the sample.

In general, the VNIR spectrometer was less likely to identify kaolinite in each of the samples when compared to QEMSCAN and X-ray diffraction.

Clay Mineralogy Identified with X-ray Diffraction

The results of the X-ray diffraction on whole rock samples did not distinguish individual clay types, therefore requiring clay seperates. X-ray scans of clay seperates of reduced and oxidized sandstones are compared in Fig. 11. The smectite peak is taller and sharper in the oxidized sample, indicating better crystallinity, the illite peak is taller and sharper in the reduced sample, also indicating better crystallinity, and the kaolinite peak is taller and sharper in the oxidized sample, indicating more defined crystallinity. The clay results of a low-grade mineralized sample were compared to those of a high-grade mineralized sample in Fig. 12. The smectite peak is larger and sharper in the mineralized sample, indicating that more smectite is present with more developed crystallinity, the illite peak is taller and sharper in the low-grade sample, indicating higher concentration and better crystallinity, and the kaolinite peak is larger and sharper in the high-grade sample, indicating more is present, with more developed crystallinity.

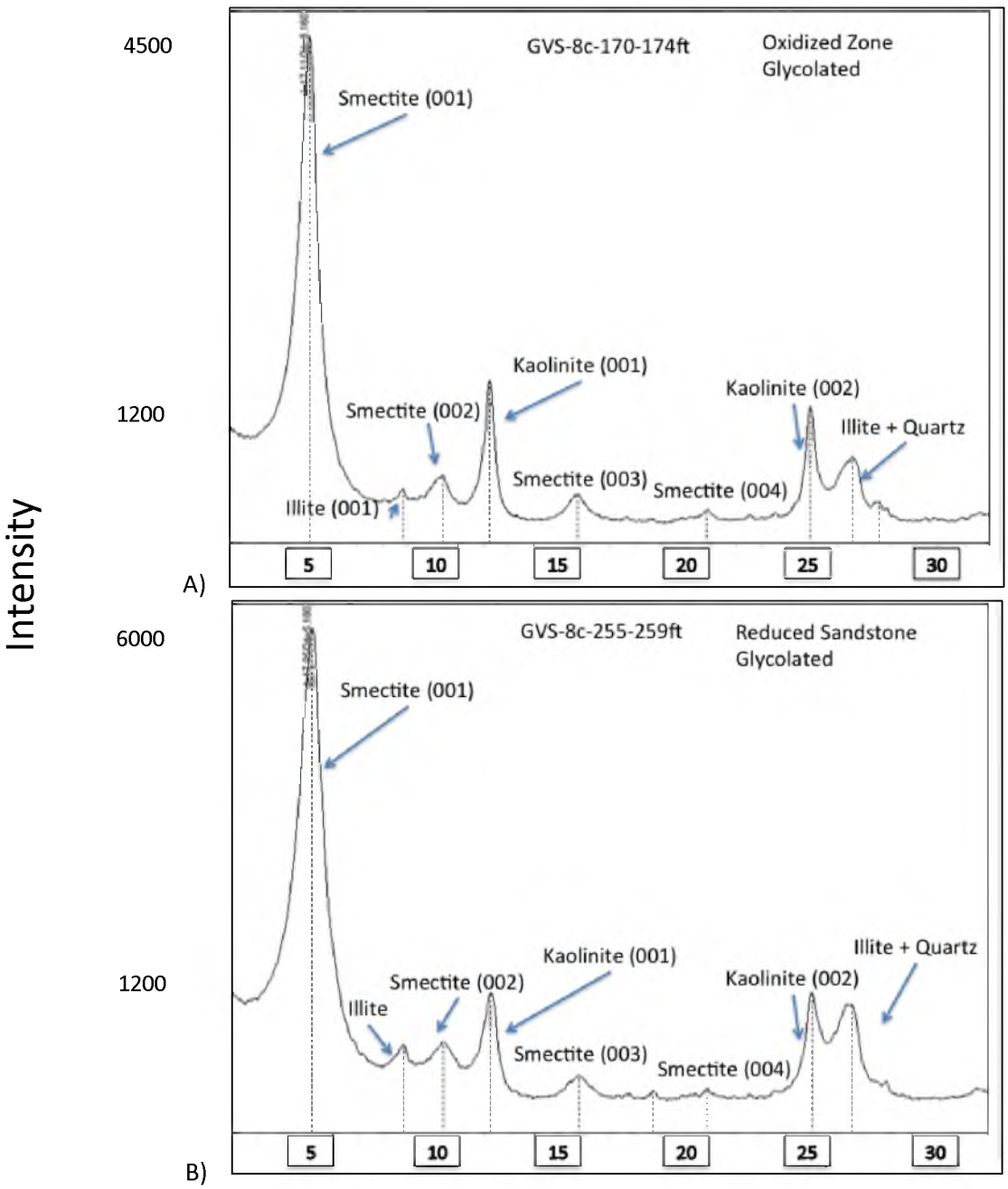

Fig. 11. Comparisons of clay separate XRD patterns for a reduced and oxidized sample. Note that the smectite peak is taller and narrower in the oxidized sample, the illite peak is taller and sharper in the reduced sample, and the kaolinite peak is taller and narrower in the oxidized sample. A) Result of clay separate for reduced sandstone in Gerge Ver borehole 8. B) Result of clay separate for oxidized sandstone in George Verr borehole 8.

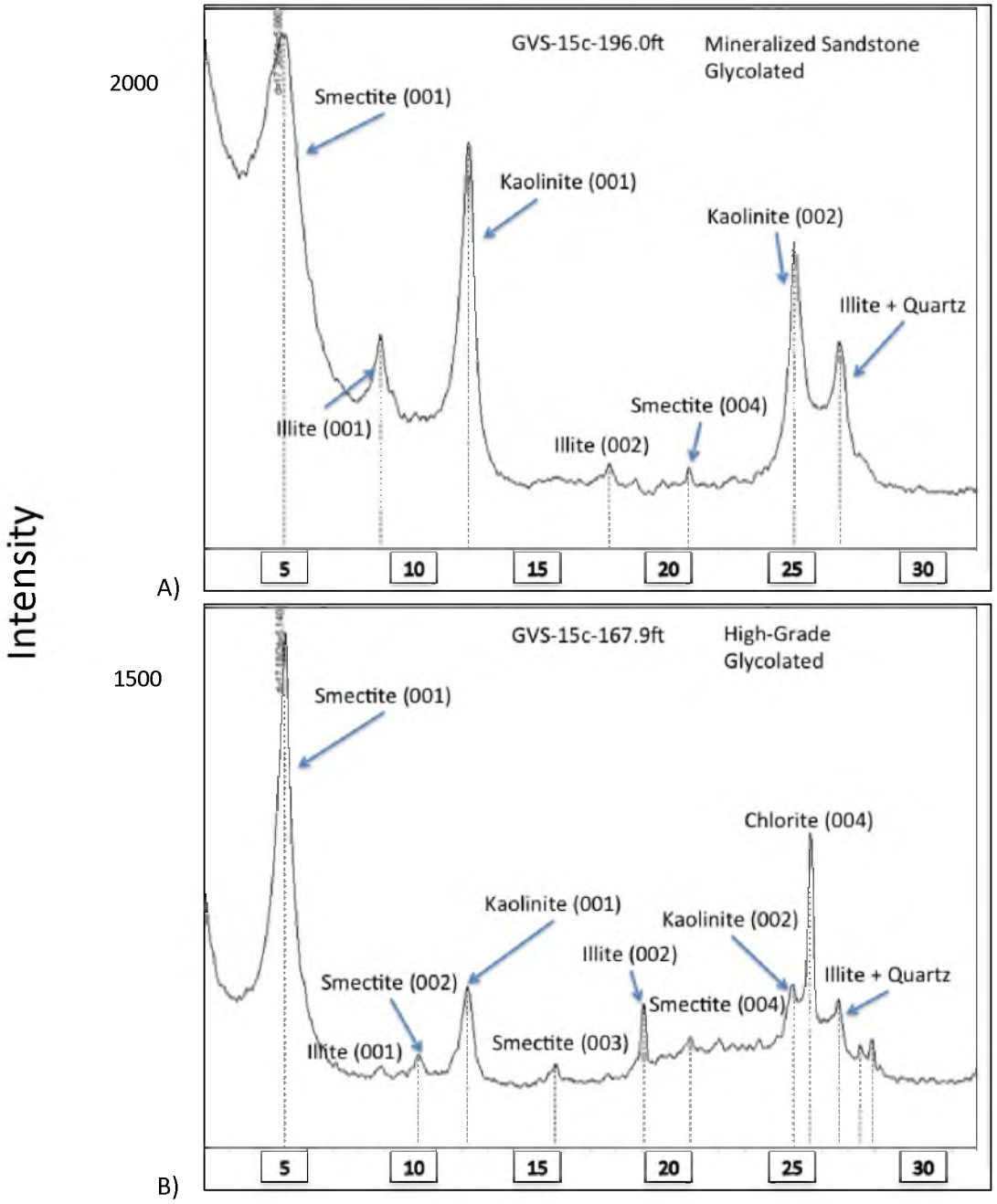

Fig. 12. Comparison of clay separate XRD patterns for a lower-grade mineralized sample (80 ppm U) and a sample from higher-grade ore (100 ppm U). Note that the smectite peak is larger and sharper in the high-grade sample, the illite peak is taller and sharper in the low-grade sample, and the kaolinite peak is larger and sharper in the high-grade sample. Both samples are from the George Ver borehole 15. A) Low-grade mineralized clay separate. B) High-grade, clay separate.

Clay Habits as Identified with QEMSCAN

Habit of Kaolinite

Three habits of kaolinite have been characterized with QEMSCAN. Each of the three habits is associated with specific sectors of the deposit – oxidized sandstone, reduced sandstone, and the mineralized orebody. The habit identified in the oxidized sandstone is defined as clumpy, as in the clay has formed individual groupings or clumps. In the ore body, there is a distinct change not only in the amount of kaolinite (7% to 11%) but the texture changes from discrete clumps to feldspar grain replacement. Downstream in the reduced sandstone, the texture is disseminated and does not form distinct clumps (Fig. 13).

Habit of Smectite

Three habits associated with the mineral smectite are identified. The habit identified in the oxidized or upstream sandstone can be described as clumpy. Moving into the ore body, there is a distinct change not only in the amount of smectite (3% to 7%) but the habit changes from clumpy to grain replacement, as seen with kaolinite. Downstream in the reduced sandstone, the texture can be described primarily as disseminated with some clumps present (Fig. 14).

Habit of Illite

Three habits of the mineral illite are identified. The texture identified in the oxidized or upstream sandstone can be described as disseminated. In the ore body,

QEMSCAN Image	Sector	Texture	Amount
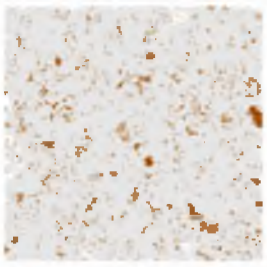	Oxidized Upstream	Clots	7%
	Mineralized	Grain Replacement	11%
	Reduced Downstream	Disseminated	5%

Fig. 13. Kaolinite texture across a roll-front deposit in the Gas Hills District; amount is reported in area percent. Kaolinite is in brown.

QEMSCAN Image	Sector	Texture	Amount
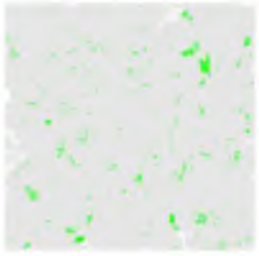	Oxidized Upstream	Clots	3%
	Mineralized	Grain Replacement	7%
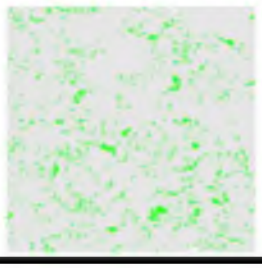	Reduced Downstream	Clumpy & Disseminated	6%

Fig. 14. Smectite texture across a roll-front deposit in the Gas Hills District; amount is reported in area percent. Smectite is in green.

there is a distinct change not only in the amount of illite (5% to 6%) but the texture changes from clot like to grain replacement, as seen with kaolinite and smectite. In the reduced sandstone, the texture is primarily clot- like (Fig. 15).

Porosity

First order-2D porosity was estimated from QEMSCAN images. The porosity in the reduced sandstone is 5 percent, an average of 8 percent through the ore zone, and 4 – 21 percent in the oxidized sandstone (Table 2).

Geochemistry

Oxidized Sandstone

In the oxidized sandstone, K and Rb have elevated values when compared to the reduced sandstone. The oxidized sandstone has a K range of 3.5 to 4.2 percent with standard deviation of 0.3 and the Rb has a range of 140 to 167 ppm with standard deviation of 9.7. Compare this to a K range in the reduced sandstone of 2.5 to 2.8 percent with standard deviation of 0.1 and a Rb range of 87 to 137 ppm with standard deviation of 18.7 (Table 3).

Correlations were considered statistically significant at a p-value of 0.05 and a 95 percent confidence interval (Table 4). In the oxidized sandstone, U correlates most significantly with As, Fe, and Co.

QEMSCAN Image	Sector	Texture	Amount
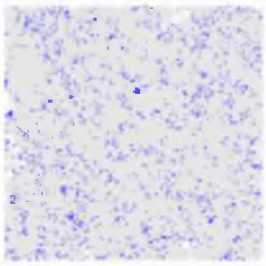	Oxidized Upstream	Disseminated	5%
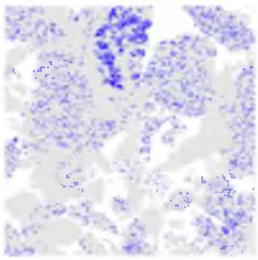	Mineralized	Grain Replacement	6%
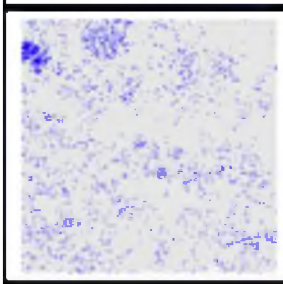	Reduced Downstream	Clumpy	4%

Fig. 15. Changes in illite texture across a roll-front deposit in the Gas Hills District; amount is reported in area percent. Illite is in blue.

Table 2: First order porosity of the George Ver and Loco Lee deposits in the Gas Hills District

Sector of Orebody	Porosity Percent
Oxidized Sandstone	21
Oxidized Interior	20
Lower Limb	10
Upper Limb	4
Mineralized Zone	6
High-Grade Ore	9
Reduced Sandstone	5

Table 3: Element assays in each sector of the Geroge Ver and Loco Lee orebodies

DESIGNATION	SAMPLE ID	U	Al	Mg	Mn	Fe	K	Ca	P	Ce	Rb	Mo	Ti
		ppm	%	%	ppm	%	%	%	%	ppm	ppm	ppm	%
Oxidized	GVS-S8-08-202.0ft	86	7.02	0.23	150	2.83	3.9	0.2	<0.01	75	153	5.0	0.15
Oxidized	GVS-8c-151-155ft	18.8	6.01	0.13	110	1.22	3.5	0.3	<0.01	41.1	140	5.0	0.06
Oxidized	GVS-s10c-191-196ft	12.9	6.69	0.17	100	1.19	4.0	0.2	<0.01	46	154	<2	0.08
Oxidized	GVS-10c-211ft-216ft	9.0	6.61	0.15	120	1.39	4.2	0.3	<0.01	33	167	2	0.07
Oxidized	GVS-8c170ft-174ft	12	6.81	0.25	360	1.19	3.6	1.9	0.02	66	142	<2	0.13
Limbs	GVS-S8-08-199.0ft	136	7.99	0.45	160	3.74	3.9	0.2	0.02	90.6	165	50	0.25
Limbs	GVS-S8-08-206.0ft	123	10.3	0.51	130	2.28	3.7	0.3	0.03	216	159	6.0	0.37
Limbs	LLS-03c-73.5ft	45.4	4.89	0.08	140	1.48	3.2	0.1	0.02		138	3.0	0.07
Limbs	LLS-03c-81.5ft	39.5	5.5	0.09	100	1.32	3.6	0.2	<0.01	28.1	146	<2	0.05
Ore Zone	GVS-S10c-08-234.2ft	88	9.74	0.40	120	2.45	3.6	0.2	0.02	182	164	77	0.3
Ore Zone	GVS-15c-196.0ft	82	9.53	0.68	150	2.2	3.5	0.3	0.03	238	189	8.0	0.43
Ore Zone	LLS-02c-77.2ft	270	4.92	0.06	80	1.28	3.2	0.2	0.23	46	124	3.0	0.06
Ore Zone	GVS-S10c-232.0ft	221	3.64	0.11	1410	3.72	2.4	12.1	0.51	21.9	95.5	18	0.02
Ore Zone	LLS-03c-60.2ft	45.8	6.47	0.32	100	5.1	2.0	0.1	0.01	60.4	89.8	2.0	0.27
Ore Zone	LLS-02c-60.0ft	67.2	7.16	0.32	90	4.61	2.1	0.2	0.01	39.7	83.3	2.0	0.3
Ore Zone	LLS-02c-84.0ft	131	6.13	0.13	80	1.12	4.1	0.2	0.01	42.5	166	<2	0.07
Ore Zone	GVS-S8-182.0ft	375	8.05	0.33	130	2.08	3.7	0.3	<0.01	98.9	161	3.0	0.22
Ore Zone	LLS-03c-85.0ft	392	6.63	0.13	130	1.22	3.6	0.2	0.01	41	156	4.0	0.05
Ore Zone	GVS-15c-167.9ft	101	5.43	0.09	120	1.06	3.6	0.2	<0.01	70	237	96	0.06
Reduced	GVS-10c-295ft-303ft	22	9.56	1.22	360	5.15	2.5	0.4	0.03	157	137	8.0	0.52
Reduced	GVS-s10c-270-274ft	32.6	8.46	0.37	130	2.22	2.8	0.2	0.02	93.3	122	11	0.29
Reduced	GVS-8c-241-245ft	6.39	8.13	0.67	170	3.49	2.5	0.4	<0.01	41	124	3.0	0.38
Reduced	GVS-8c-255ft-259ft	2.4	6.48	0.47	200	2.05	2.7	0.5	<0.01	34	86.6	<2	0.18

Table 3 cont: Element assays in each sector of the Geroge Ver and Loco Lee orebodies

DESIGNATION	SAMPLE ID	Zr	Sr	V	Th	Co	Cs	Tl	As	Ni	Zn	Cu	Sc	Y
		ppm	ppm	ppm	ppm	ppm	ppm	ppm	ppm	ppm	ppm	ppm	ppm	ppm
Oxidized	GVS-S8-08-202.0ft	209	72	29	29.2	3.9	5.2	1.2	282	13	30	6.0	<5	25.8
Oxidized	GVS-8c-151-155ft	101	69.7	29	16.9	3.2	1.9	1.4	40	14	14	7.0	<5	13.5
Oxidized	GVS-s10c-191-196ft	130	81.3	40	18.1	2.9	3.9	1.0	<5	11	17	<5	<5	19.3
Oxidized	GVS-10c-211ft-216ft	95	79	24	14.7	2.7	3.0	1.1	9.0	12	9.0	<5	<5	15.3
Oxidized	GVS-8c170ft-174ft	233	88	26	28.5	2.9	5.3	0.9	<5	12	21	7	<5	29.3
Limbs	GVS-S8-08-199.0ft	251	85.8	63	36.5	8.6	11.7	1.6	171	23	53	16	17	31.6
Limbs	GVS-S8-08-206.0ft	192	94.8	60	71.8	9.3	13.9	2.0	56	31	56	22	11	55.7
Limbs	LLS-03c-73.5ft	137	73.9	95	42.5	1.0	2.1	13.1	169	8.0	<5	<5	<5	32.7
Limbs	LLS-03c-81.5ft	85.2	66.7	112	18.4	1.8	4.7	3.4	75	16	<5	8.0	<5	10.7
Ore Zone	GVS-S10c-08-234.2ft	153	104	48	56.9	13.1	15.4	2.2	92	49	55	27	12	40.8
Ore Zone	GVS-15c-196.0ft	259	141	82	54.8	11.6	23.8	1.1	26	34	79	44	11	62.6
Ore Zone	LLS-02c-77.2ft	83	76	55	18.1	0.7	2.0	11.1	570	8	<5	10	<5	13.1
Ore Zone	GVS-S10c-232.0ft	54.5	115	121	5.9	10.6	1	3.8	1790	18	14	<5	<5	10.4
Ore Zone	LLS-03c-60.2ft	297	43.2	60	22.5	8.7	12.8	0.6	156	33	44	9.0	8	27.2
Ore Zone	LLS-02c-60.0ft	287	59.5	64	41.2	9.3	10.4	0.8	266	26	65	20	10	30.9
Ore Zone	LLS-02c-84.0ft	131	80.7	84	20.5	1.5	4.8	6.7	97	24	9.0	6.0	<5	13.7
Ore Zone	GVS-S8-182.0ft	274	95.9	32	35.3	8.6	13.3	1.0	39	24	33	11	6	31.4
Ore Zone	LLS-03c-85.0ft	83	71	138	16.8	6.2	9.3	85.4	69	429	10	15	<5	11.9
Ore Zone	GVS-15c-167.9ft	192	68	39	27.3	5.1	2.7	2.2	84	10	13	<5	<5	17.5
Reduced	GVS-10c-295ft-303ft	82.2	174	173	37.5	35.1	11	0.7	215	113	330	77	15	35.6
Reduced	GVS-s10c-270-274ft	122	159	79	26.6	9.1	9.9	0.9	19	41	65	50	8	23.9
Reduced	GVS-8c-241-245ft	149	174	85	25.8	13	8.8	0.6	18	51	78	41	11	16
Reduced	GVS-8c-255ft-259ft	116	117	42	12.7	8.0	2.3	<0.5	<5	31	37	16	<5	9.4

Table 4. Pearson Correlation for Oxidized Sandstone in the George Ver and Loco Lee Deposits

Zn	Zn						**V**	V						
	1							1						
Al	Al						**Th**	Th	Zr	Ti	Mg			
	1							1	0.98	0.97	0.95			
Cr	Cr	Cs	Mg				**U**	U	As	Fe	Co			
	1	0.97	0.95					1	1.00	0.98	0.96			
Ni	Ni						**Cs**	Cs	Cr	Mg				
	1							1	0.97	0.97				
Co	Co	U	As				**Tl**	Tl	Sr					
	1	0.96	0.96					1	-0.96					
Mg	Mg	Zr	Cs	Th	Cr	Ti	**As**	As	U	Fe	Co			
	1	0.98	0.97	0.95	0.95	0.95		1	1.00	0.98	0.96			
K	K	Rb					**Fe**	Fe	As	U				
	1	0.98						1	0.98	0.98				
Ca	Ca	P	Mn				**Mn**	Mn	P	Ca				
	1	1.00	0.98					1	0.99	0.98				
P	P	Ca	Mn				**Cu**	Cu						
	1	1.00	0.99					1						
Ti	Ti	Th	Mg				**Mo**	Mo						
	1	0.97	0.95					1						
Zr	Zr	Mg	Th				**Rb**	Rb	K					
	1	0.98	0.98					1	0.98					
Sr	Sr	Tl												
	1	-0.96												

Mineralized Sandstone

Within the mineralized sandstone, there was detectable P, V, Zr, Cs, As, and Tl are higher in the reduced and oxidized sandstones (Table 3). U concentration in the mineralized sandstone is over 300 ppm; this is well above the oxidized and reduced sandstones, which are closer to 20 ppm on average. This is a 15x enrichment factor. The Pearson correlation for the mineralized sandstone with statistically significant correlations can be seen in Table 5. In the mineralized sandstone, U is most highly correlated with Tl, although based on the 0.05 cutoff for significance, U does not correlate with any element in particular in the mineralized portion. In the mineralized limbs of the deposit, U correlates positively with Zn, Co, and Mg, but has a negative correlation with V (Table 6).

Reduced Sandstone

A comparison of the relative values in the amount of primary elements and trace elements in the reduced sandstone, mineralized sandstone, and oxidized sandstone can be seen in Fig. 16 and Fig. 17. The elements that decrease in value in the reduced sandstone when compared to the oxidized and mineralized sandstones are K, P, Zr, V, Th, U, Tl, As, Cs, Mo, and Rb, as seen in Table 3. Iron content is much lower in the oxidized sandstone compared to the reduced sandstone (Fig. 18). The reduced sandstone contains higher amounts of the elements Zn, Cr, Co, Mg, Sr, Mn, Cu (similar values in ore body), and Ni when compared

Table 5. Pearson Correlation for the Mineralized Sandstone in the George Ver and Loco Lee Deposits

Zn	Zn	Ti		**V**	V		
	1	0.97			1		
Al	Al			**Th**	Th		
	1				1		
Cr	Cr			**U**	U		
	1				1		
Ni	Ni	Tl		**Cs**	Cs	Mg	
	1	0.98			1	0.96	
Co	Co			**Tl**	Tl	Ni	
	1				1	0.98	
Mg	Mg	Cs	Ti	**As**	As	P	
	1	0.96	0.96		1	0.98	
K	K			**Fe**	Fe		
	1				1		
Ca	Ca	Mn		**Mn**	Mn	Ca	
	1	0.99			1	0.99	
P	P	As		**Cu**	Cu		
	1	0.98			1		
Ti	Ti	Zn	Mg	**Mo**	Mo		
	1	0.97	0.96		1		
Zr	Zr			**Rb**	Rb		
	1				1		
Sr	Sr						
	1						

Table 6. Pearson Correlation for the Limb Sandstone in the George Ver and Loco Lee Deposits

Zn	Zn	Mg	Co	U	Cs	V	Ti		
	1	1.00	1.00	0.99	0.97	-0.96	0.96		
Al	Al								
	1								
Cr	Cr	Ti	Cu	Sr					
	1	0.98	0.96	0.95					
Ni	Ni	Cu	Cs	Ca					
	1	0.99	0.97	0.96					
Co	Co	Mg	Zn	Cs	U	Cu	Ti	Rb	
	1	1.00	1.00	0.99	0.98	0.96	0.96	0.95	
Mg	Mg	Zn	Co	Cs	U	Ti	Cu	V	Sr
	1	1.00	1.00	0.98	0.98	0.97	0.96	-0.95	0.95
K	K	Tl							
	1	-0.95							
Ca	Ca	Ni							
	1	0.96							
P	P								
	1								
Ti	Ti	Sr	Cr	Mg	Cu	Zn	Co	Cs	
	1	0.98	0.98	0.97	0.97	0.96	0.96	0.96	
Zr	Zr	Fe							
	1	0.95							
Sr	Sr	Ti	V	Cr	Mg				
	1	0.98	-0.97	0.95	0.95				

V	V	Sr	U	Zn	Mg		
	1	-0.97	-0.96	-0.96	-0.95		
Th	Th						
	1						
U	U	Zn	Co	Mg	V		
	1	0.99	0.98	0.98	-0.96		
Cs	Cs	Cu	Co	Mg	Zn	Ni	Ti
	1	0.99	0.99	0.98	0.97	0.97	0.96
Tl	Tl	K					
	1	-0.95					
As	As						
	1						
Fe	Fe	Mo	Zr				
	1	0.95	0.95				
Mn	Mn						
	1						
Cu	Cu	Ni	Cs	Ti	Mg	Co	Cr
	1	0.99	0.99	0.97	0.96	0.96	0.96
Mo	Mo	Fe					
	1	0.95					
Rb	Rb	Co					
	1	0.95					

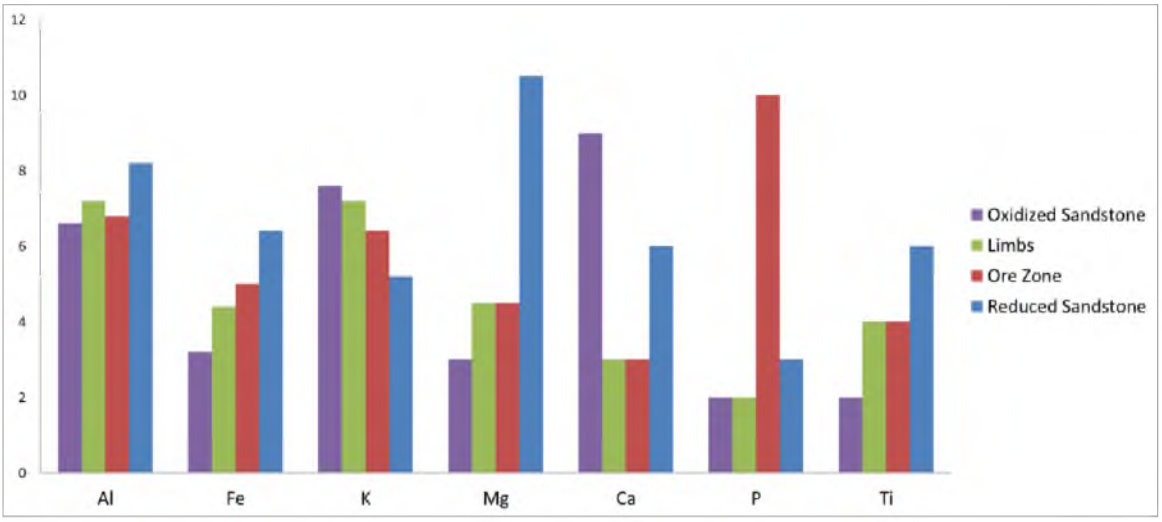

Fig. 16. Average primary element comparison from the reduced sandstone, ore zone, mineralized limbs, and oxidized sandstone (element values have been weighted to fit on the same scale). Al values had no multiplier, Fe and K values were multiplied by 2, Mg and Ca values multiplied by 15, P values multiplied by 100, and Ti values multiplied by 20.

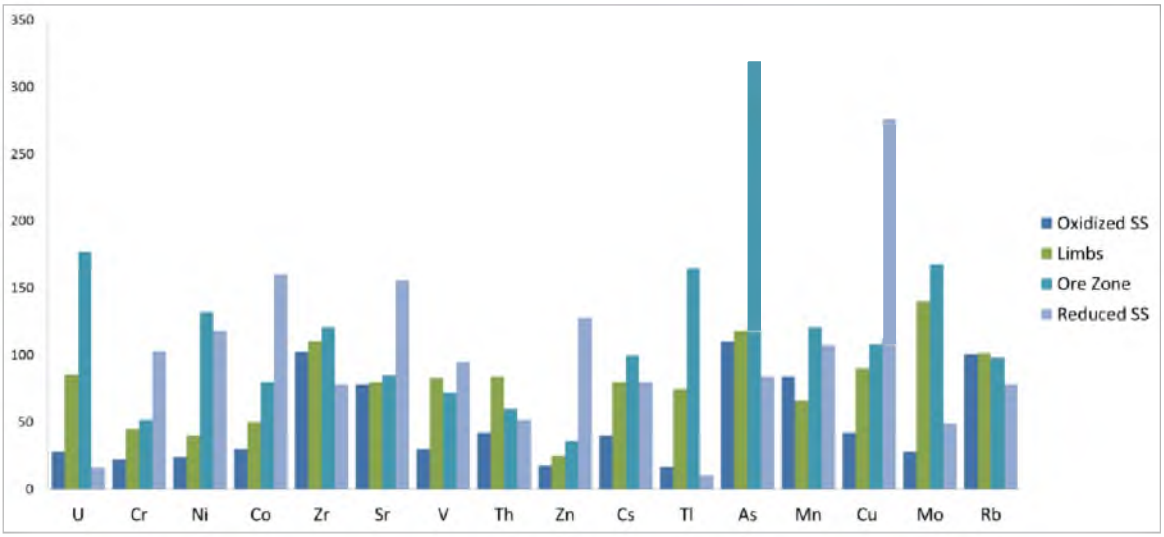

Fig. 17. Average trace element comparison from the reduced sandstone, ore zone, mineralized limbs, and oxidized sandstone (element values have been weighted to fit on the same scale). Ni values were multiplied by 2, Co values multiplied by 10, Zr values divided by 1.5, Th values multiplied by 2, Cs values multiplied by 10, Tl values multiplied by 15, Mn values were divided by 2, Cu and Mo values were multiplied by 7, and Rb values were divided by 1.5.

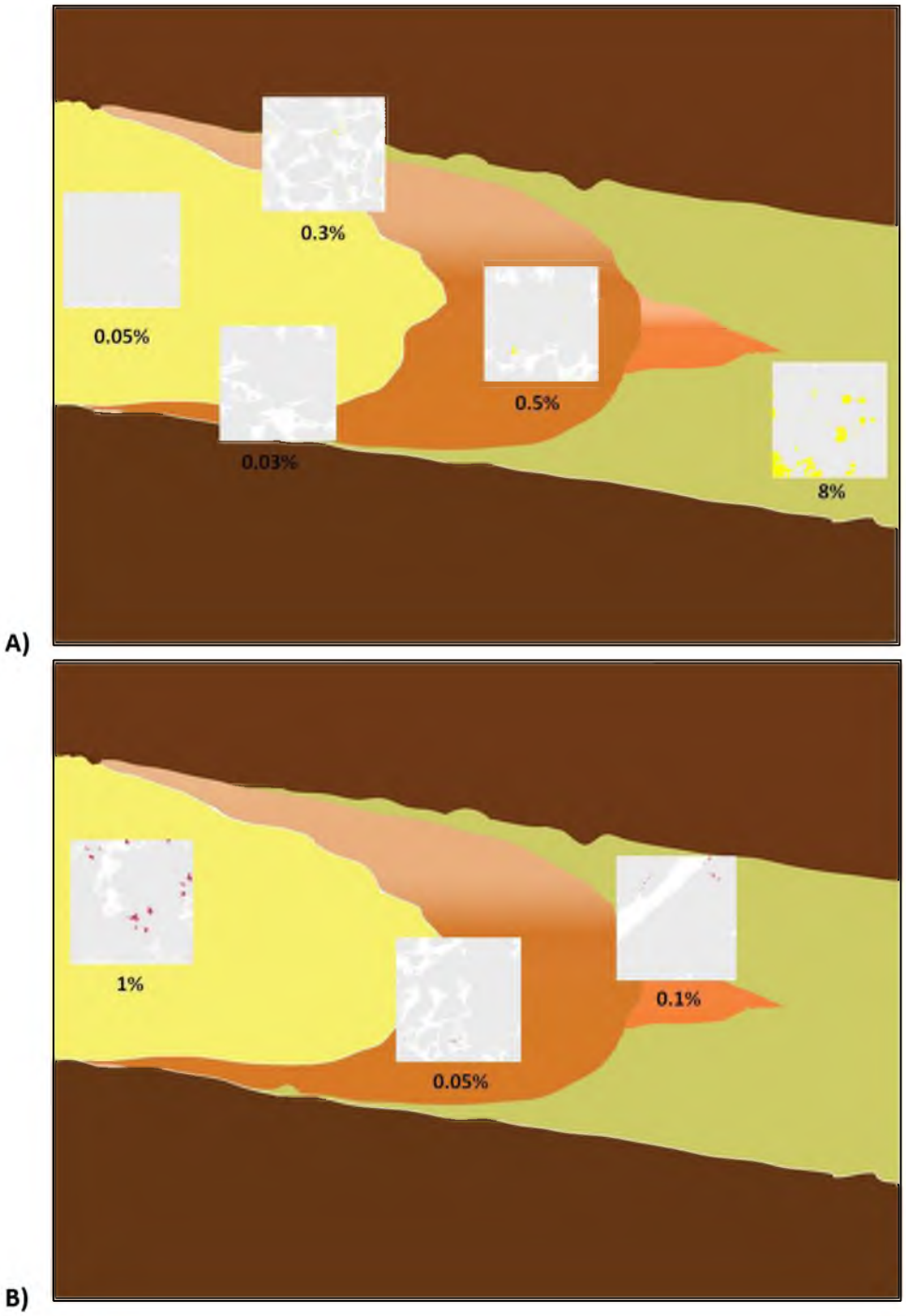

Fig. 18. QEMSCAN images of pyrite and gypsum abundance across the roll-front. A) Pyrite distribution in the George Ver and Loco Lee deposits. Almost 100% of the pyrite content resides in the reduced sandstone and pockets of reduced sandstone in the ore body. B) Distribution of gypsum in the George Ver and Loco Lee deposits.

to the oxidized sandstone (Table 3). Based on the correlation in the reduced sandstone, U correlates most strongly with Mo and Tl, as seen in Table 7.

Rare Earth Element Geochemistry

The reduced sandstone contains more rare earth elements than the oxidized sandstone by a factor of two (Table 8). The reduced sandstone rare earth content is above average when compared to the chondrite (Sun and McDonough, 1989) (Fig. 19). When compared to the North American Granite Composite, the values are almost identical (Fig. 20).

Ore zone values of rare earth elements are almost double those of the reduced sandstone. When compared to the oxidized sandstone, the values are increased by a factor of three. The LREE do not move in sync within the oxidized, reduced, and mineralized sandstones. It is observed that the HREE move in sync between the oxidized and reduced sandstones (Fig. 19).

Table 7. Pearson Correlation for Reduced Sandstone in the George Ver and Loco Lee Deposits

Zn	Zn	As	Co	Ni	V	Mg		**V**	V	Ni	Zn	Co	As	Ti	Cu	Fe
	1	1.00	1.00	0.99	0.97	0.96			1	0.99	0.97	0.97	0.96	0.96	0.95	0.95
Al	Al	Th	Cu	Rb	Cs			**Th**	Th	Al	Cu	Rb	Ti			
	1	1.00	0.99	0.97	0.96				1	1.00	0.99	0.97	0.95			
Cr	Cr	Fe	Ti					**U**	U	Mo	Tl					
	1	0.99	0.97						1	1.00	0.95					
Ni	Ni	Co	Zn	V	As	Mg	Fe	**Cs**	Cs	Rb	Al					
	1	1.00	0.99	0.99	0.99	0.97	0.96		1	0.98	0.96					
Co	Co	Ni	Zn	As	Mg	V	Fe	**Tl**	Tl	Mo	U	Ca				
	1	1.00	1.00	0.99	0.98	0.97	0.96		1	0.96	0.95	-0.95				
Mg	Mg	Co	Fe	Ni	Zn	As		**As**	As	Zn	Co	Ni	V	Mg		
	1	0.98	0.98	0.97	0.96	0.95			1	1.00	0.99	0.99	0.96	0.95		
K	K							**Fe**	Fe	Cr	Mg	Ni	Ti	Co	V	
	1								1	0.99	0.98	0.96	0.96	0.96	0.95	
Ca	Ca	Tl						**Mn**	Mn							
	1	-0.95							1							
P	P							**Cu**	Cu	Th	Al	V				
	1								1	0.99	0.99	0.95				
Tl	Ti	Cr	Fe	V	Th			**Mo**	Mo	U	Tl					
	1	0.97	0.96	0.96	0.95				1	1.00	0.96					
Zr	Zr							**Rb**	Rb	Cs	Al	Th	Sr			
	1								1	0.98	0.97	0.97	0.97			
Sr	Sr	Rb														
	1	0.97														

Table 8: Rare earth element assays in each sector of the George Ver and Loco Lee orebodies in the Gas Hills

DESIGNATION	SAMPLE ID		La	Ce	Pr	Nd	Sm	Eu	Gd	Dy	Er	Tb	Yb	Ho	Lu
			ppm	ppm	ppm	ppm	ppm	ppm	ppm	ppm	ppm	ppm	ppm	ppm	ppm
Oxidized	GVS-S8-08-202.0ft	<0.01	40.5	75	8.67	26.3	5.7	0.55	4.83	4.71	2.63	0.78	2.5	0.89	0.47
Oxidized	GVS-8c-151-155ft	<0.01	23.5	41.1	4.92	14.8	3.3	0.39	2.74	2.23	1.24	0.44	1.2	0.39	0.18
Oxidized	GVS-s10c-191-196ft	<0.01	26.5	46	5.71	16.4	4.2	0.55	3.46	3.04	1.93	0.54	1.6	0.62	0.26
Oxidized	GVS-10c-211ft-216ft	<0.01	20	33	4.22	12.3	2.9	0.37	2.66	2.3	1.53	0.4	1.3	0.48	0.21
Oxidized	GVS-8c170ft-174ft	0.02	36.4	66	8.1	23.6	5.4	0.6	4.73	4.46	2.79	0.8	2.8	0.89	0.4
Ore Zone	GVS-S10c-08-234.2ft	0.02	89.8	182	19.5	57.6	12.5	1.46	10.2	7.96	4.14	1.6	3.5	1.47	0.62
Ore Zone	GVS-15c-196.0ft	0.03	104	238	25.0	80.5	16.7	2.62	14.7	11.9	6.26	2.26	5.1	2.08	0.69
Ore Zone	LLS-02c-77.2ft	0.23	24.1	46	4.92	13.4	2.8	0.12	2.34	1.92	1.16	0.33	1	0.4	0.18
Ore Zone	GVS-S10c-232.0ft	0.51	18.2	21.9	2.3	6.6	1.3	0.2	1.27	1.28	0.88	0.22	0.7	0.27	0.11
Ore Zone	LLS-03c-60.2ft	0.01	31.9	60.4	7.39	23.9	4.9	0.71	4.81	4.27	2.81	0.74	2.7	0.88	0.42
Ore Zone	LLS-02c-60.0ft	0.01	23.3	39.7	5.63	18.2	4.1	0.65	3.91	4.12	3.01	0.67	3.1	0.89	0.5
Ore Zone	LLS-02c-84.0ft	0.01	24.2	42.5	5.02	14.1	3	0.2	2.46	2.11	1.3	0.35	1.3	0.45	0.22
Ore Zone	GVS-S8-182.0ft	<0.01	51.4	98.9	11.1	33.2	6.6	0.77	5.64	4.66	2.93	0.89	2.8	0.94	0.5
Ore Zone	LLS-03c-85.0ft	0.01	17.9	41	4.36	12.2	3.1	0.35	2.42	1.95	1.27	0.36	1.2	0.38	0.2
Ore Zone	GVS-15c-167.9ft	<0.01	38.8	70	8.09	24.1	5.3	0.37	3.75	3.07	1.88	0.69	1.9	0.61	0.34
Limbs	GVS-S8-08-199.0ft	0.02	48.5	90.6	10.8	32.4	7.5	0.86	6.47	5.69	3.35	1.04	3.4	1.1	0.49
Limbs	GVS-S8-08-206.0ft	0.03	100	216	23.7	71	15.1	1.91	13	10.5	5.38	2.03	4.3	1.86	0.57
Limbs	LLS-03c-73.5ft	0.02	92.2	175	20.1	58.3	12	0.39	9.08	5.82	3.01	1.16	2.8	1.02	0.41
Limbs	LLS-03c-81.5ft	<0.01	17.7	28.1	3.45	10.2	2.1	0.17	1.9	1.65	1.06	0.26	1.1	0.31	0.18
Reduced	GVS-10c-295ft-303ft	0.03	77.8	157	16.6	48.8	10	1.54	8.65	6.76	3.43	1.2	2.6	1.2	0.48
Reduced	GVS-s10c-270-274ft	0.02	54.1	93.3	10.6	33	6.9	1.24	6.15	4.5	2.35	0.81	2.1	0.79	0.32
Reduced	GVS-8c-241-245ft	<0.01	23.7	41	5.21	15.7	3.4	0.59	3.19	2.88	1.73	0.49	1.7	0.53	0.26
Reduced	GVS-8c-255ft-259ft	<0.01	20.6	34	4.05	12.3	2.7	0.55	2.33	1.87	1.03	0.32	1	0.32	0.18

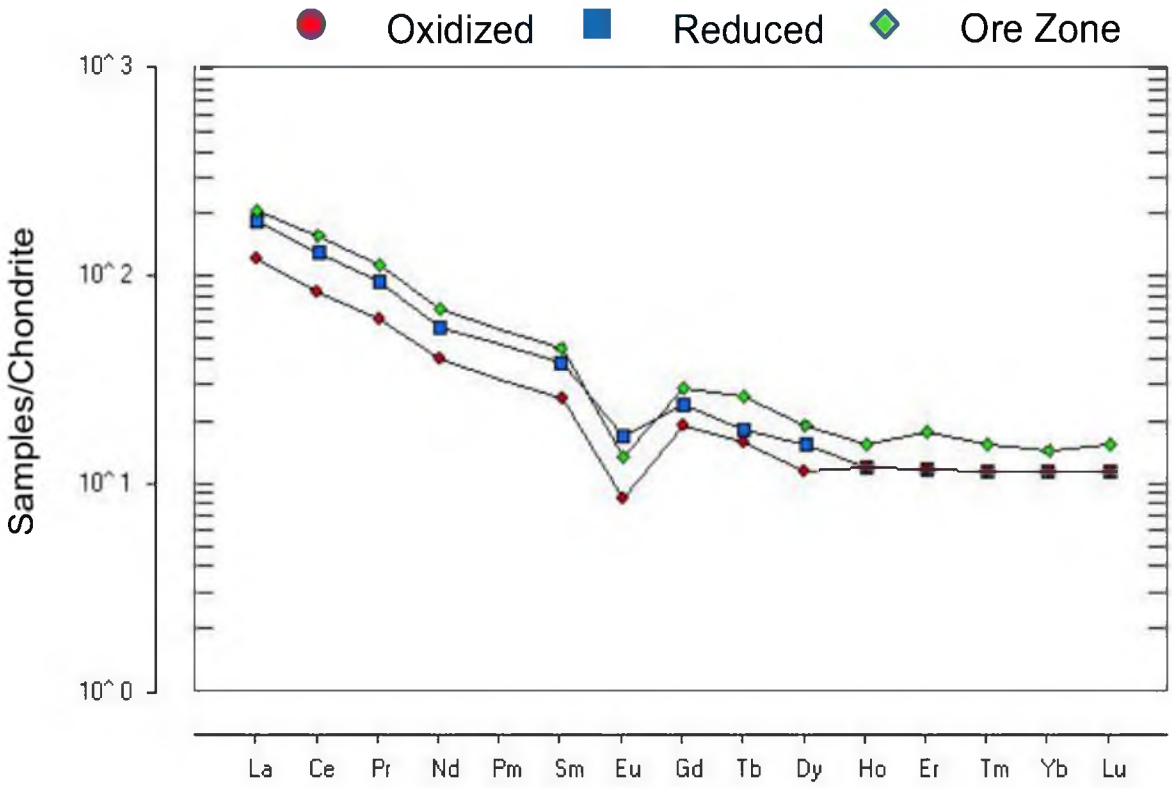

Fig. 19. Average rare earth element distribution in the ore zone, oxidized sandstone, and the reduced sandstone from the George Ver and Loco Lee deposits divided by the average chondrite value. Note the Eu anomaly as well as the separation in LREE between the oxidized and reduced sandstone.

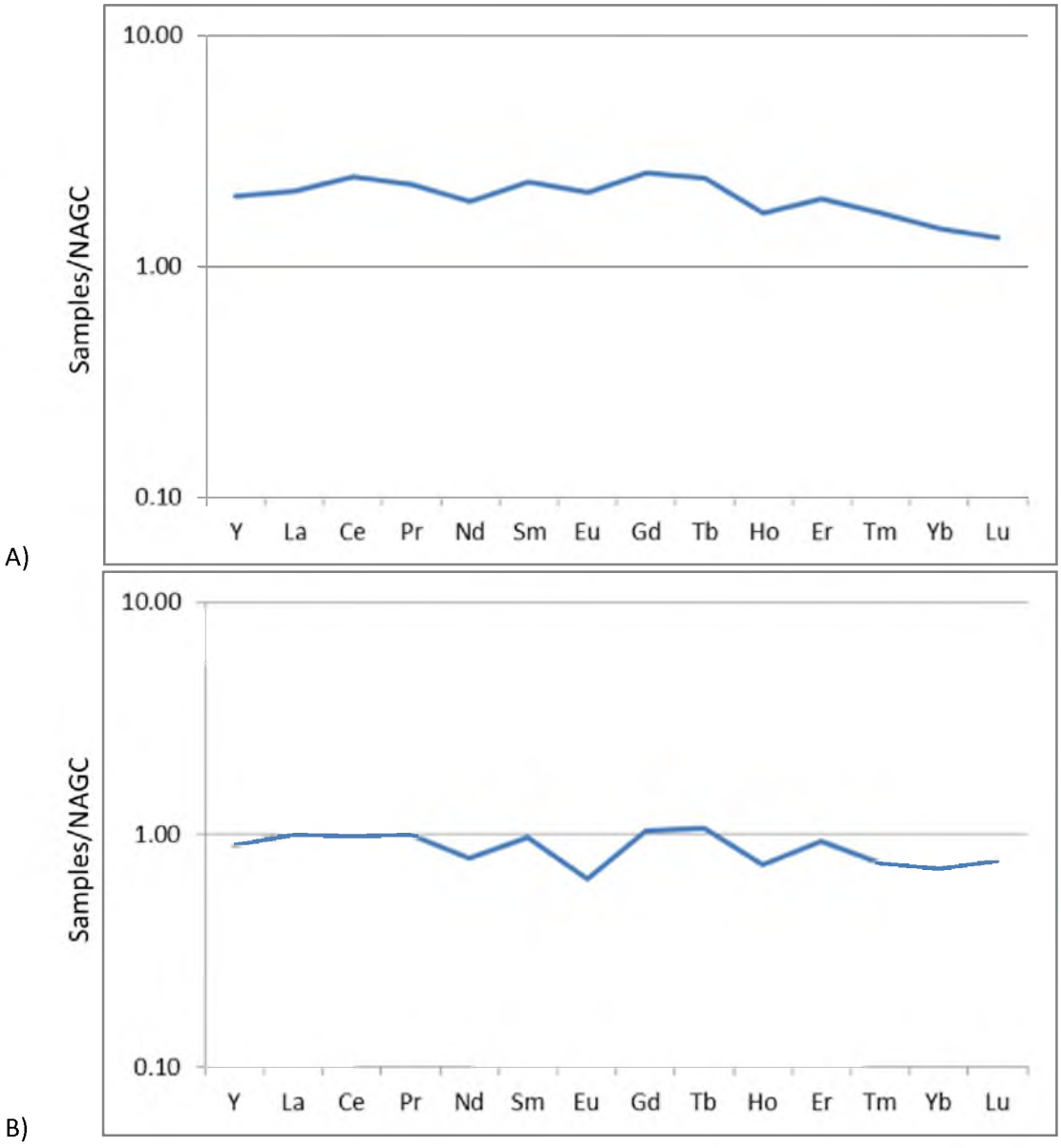

Fig. 20. Select samples normalized to the North American Granite Composite. A) Ore zone sample 15C-196 normalized to the North American Granite Composite. B) Average rare earth content in the ore zone normalized to the North American Granite Composite.

CHAPTER 5

DISCUSSION

Clay Alteration in the George Ver and Loco Lee Deposits

The Gas Hills has a clay mineral assemblage that includes kaolinite, smectite, and illite. This is a result of diagenetic processes as well as from alteration of the sandstone during low temperature argillic alteration accompanying mineralization.

The unaltered reduced rock has a clay composition of 5% kaolinite with a disseminated habit, 6% smectite that is clumpy and disseminated, and 4% illite that is clot like. The porosity prior to alteration is 5% and uranium content in the reduced sandstone is approximately 30 ppm (Fig. 21).

Later in time (Fig. 21b), the amount of kaolinite increases, on average, to 11%. This increase is due to alteration of feldspars. Smectite increases to 7% and illite increases from 4% to 6%. Porosity increases to 8%. The uranium content increases from 30 ppm to 300 ppm as uranium is changing oxidation state from 6^+ to 4^+, dropping out of solution and concentrating at the reducing interface. This is when the majority of uranium mineralization takes place. The mineralized zone migrates down dip as pulses of oxidized groundwater alter the orebody and re-deposited uranium down-dip. A continuous supply of uranium and associated elements in the mineralizing solution

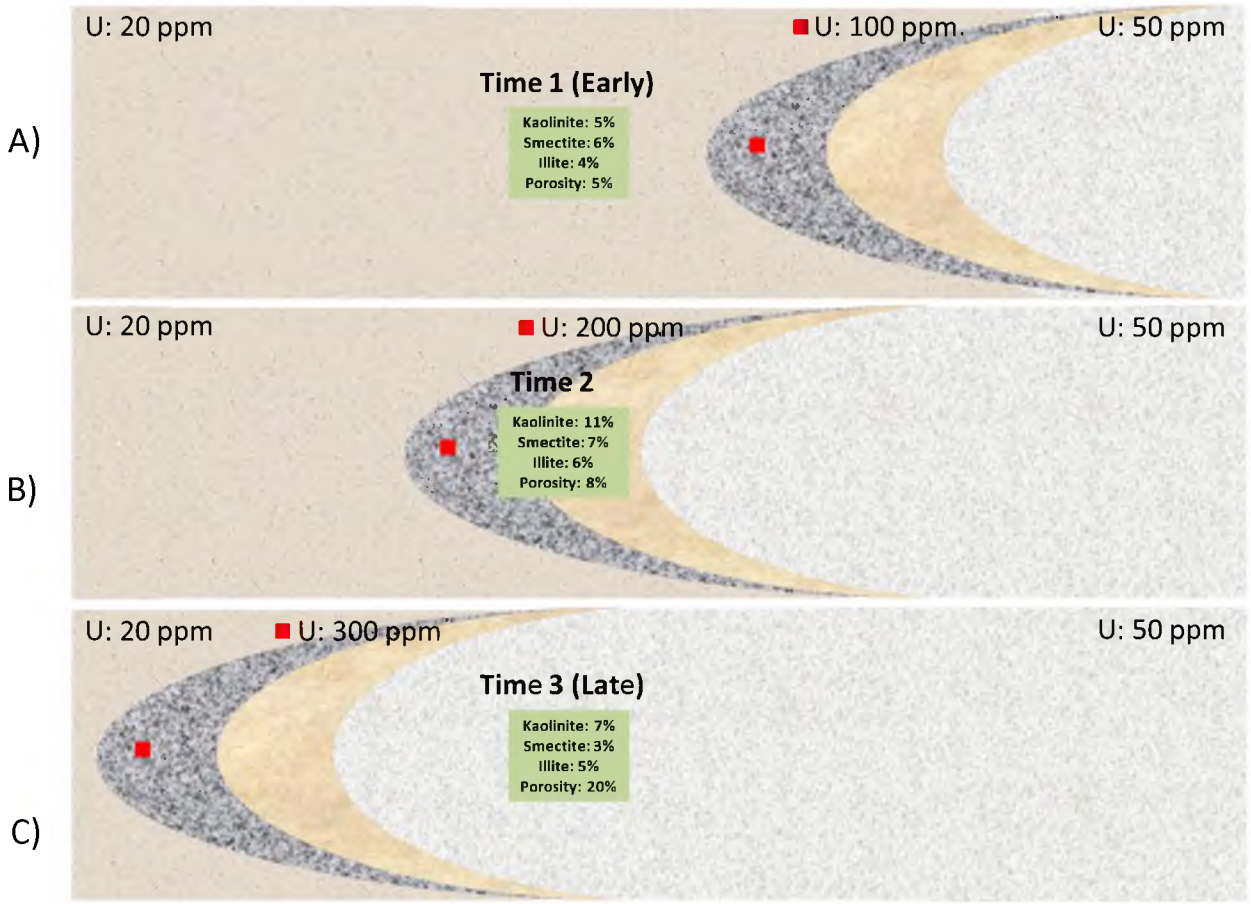

Fig. 21. The green box represents a rock volume through time as the uranium roll-front progresses. Over time, the porosity increases by 300% through dissolution of mineral grains. The clay content is highest during mineralization. As the roll-front progresses, the U is high-graded at the roll-front in the redox interface.

passing through this interface increases the grade and size of the deposit. The extent of mineralization is governed by the supply of oxygen and uranium, the amount of pyrite and organic material, and the rate of flow of the groundwater.

Late in the alteration cycle, the kaolinite decreases from 11% to 7%, the smectite decreases from 6% to 3% as it is destroyed, and the illite stays about the same with a slight gain to 5%. The porosity increases significantly to 20%. This is due to the destruction of the clay minerals. The uranium content at this point has decreased to approximately 50 ppm (likely the irreducible level) as the roll-front continues progressing into the reduced sandstone. Uranium is constantly changing oxidation state and going back into solution as oxidized fluid continues to flow through.

The clay content is not all originally diagenetic. Some is related to much later alteration processes from the flow of oxygen-rich fluid through the sandstone host rock. Granger and Warren (1978) postulated that 4,000 volumes of water are needed to oxidize one volume of pyrite-bearing rock in a typical ore-host rock. The oxidizing capacity of the fluid is limited by how much oxygen can be dissolved at and near the surface. It was this volume of neutral to slightly acidic fluid that generated 29% more kaolinite and 44% more illite in the orebody when compared to the amount of clay in the reduced sandstone. Smectite was reduced by up to 50% in the orebody when compared to original unaltered amounts.

The greatest abundance of smectite can be found in the reduced sandstone, followed by the oxidized sandstone; the ore body has the least amount of smectite. This suggests that the smectite was the first clay to form in the system as a result of early

diagenesis, as it is the most abundant clay in the relatively unaltered reduced sandstone. The smectite is primarily being replaced by the illite since the smectite content decreases and the illite content increases in the mineralized sandstone as a function of pH (Fig 22).

The discrete clot habit associated with the clays in the oxidized sandstone is likely due to the destruction of feldspar and mica. As fluid flows through the system, individual grains of feldspar are replaced by kaolinite (pH around 6). The disseminated habit of the kaolinite associated with the reduced sandstone is typical of earlier, diagenetic kaolinite.

The increase in kaolinite content in the oxidized sandstone represents the dissolution of feldspar grains due to acid hydrolosis. Because the oxidized sandstone kaolinite is more clot-like than the reduced sandstone clay, this suggests an increase in the destruction of feldspar and increased clay content in the altered sandstone.

Shallow groundwater likely becomes acidic due to interaction with the organic material and pyrite in the Wind River Formation, both of which are found in abundance and identified in this study. Feldspar is replaced by kaolinite, and smectite replaces volcanic ash.

Smectite is less abundant in the oxidized sandstone when compared to the reduced sandstone; therefore, it is being destroyed or replaced as the ore fluid is altering the sandstone. The source of the smectite is from the original alteration of volcanic ash as well as formation during early diagenesis. It is possible that the semctite is converted to kaolinite, which would explain the increase of kaolinite in the oxidized

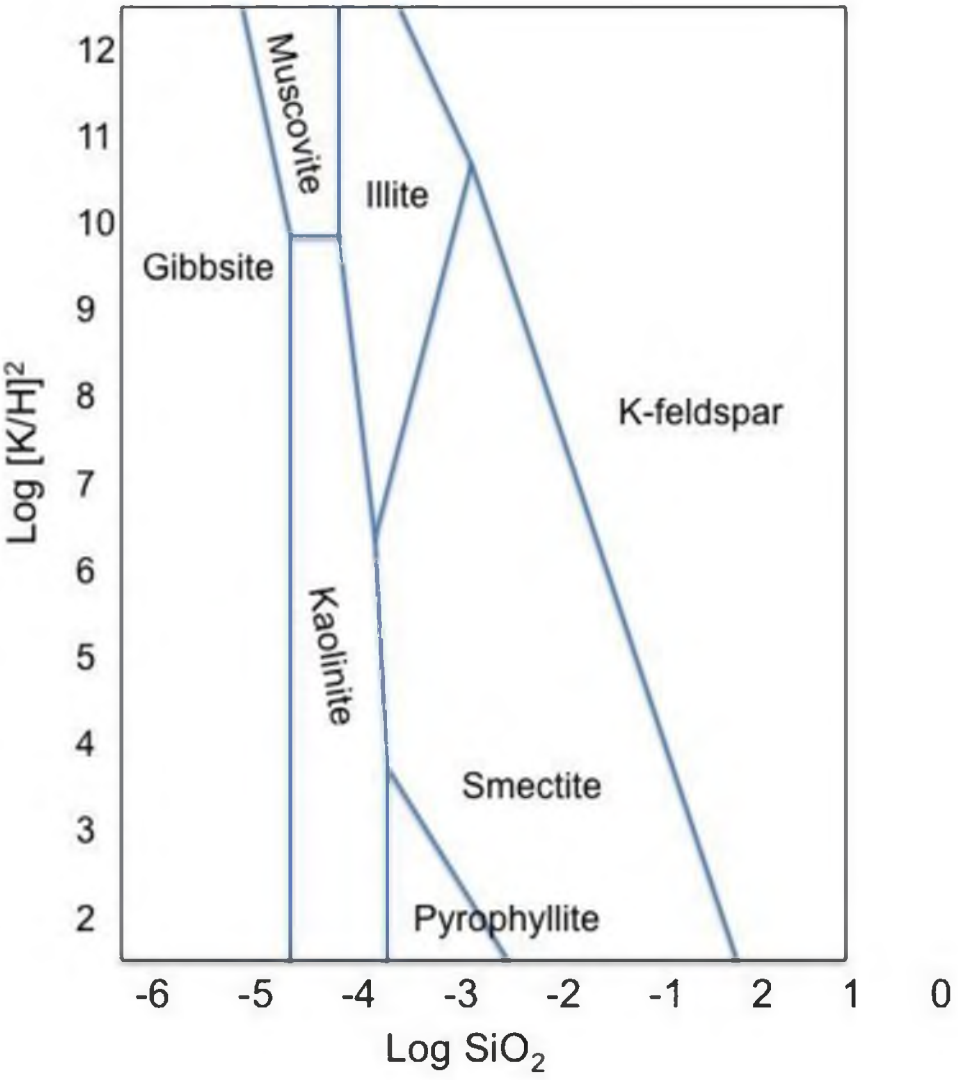

Fig. 22. Theoretical plot of ion activites showing stabilities of phases using idealized compositions (after Garrels, 1984).

sandstone and the decrease in the amount of smectite as observed by Amouric and Olives (2000).

Alteration and Porosity

The more altered the rock, meaning an increase in kaolinite and illite, the greater the porosity. Formation of kaolinite and illite indicate that secondary porosity has been created. Acid created by the alteration of organic material and pyrite likely increased porosity and permeability in the upstream, oxidized portions of the roll-front deposit by progressively removing calcite.

Petroleum compounds are strong reductants for uranium. Experimental oil-sandstone-water reactions in hydrocarbon reservoirs (Shebl and Surdam, 1996) shows that crude oil can reduce oxidized mineral phases. For example, Fe-oxide reduction to pyrite by hydrocarbons causes oxidation of the hydrocarbons and releases $C0_2$ and organic acids. These organic acids dissolved silicate minerals (quartz and feldspar) and cements in sandstone. The original porosity of the sandstone was increased by 10% to 20% (Fig. 23).

Several large oil and gas deposits occur in the Gas Hills District and gas accumulations have been produced from the Wind River formation in the basin. This is the likely source of the organic acids that enhanced sandstone porosity and facilitated migration of the ore bearing fluids and deposition of uranium minerals. When the individual clay areas are plotted against porosity for the oxidized sandstone, reduced sandstone, and ore zone, several trends can be identified (Fig. 24).

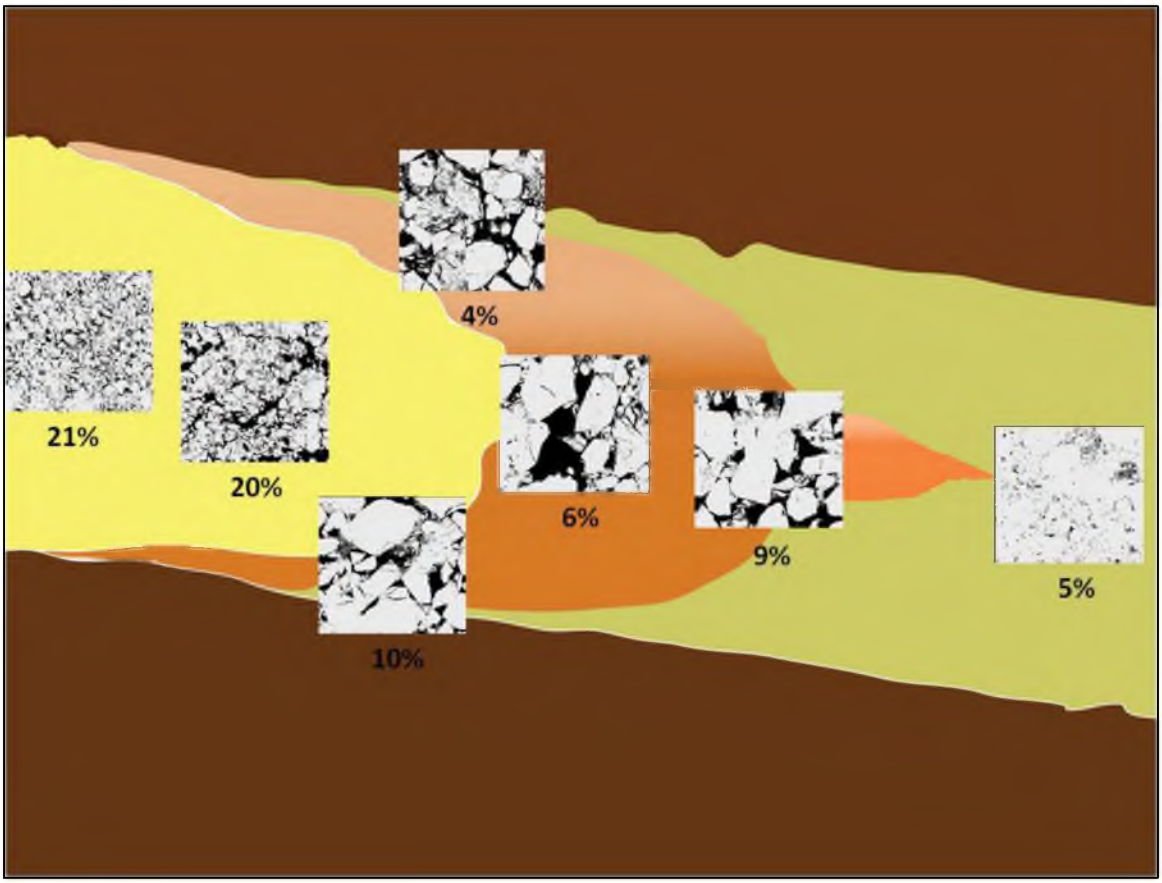

Fig. 23. Net porosity consistently increases as the sandstone becomes more oxidized.

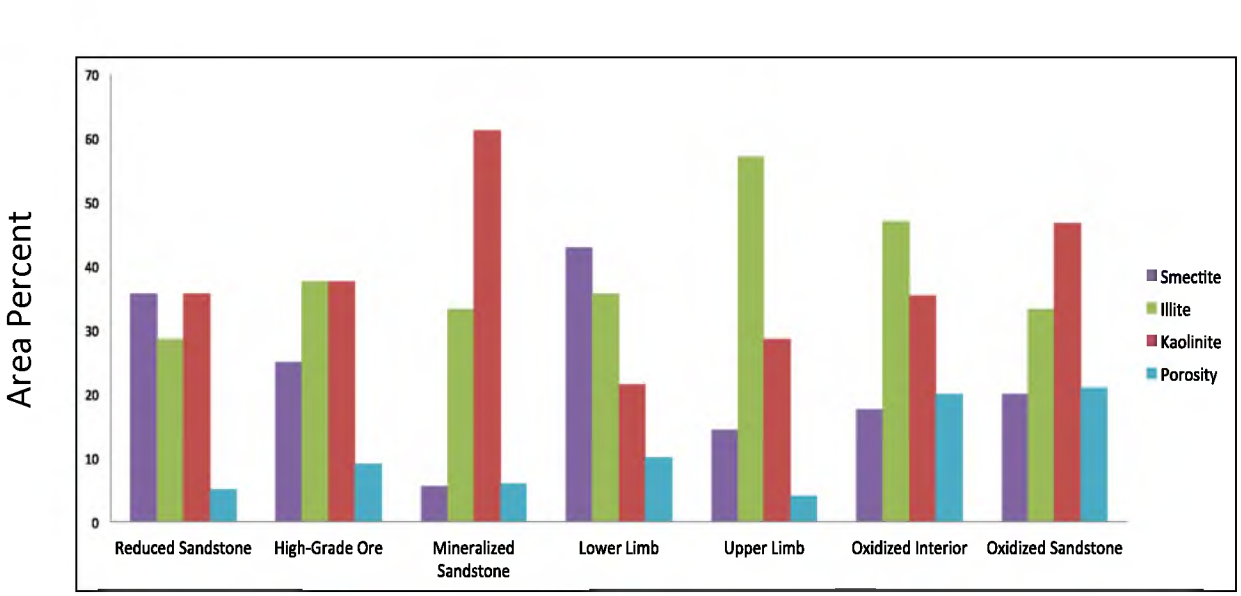

Fig. 24. Clay type and abundance across a uranium roll-front system in the Geroge Ver and Loco Lee deposits of the Gas Hills.

When illite concentration is at its highest, porosity values are highest. This suggests that illite has very little impact on pore occlusion in this deposit. When kaolinite concentration is highest, the porosity values are lowest, suggesting that the authigenic kaolinite is pore occluding and plays a big role in the large decrease in porosity. Smectite has relatively constant values in the oxidized sandstone, reduced sandstone, and the ore zone and has little bearing on the overall porosity of the system. If anything, destruction of smectite in the oxidized sandstone has helped increase the porosity.

Porosity is also at its highest when quartz abundance is at its lowest and K-feldspar is relatively high (Fig. 25). Where porosity is at its lowest, overall clay content, feldspar, pyrite, and quartz are at their highest concentrations. K-feldspar seems to be at its lowest abundance when porosity is at its lowest.

Harshman (1962) proposed that uranium was transported by weakly acidic, moderately oxidizing ground water. Subsequently, Harshman (1966) concluded that the alteration accompanying the deposits was caused by neutral to somewhat alkaline, oxidizing groundwater. Melin (1969) proposed that in Shirley Basin, the ore fluid was acid (pH around 5), depleted of oxygen, and charged with H_2S and CO_2. The source of the acidity and H_2S was sour gas from a ruptured petroleum reservoir. Mineral deposition from the acidic solution was caused by an increase in pH at the edge of the altered tongue. Investigators propose slightly alkaline oxidizing ground water as the mineralizing solution (Files, 1970; Harshman, 1974). The findings of this study are in agreement with Harshman (1962) that the fluid must have become weakly acidic in

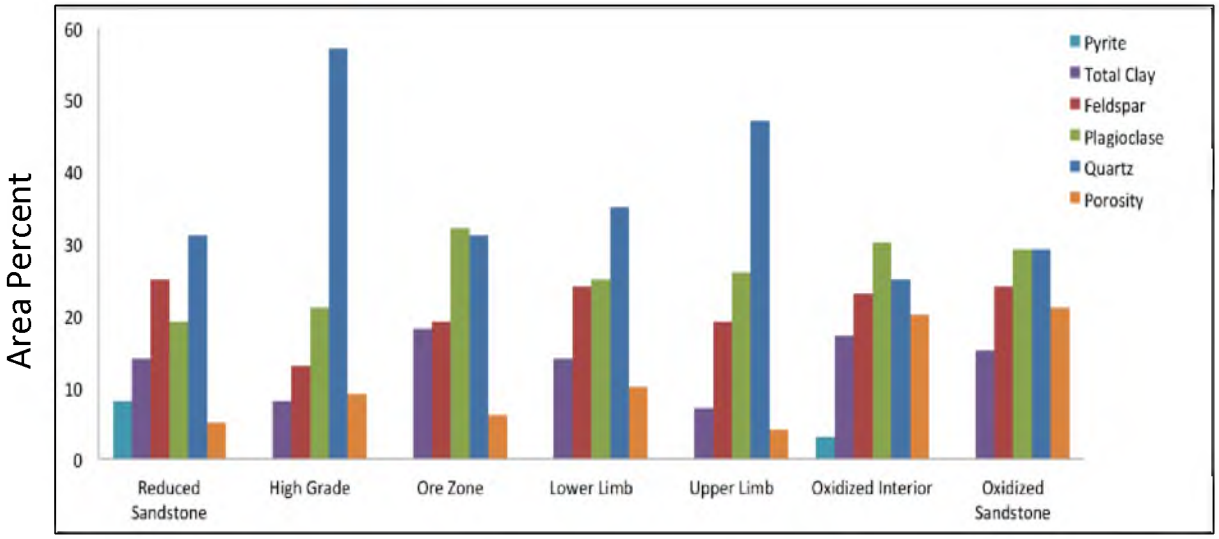

Fig. 25. Average primary mineral abundance and porosity in each main section of the uranium roll front deposit.

moderately oxidizing groundwater at the time of roll-front development.

The Use of ASD (VNIR) for Rapid Clay Detection

The VNIR spectrometer, or ASD spectrometer, is a good tool for rapid clay detection. While more work, preferably from different deposits within the district, would enhance validation, we can conclude that the ASD tool identifies most of the clay minerals shown using X-ray diffraction clay separates and QEMSCAN analysis.

Complications of interpretation arise when multiple clay types are present in a sample. These difficulties impede the interpretation of the recorded spectra, where mineral identification is based on a comparison to reference spectra using features such as the wavelength positions, the intensity and shape of absorption troughs, and the overall shape of the entire spectrum. The VNIR spectrometer, when calibrated according to the mineral assemblages that exist in the Gas Hills, proved to be a useful tool to identify clay minerals.

The spectrometer can give valuable information as to the slight variations in mineral color. An untrained geologist can use this information to determine whether the rock is reduced or oxidized. It was found that on average, the oxidized sandstone is more reflective than the reduced sandstone. The more oxidized sandstones indicate more red tones with peaks in the 570-650 nm range while the less reflective reduced sandstones indicate more green tones with peaks generally in the 510-570 nm range. The mineralized sandstone including the limbs can be a mixture of red and green tones or can take on a green or red tone.

Without proper calibration, the ASD is not likely to be very useful. It is important to calibrate the ASD to samples with known compositions of clay minerals. This will make identifying the often-indistinct peaks and troughs much easier. The ASD is the ideal tool for identification in the field. It is portable and easy to use. Hundreds of samples can be tested at the rate of 2 seconds per sample. In the lab, X-ray diffraction clay separates and QEMSCAN analysis will likely give the most accurate results when unraveling the clay mineralogy. These results can help guide the interpretation of the ASD analysis. Using ASD is ineffective unless upstream and downstream sandstone samples have already been analyzed using XRD or QEMSCAN; otherwise, it can be challenging to interpret the clay compositions when multiple clays are present. Data processing, as shown below, can be used to make better interpretations that might not be obvious from the initial spectra.

In particular, it was very difficult to determine if there was kaolinite present in the samples. There tends to be a dominant clay signature in each sample, but based on the XRD analysis, it is known that kaolinite is present in the clay separates. To identify the kaolinite peaks that are at 1393 and 1410, the derivative of the spectra was calculated and plotted (Fig. 26). When the derivative is plotted, it can be seen that the slope of the curves is plotted for the kaolinite peaks as they change from a positive slope to a negative slope.

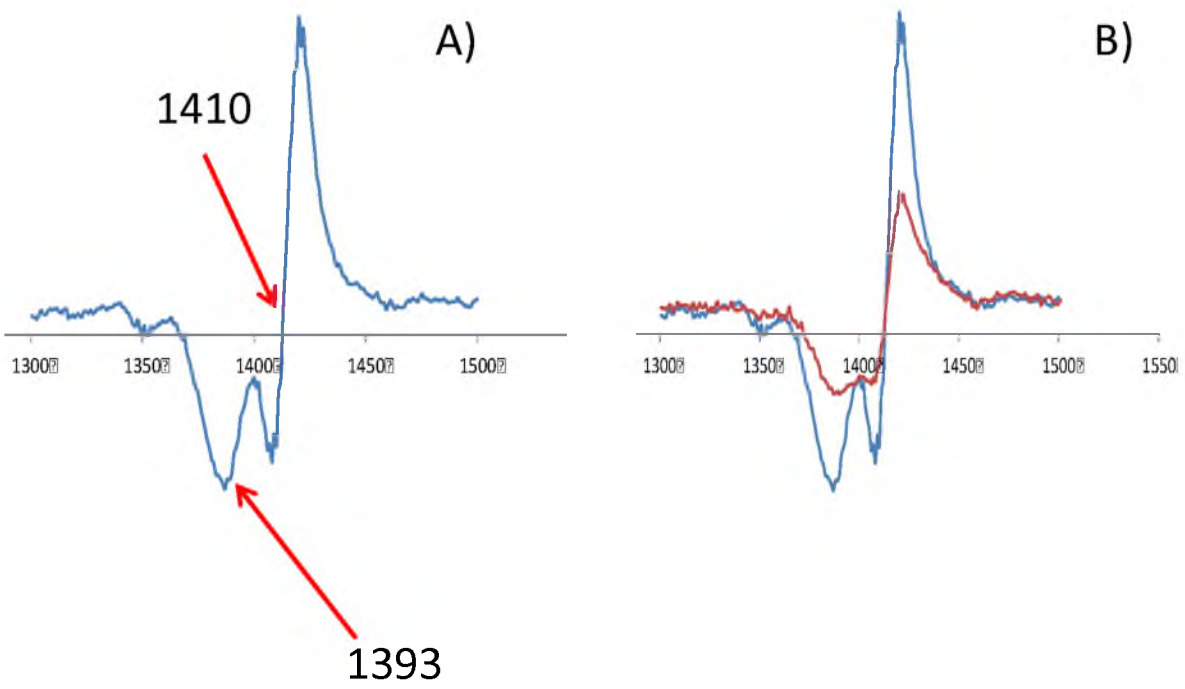

Fig. 26. Taking the derivative of the spectra (blue line) allows for the slopes of the kaolinite troughs at 1393 and 1410 to be seen, proving that, while the troughs can be hard to find, they do exist. This is a comparison of the mineralized ASD spectra (A) which has the most kaolinite to the reduced spectra (B) in red, which has the least.

Chemical Variation in the George Ver and Loco Lee Deposits

Mineralized Sandstone

Strong positive correlations exist between uranium and the elements Zn, Co, and Mg. This indicates that uranium has likely been mobilized with these elements. There is also a strong negative correlation with V, indicating that V is depleted by the same reaction that precipitates U. Uranium is soluble under oxidizing conditions while V is soluble under reducing conditions. At the time when U and V are in solution, U is precipitated at the reducing interface while V stays in solution and is precipitated further downstream. Uranium has a strong correlation with Al, which also indicates an association with clay minerals. Based on the geochemical correlations, Mg, Al, and K have strong correlations; this would indicate illite as being present in the mineralized sandstone. This correlation is not nearly as prevalent in the reduced and oxidized sandstones. The correlation of Al and K being relatively strong indicates that K-feldspar is present. QEMSCAN and XRD analysis shows that K-feldspar is present in the mineralized sandstone and illite and smectite are at the highest concentration, which confirms the geochemical results.

Oxidized Sandstone

In the oxidized sandstone, uranium correlates most strongly with As, Fe, and Co, indicating that after oxidation, U is most stable in minerals that have these associated elements. These elements are likely contained in the clays, particularly in smectite. Aluminum has a strong correlation with Mg, suggesting the presence of smectite

(correlation coefficient of 0.80). There is much less Fe in the oxidized sandstone, primarily because it has moved out of the system in solution and been re-deposited downstream in the reduced sandstone.

Reduced Sandstone

There are strong positive correlations between U, Mo, and Tl in the reduced sandstone. This could indicate that U is associated with these elements prior to alteration, but could also indicate that Mo and U are mobile in hydroxyl complexes and precipitate under similar reducing conditions. U and Mo become immobilized when sulfides appear in the reducing environment. Based on the correlation results, Al has a much weaker correlation with Mg (correlation coefficient of 0.70), which indicates smectite might not be as prevalent.

Rare Earth Element Geochemistry

Rare earth element concentration is highest in the ore zone. There is not a significant concentration of other rare earth bearing minerals, such as monazite, so the likely minerals containing the rare earth elements are the feldspars. Based on a correlation analysis, the heavy and the light rare earth elements correlate strongly with Al, with a Pearson correlation coefficient of 0.85 (Fig. 27). Al is primarily found in feldspar, so this is the mineral in which the REE are contained. The LREE are more susceptible to alteration due to the concentration difference found in the reduced, oxidized, and mineralized sandstones.

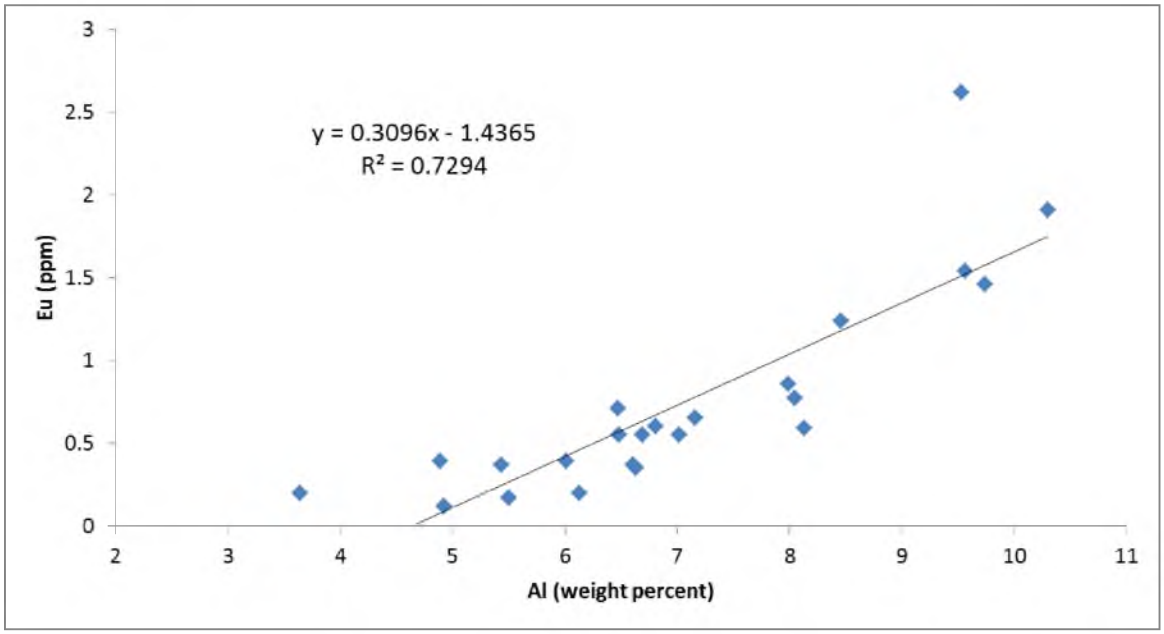

Fig. 27. Eu correlation with Al. This strong correlation (R^2 of 0.73) suggests that the REE are associated with feldspar. All REE behave this way.

When comparing the oxidized sandstone (normalized to the chondrite composite) to the ore zone, the ore zone has three times the amount of rare earth elements compared to the oxidized samples. When compared to the chondrite composite, the average ore zone sample is significantly more elevated (factor of 2). The REE content would be higher due to volume loss. As feldspar is altered to clay, the REE content would stay the same and be inherited.

The rare earth element assay values for the orebody in the George Ver and Loco Lee are very similar, almost identical to the values that can be found in the average North American Granite Composite (Fig. 19). This suggests that the probable source of the rare earth elements is from detritus shed from the Granitic Mountains. Individual samples from the orebody locally contain much higher amounts, as great as a factor of 4 (approximately 100 ppm vs. 450 ppm) of rare earth elements when compared to the North American Granite Composite.

CHAPTER 6

CONCLUSIONS

Three distinct clays occur in the George Ver and Loco Lee deposits that constitute argillic alteration. Kaolinite has a range of 2 to 11 percent, with overall highest concentrations in the oxidized sandstone. Smectite has a range of 1 to 6 percent with the highest concentrations in the reduced sandstone and illite has a range of 3 to 8 percent with overall highest concentration in the ore zone (Fig. 28). Much of the clay can be attributed to original diagenetic processes, although approximately 29% kaolinite and 44% illite was gained due to argillic alteration calculated from an area percent using QEMSCAN. Overall, smectite was destroyed by up to 50% during the alteration process. It is likely that much of the smectite was converted to illite during mineralization.

Porosity changes significantly across the downstream length of a deposit. From reduced sandstone through the oxidized sandstone, there is a range of 5 to 21 percent. The controls on porosity include the distribution of clays, the habit and texture of the clay, and the presence of authigenic quartz.

Three distinct habits are associated with the clays from the reduced sandstone to the oxidized sandstone. These textural changes are a result of changes in fluid

Fig. 28. Summary of the overall relationships between clay content, mineral abundance, and elemental trends. The top box is the schematic of a roll-front deposit and the second box represents the relative change in the given variable.

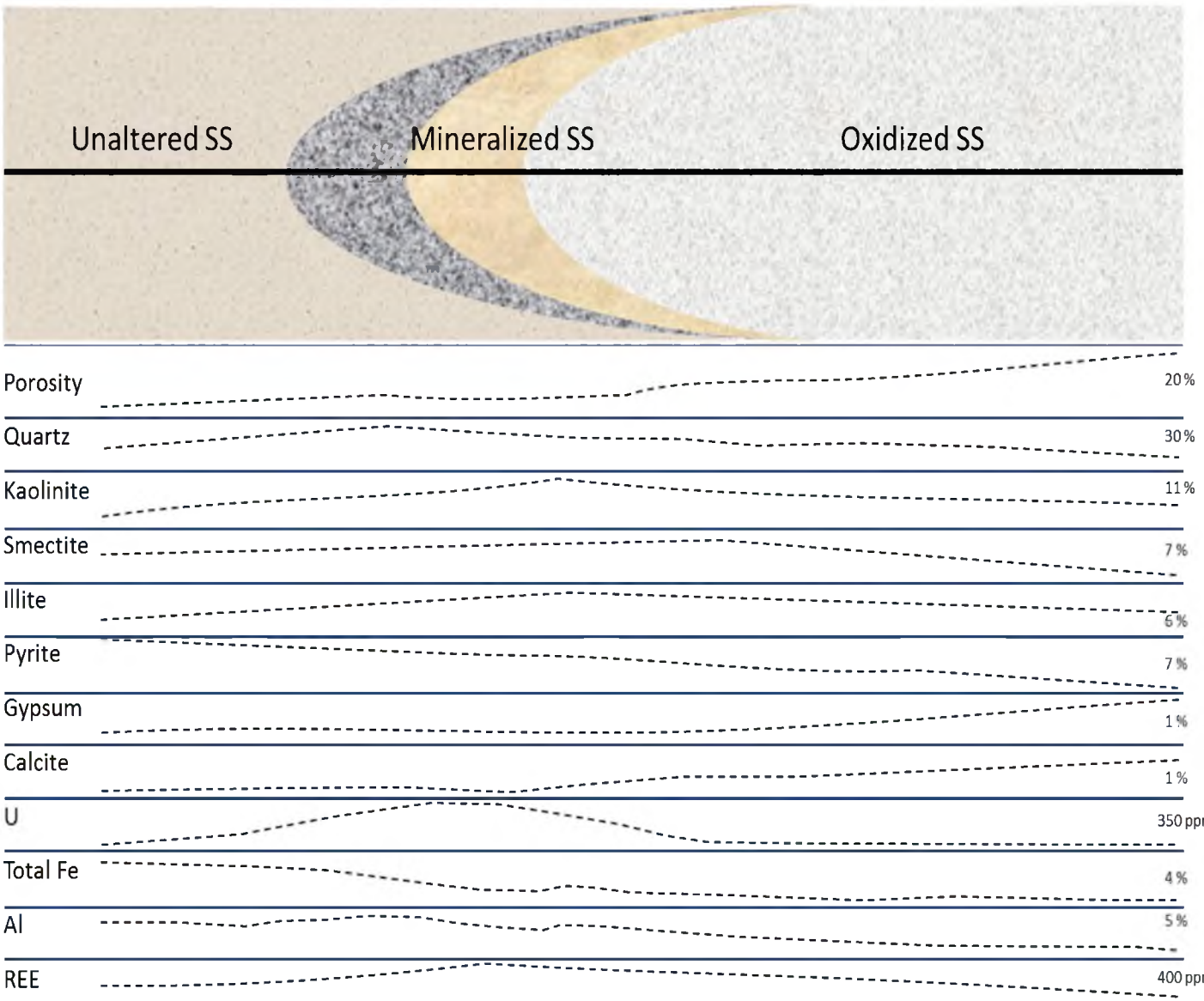
Unaltered SS
Mineralized SS
Oxidized SS
Porosity
20 %
Quartz
30 %
Kaolinite
11 %
Smectite
7 %
Illite
6 %
Pyrite
7 %
Gypsum
1 %
Calcite
1 %
U
350 ppm
Total Fe
4 %
Al
5 %
REE
400 ppm

composition over time. The disseminated texture is likely from original diagenetic formation, the clot-like texture was created at the onset of oxidation and near surface weathering, and the grain replacement texture is a result of alteration during mineralization.

In the mineralized sandstone, it was found that U correlates strongly with Zn, Co, Mg and has negative correlation with V. This is due to the elements precipitating under similar geochemical environments, while V precipitates further downstream. In the reduced sandstone, U correlates with Mo and Tl. In the oxidized sandstone, U has a strong correlation with As, Fe, and Co, which likely indicates that these elements are in clay minerals. Positive correlations of Al, K, and Mg exist, confirming the presence of the clays in the respective sections.

Comparing the George Ver and Loco Lee to other Wyoming uranium districts, calcite and sulfates exist in the oxidized sandstone and not in the reduced sandstone (Table 5). In contrast to other studies in the Gas Hills, V has highest concentration in the reduced sandstone, not in the orebody. Quartz is significantly increased in the orebody compared to the reduced sandstone and the oxidized sandstone.

This combination of new analytical techniques and research resulted in a better understanding of the alteration associated with roll-front uranium deposits in the Gas Hills District. The model has been updated by adding a quantitative abundance and distribution of primary minerals, as well as defining the individual clays that make up each zone of the system and determining which were formed due to diagenesis and which were results of argillic alteration. There is now a first order approximation for

porosity as well as a better understanding of the controls on porosity. Rare earth elements increase in the ore zone and are associated with feldspar. Targeting Zn, Co, and Tl could lead to U when exploring new areas near these orebodies.

ASD spectroscopy was found to be an efficient tool for identifying clay minerals. The data accumulated from the ASD can be used effectively with the data produced from the X-ray diffraction and QEMSCAN analysis. Because the ASD can analyze samples quickly, it eliminates the need to increase the sample density using the more expensive X-ray diffraction or QEMSCAN. Our ASD spectra agree with the clay minerals identified with X-ray diffraction, petrographic, and QEMSCAN analysis. To the untrained eye, the samples take on a very similar shade of color. The spectrometer indicated that the oxidized sample was redder while the reduced sample was less reflective and greener.

APPENDIX

Table 9. Georege Ver borehole S8 samples and tests

Borehole	Sample	Depth (ft)	Thin Section	ASD	XRD	Whole-Rock	QEMSCAN	Description
GVS-S8-08	GVS-8c151ft-155ftoxi	151-155	X	X		X		Up Stream Oxidized
GVS-S8-08	GVS-8c170ft-174ftoxi	170-174	X	X	X	X	X	Up Stream Oxidized
GVS-S8-08	GVS-S8-08-00004	174.2		X				Mineralized Zone
GVS-S8-08	GVS-S8-08-174.5ft	174.5	X	X				Mineralized Zone
GVS-S8-08	GVS-S8-08-00007	176		X				Mineralized Zone
GVS-S8-08	GVS-S8-08-00000	177.2		X				Mineralized Zone
GVS-S8-08	GVS-S8-08-00003	178.5		X				Heart
GVS-S8-08	GVS-S8-08-00008	179.2		X				Heart
GVS-S8-08	GVS-S8-08-00011	180.8		X				Heart
GVS-S8-08	GVS-S8-08-00012	181.4		X				Heart
GVS-S8-08	GVS-S8-08-182.0ft	182	X	X		X		Heart
GVS-S8-08	GVS-S8-08-00015	182.8		X				Heart
GVS-S8-08	GVS-S8-08-00016	183.4		X				Heart
GVS-S8-08	GVS-S8-08-00019	184.8		X				Mineralized Zone
GVS-S8-08	GVS-S8-08-00020	185.2		X				Mineralized Zone
GVS-S8-08	GVS-S8-08-185.5ft	185.5	X	X				Mineralized Zone

Table 9 cont. Georege Ver borehole S8 samples and tests

Borehole	Sample	Depth (ft)	Thin Section	ASD	XRD	Whole-Rock	QEMSCAN	Description
GVS-S8-08	GVS-S8-08-00023	186.8		X				Mineralized Zone
GVS-S8-08	GVS-S8-08-00024	187.4		X				Mineralized Zone
GVS-S8-08	GVS-S8-08-00027	188.8		X				Mineralized Zone
GVS-S8-08	GVS-S8-08-00028	189.4		X				Mineralized Zone
GVS-S8-08	GVS-S8-08-00031	190.8		X				Mineralized Zone
GVS-S8-08	GVS-S8-08-00032	191.2		X				Mineralized Zone
GVS-S8-08	GVS-S8-08-00035	192.8		X				Mineralized Zone
GVS-S8-08	GVS-S8-08-00036	193.4		X				Mineralized Zone
GVS-S8-08	GVS-S8-08-195.0ft	195	X	X				Mineralized Zone
GVS-S8-08	GVS-S8-08-00040	196		X				Upper Limb
GVS-S8-08	GVS-S8-08-00043	197.8		X				Upper Limb
GVS-S8-08	GVS-S8-08-00044	198.4		X				Upper Limb
GVS-S8-08	GVS-S8-08-199.0ft	199	X	X	X	X	X	Upper Limb
GVS-S8-08	GVS-S8-08-00047	199.6		X				Upper Limb
GVS-S8-08	GVS-S8-08-00048	200.6		X				Upper Limb

Table 9 cont. Georege Ver borehole S8 samples and tests

Borehole	Sample	Depth (ft)	Thin Section	ASD	XRD	Whole-Rock	QEMSCAN	Description
GVS-S8-08	GVS-S8-08-00051	201.8		X				Interior
GVS-S8-08	GVS-S8-08-202.0ft	202	X	X	X	X	X	Interior
GVS-S8-08	GVS-S8-08-206.0ft	206	X	X	X	X	X	Lower Limb
GVS-S8-08	GVS-S8-08-00052	206.6		X				Lower Limb
GVS-S8-08	GVS-S8-08-00055	207.8		X				Lower Limb
GVS-S8-08	GVS-S8-08-208.5ft	208.5	X	X				Lower Limb
GVS-S8-08	GVS-S8-08-00056	208.8		X				Mineralized Zone
GVS-S8-08	GVS-S8-08-00059	209.8		X				Mineralized Zone
GVS-S8-08	GVS-S8-08-00060	210.8		X				Mineralized Zone
GVS-S8-08	GVS-S8-08-00063	211.8		X				Mineralized Zone
GVS-S8-08	GVS-S8-08-212.0ft	212	X	X				Mineralized Zone
GVS-S8-08	GVS-8c-241ft-245ftredu	241-245	X	X		X		Down Stream Reduced
GVS-S8-08	GVS-8c-255ft-259ftredu	255-259	X	X	X	X	X	Down Stream Reduced

Table 10. Georege Ver borehole S10 samples and tests

Borehole	Sample	Depth (ft)	Thin Section	ASD	XRD	Whole-Rock	QEMSCAN	Description
GVS-S10-08	GVS-10c-192ft-196ftoxi	192-196	X	X		X		Upstream oxidized
GVS-S10-08	GVS-10c-211ft-216ftoxi	211-216	X	X	X	X	X	Upstream oxidized
GVS-S10-08	GVS-S10-08-00002	218		X				Unknown
GVS-S10-08	GVS-S10-08-00003	219		X				Unknown
GVS-S10-08	GVS-S10-08-00004	220		X				Unknown
GVS-S10-08	GVS-S10c-08-220.6ft	220.6	X	X				Unknown
GVS-S10-08	GVS-S10-08-00005	221		X				Unknown
GVS-S10-08	GVS-S10-08-00006	222		X				Unknown
GVS-S10-08	GVS-S10-08-00007	226.8		X				Unknown
GVS-S10-08	GVS-S10-08-00008	227.8		X				Unknown
GVS-S10-08	GVS-S10-08-00009	228.5		X				Unknown
GVS-S10-08	GVS-S10-08-00010	229.7		X				Unknown
GVS-S10-08	GVS-S10-08-00011	231.2		X				Unknown
GVS-S10-08	GVS-S10c-08-232.0ft	232	X	X		X		Seep
GVS-S10-08	GVS-S10-08-00013	232.8		X				Seep
GVS-S10-08	GVS-S10-08-00014	233.6		X				Seep
GVS-S10-08	GVS-S10c-08-234.2ft	234.2	X	X	X	X	X	Seep
GVS-S10-08	GVS-S10-08-00015	234.6		X				Seep
GVS-S10-08	GVS-S10-08-00016	235.4		X				Seep
GVS-S10-08	GVS-S10-08-00017	236.8		X				Seep
GVS-S10-08	GVS-S10-08-00018	237.4		X				Unknown
GVS-S10-08	GVS-S10-08-00019	238.5		X				Unknown

Table 10 cont. Georege Ver borehole S10 samples and tests

Borehole	Sample	Depth (ft)	Thin Section	ASD	XRD	Whole-Rock	QEMSCAN	Description
GVS-S10-08	GVS-S10-08-00020	240		X				Unknown
GVS-S10-08	GVS-S10-08-00021	241		X				Unknown
GVS-S10-08	GVS-S10-08-00022	242.2		X				Unknown
GVS-S10-08	GVS-S10-08-00023	243.6		X				Unknown
GVS-S10-08	GVS-S10-08-00024	244.4		X				Unknown
GVS-S10-08	GVS-S10c-08-244.5ft	244.5	X	X				Unknown
GVS-S10-08	GVS-S10-08-00025	245.8		X				Unknown
GVS-S10-08	GVS-S10-08-00026	246.4		X				Unknown
GVS-S10-08	GVS-S10-08-00027	247.6		X				Unknown
GVS-S10-08	GVS-S10c-08-248.0ft	248	X	X				Unknown
GVS-S10-08	GVS-S10-08-00028	248.4		X				Unknown
GVS-S10-08	GVS-S10-08-00029	250.8		X				Unknown
GVS-S10-08	GVS-S10-08-00030	251.6		X				Unknown
GVS-S10-08	GVS-S10-08-00031	252		X				Unknown
GVS-S10-08	GVS-S10-08-00032	252.8		X				Unknown
GVS-S10-08	GVS-S10-08-00033	253.8		X				Unknown
GVS-S10-08	GVS-S10-08-00034	255		X				Unknown
GVS-S10-08	GVS-S10-08-00035	257.6		X				Unknown
GVS-S10-08	GVS-S10c-08-258.0ft	258	X	X				Unknown
GVS-S10-08	GVS-S10-08-00036	258.2		X				Unknown
GVS-S10-08	GVS-S10-08-00037	258.8		X				Unknown
GVS-S10-08	GVS-10c-270ft-274ftredu	270-274	X	X		X		Down Stream Reduced
GVS-S10-08	GVS-10c-295ft-303ftredu	295-303	X	X	X	X	X	Down Stream Reduced

Table 11. Georege Ver borehole 15C samples and tests

Borehole	Sample	Depth (ft)	Thin Section	ASD	XRD	Whole-Rock	QEMSCAN	Description
GVS-15c	GVS-15c-162.0ft	162	X	X				Mineralized Zone
GVS-15c	GVS-15c-00002	167.5		X				Heart
GVS-15c	GVS-15c-167.9ft	167.9	X	X	X	X	X	Heart
GVS-15c	GVS-15c-00003	168		X				Heart
GVS-15c	GVS-15c-168.2ft	168.2	X	X				Heart
GVS-15c	GVS-15c-00004	168.7		X				Heart
GVS-15c	GVS-15c-00005	169.5		X				Heart
GVS-15c	GVS-15c-00006	171.2		X				Heart
GVS-15c	GVS-15c-00007	172		X				Heart
GVS-15c	GVS-15c-00008	172.6		X				Heart
GVS-15c	GVS-15c-00009	190.8		X				Seep
GVS-15c	GVS-15c-00010	191.5		X				Seep
GVS-15c	GVS-15c-00011	192		X				Mineralized Zone
GVS-15c	GVS-15c-192.7ft	192.7	X	X				Mineralized Zone
GVS-15c	GVS-15c-00012	192.8		X				Mineralized Zone
GVS-15c	GVS-15c-00013	193.4		X				Mineralized Zone
GVS-15c	GVS-15c-00014	194.8		X				Mineralized Zone
GVS-15c	GVS-15c-00015	195.4		X				Mineralized Zone
GVS-15c	GVS-15c-196.0ft	196	X	X	X	X	X	Mineralized Zone
GVS-15c	GVS-15c-00017	196.7		X				Mineralized Zone
GVS-15c	GVS-15c-00018	197.8		X				Mineralized Zone

Table 12. Loco Lee borehole 2C samples and test

Borehole	Sample	Depth (ft)	Thin Section	ASD	XRD	Whole-Rock	QEMSCAN	Description
LLS-02c	LLS-02c-00000	53		X				Mineralized Zone
LLS-02c	LLS-02c-00003	57		X				Mineralized Zone
LLS-02c	LLS-02c-60.0ft	60	X	X		X		Mineralized Zone
LLS-02c	LLS-02c-00007	60.4		X				Mineralized Zone
LLS-02c	LLS-02c-00004	62.8		X				Mineralized Zone
LLS-02c	LLS-02c-00011	64.2		X				Mineralized Zone
LLS-02c	LLS-02c-00008	65		X				Mineralized Zone
LLS-02c	LLS-02c-00015	66		X				Heart
LLS-02c	LLS-02c-00012	67		X				Heart
LLS-02c	LLS-02c-00019	68		X				Heart
LLS-02c	LLS-02c-00016	69		X				Heart
LLS-02c	LLS-02c-00023	70		X				Heart
LLS-02c	LLS-02c-00020	71		X				Heart
LLS-02c	LLS-02c-00027	72		X				Heart
LLS-02c	LLS-02c-00024	73.5		X				Heart
LLS-02c	LLS-02c-77.2ft	77.2	X	X	X	X	X	Heart
LLS-02c	LLS-02c-00031	77.8		X				Heart
LLS-02c	LLS-02c-00028	78.8		X				Heart
LLS-02c	LLS-02c-00035	79.8		X				Heart
LLS-02c	LLS-02c-00032	80.2		X				Heart
LLS-02c	LLS-02c-00039	82		X				Heart
LLS-02c	LLS-02c-00036	83		X				Heart
LLS-02c	LLS-02c-00043	83.8		X				Heart
LLS-02c	LLS-02c-84.0ft	84	X	X		X		Heart
LLS-02c	LLS-02c-00040	84.2		X				Heart

Table 13. Loco Lee borehole 3C samples and tests

Borehole	Sample	Depth (ft)	Thin Section	ASD	XRD	Whole-Rock	QEMSCAN	Description
LLS-03c	LLS-03c-60.2ft	60.2	X	X		X		Mineralized Zone
LLS-03c	LLS-03c-00003	61.2		X				Mineralized Zone
LLS-03c	LLS-03c-00004	62		X				Mineralized Zone
LLS-03c	LLS-03c-00007	63		X				Mineralized Zone
LLS-03c	LLS-03c-00008	64		X				Mineralized Zone
LLS-03c	LLS-03c-00011	65		X				Mineralized Zone
LLS-03c	LLS-03c-00012	65.8		X				Mineralized Zone
LLS-03c	LLS-03c-00015	66		X				Mineralized Zone
LLS-03c	LLS-03c-00016	67		X				Upper Limb
LLS-03c	LLS-03c-67.5ft	67.5	X	X				Upper Limb
LLS-03c	LLS-03c-00019	68		X				Upper Limb
LLS-03c	LLS-03c-00020	68.8		X				Upper Limb
LLS-03c	LLS-03c-00023	70		X				Upper Limb
LLS-03c	LLS-03c-00024	70.8		X				Upper Limb
LLS-03c	LLS-03c-00027	72		X				Upper Limb
LLS-03c	LLS-03c-00028	73		X				Upper Limb
LLS-03c	LLS-03c-73.5ft	73.5	X	X	X	X	X	Upper Limb

Table 13 cont. Loco Lee borehole 3C samples and tests

Borehole	Sample	Depth (ft)	Thin Section	ASD	XRD	Whole-Rock	QEMSCAN	Description
LLS-03c	LLS-03c-00031	73.9		X				Upper Limb
LLS-03c	LLS-03c-00032	74.4		X				Upper Limb
LLS-03c	LLS-03c-00035	75.8		X				Lower Limb
LLS-03c	LLS-03c-00036	76.4		X				Lower Limb
LLS-03c	LLS-03c-77.0ft	77	X	X				Lower Limb
LLS-03c	LLS-03c-00039	77.8		X				Lower Limb
LLS-03c	LLS-03c-00040	78.8		X				Lower Limb
LLS-03c	LLS-03c-00043	79.2		X				Lower Limb
LLS-03c	LLS-03c-00044	79.8		X				Lower Limb
LLS-03c	LLS-03c-00047	81		X				Lower Limb
LLS-03c	LLS-03c-81.5ft	81.5	X	X	X	X	X	Lower Limb
LLS-03c	LLS-03c-00048	82		X				Lower Limb
LLS-03c	LLS-03c-00051	83		X				Mineralized Zone
LLS-03c	LLS-03c-00052	83.8		X				Mineralized Zone
LLS-03c	LLS-03c-85.0ft	85	X	X	X	X	X	Mineralized Zone
LLS-03c	LLS-03c-00056	85.9		X				Mineralized Zone
LLS-03c	LLS-03c-00059	87		X				Mineralized Zone
LLS-03c	LLS-03c-00060	88		X				Mineralized Zone
LLS-03c	LLS-03c-00063	89.2		X				Mineralized Zone
LLS-03c	LLS-03c-00065	90		X				Mineralized Zone

Table 14. Pearson Correlation for the Mineralized Sandstone in the George Ver and Loco Lee Deposits

Zn	Zn	Ti	Mg	Cs	Th	Cu	Al	Cr	Co	Zr	U	Fe	Tl	P	As	Sr	K	V	Ni	Mn	Ca	Rb	Mo
	1	0.97	0.93	0.86	0.84	0.82	0.77	0.75	0.75	0.72	-0.55	0.51	-0.38	-0.36	-0.32	0.31	-0.28	-0.24	-0.23	-0.22	-0.20	-0.10	-0.03
Al	Al	Th	Cs	Mg	Ti	Cu	Zn	Cr	As	P	Co	Mn	Zr	Ca	Sr	V	K	Rb	U	Mo	Tl	Ni	Fe
	1	0.92	0.91	0.85	0.84	0.82	0.77	0.68	-0.68	-0.66	0.55	-0.54	0.53	-0.49	0.35	-0.31	0.30	0.29	-0.22	0.10	-0.09	0.05	0.00
Cr	Cr	Cs	Zn	Ti	Mg	Cu	Al	Zr	Th	Co	P	As	Fe	Ca	Ni	Mn	Mo	Tl	K	U	Rb	V	Sr
	1	0.82	0.75	0.75	0.72	0.70	0.68	0.56	0.54	0.54	-0.54	-0.48	0.42	-0.40	0.40	-0.38	-0.28	0.25	-0.25	-0.22	-0.19	0.15	-0.02
Ni	Ni	Tl	V	U	Cr	Zr	Fe	Ti	Zn	Th	K	P	As	Mo	Mg	Sr	Ca	Mn	Rb	Cs	Cu	Al	Co
	1	0.98	0.66	0.55	0.40	-0.34	-0.26	-0.25	-0.23	-0.21	0.20	-0.20	-0.19	-0.17	-0.16	-0.15	-0.14	-0.11	0.06	0.06	0.06	0.05	-0.05
Co	Co	Zn	Mg	Ti	Cs	Th	Cu	Al	Fe	Cr	Sr	Zr	K	Mn	Ca	U	Tl	Mo	Rb	As	Ni	P	V
	1	0.75	0.70	0.66	0.64	0.57	0.57	0.55	0.55	0.54	0.46	0.37	-0.32	0.29	0.29	-0.28	-0.21	0.20	-0.14	0.10	-0.05	0.03	0.02
Mg	Mg	Cs	Ti	Zn	Cu	Al	Th	Cr	Co	Zr	Sr	U	As	P	Tl	Fe	Mn	V	Ca	Ni	Rb	Mo	K
	1	0.96	0.96	0.93	0.89	0.85	0.83	0.72	0.70	0.65	0.51	-0.39	-0.38	-0.38	-0.31	0.30	-0.24	-0.19	-0.19	-0.16	0.08	-0.08	-0.03
K	K	Fe	Rb	As	Mn	Sr	P	U	Co	Al	Zr	Zn	Ca	Mo	Cr	Tl	Ni	Th	Ti	Cu	V	Cs	Mg
	1	-0.91	0.81	-0.45	-0.35	0.35	-0.34	0.34	-0.32	0.30	-0.28	-0.28	-0.27	0.26	-0.25	0.23	0.20	0.20	-0.18	0.11	-0.08	0.07	-0.03
Ca	Ca	Mn	As	P	Sr	Al	V	Zr	Th	Cr	Cs	Ti	Co	Rb	K	Cu	Fe	Zn	Mg	U	Ni	Tl	Mo
	1	0.99	0.92	0.89	0.49	-0.49	0.47	-0.46	-0.42	-0.40	-0.35	-0.34	0.29	-0.29	-0.27	-0.22	0.21	-0.20	-0.19	0.18	-0.14	-0.12	-0.05
P	P	As	Mn	Ca	Al	Zr	Th	Cr	Cs	Ti	Rb	V	Mg	Zn	K	Sr	Cu	U	Ni	Fe	Tl	Mo	Co
	1	0.98	0.90	0.89	-0.66	-0.61	-0.56	-0.54	-0.53	-0.47	-0.41	0.40	-0.38	-0.36	-0.34	0.33	-0.32	0.21	-0.20	0.16	-0.11	-0.11	0.03
Ti	Ti	Zn	Mg	Cs	Th	Al	Cu	Zr	Cr	Co	U	P	As	Fe	Tl	Mn	V	Ca	Sr	Ni	K	Mo	Rb
	1	0.97	0.96	0.92	0.86	0.84	0.82	0.77	0.75	0.66	-0.50	-0.47	-0.45	0.43	-0.39	-0.37	-0.35	-0.34	0.28	-0.25	-0.18	-0.07	-0.04
Zr	Zr	Ti	Zn	Mg	Cs	P	V	Th	Cr	As	Al	Fe	Mn	Tl	Ca	U	Co	Cu	Ni	K	Sr	Mo	Rb
	1	0.77	0.72	0.65	0.63	-0.61	-0.57	0.56	0.56	-0.54	0.53	0.49	-0.47	-0.46	-0.46	-0.44	0.37	0.34	-0.34	-0.28	-0.17	-0.10	-0.03
Sr	Sr	Cu	Mg	Ca	Co	Cs	Mn	Th	K	Al	P	Zn	Rb	Ti	As	Fe	Tl	V	Zr	Ni	U	Mo	Cr
	1	0.58	0.51	0.49	0.46	0.40	0.39	0.38	0.35	0.35	0.33	0.31	0.30	0.28	0.25	-0.23	-0.18	0.18	-0.17	-0.15	0.07	0.06	-0.02
V	V	Tl	Ni	Zr	Mn	Th	Ca	As	P	Mo	Ti	Al	U	Zn	Rb	Mg	Sr	Cr	Cs	K	Co	Fe	Cu
	1	0.68	0.66	-0.57	0.50	-0.47	0.47	0.43	0.40	-0.37	-0.35	-0.31	0.31	-0.24	-0.24	-0.19	0.18	0.15	-0.15	-0.08	0.02	-0.01	0.00
Th	Th	Al	Ti	Zn	Mg	Cu	Cs	Co	As	Zr	P	Cr	Mn	V	U	Ca	Sr	Tl	Rb	Mo	Ni	K	Fe
	1	0.92	0.86	0.84	0.83	0.82	0.81	0.57	-0.57	0.56	-0.56	0.54	-0.48	-0.47	-0.43	-0.42	0.38	-0.33	0.31	0.29	-0.21	0.20	0.05
U	U	Tl	Zn	Ni	Ti	Fe	Zr	Th	Mg	K	Mo	V	Cu	Co	Cs	Cr	Al	P	Ca	As	Mn	Sr	Rb
	1	0.62	-0.55	0.55	-0.50	-0.45	-0.44	-0.43	-0.39	0.34	-0.32	0.31	-0.28	-0.28	-0.25	-0.22	-0.22	0.21	0.18	0.13	0.13	0.07	0.03
Cs	Cs	Mg	Ti	Al	Cu	Zn	Cr	Th	Co	Zr	As	P	Sr	Mn	Ca	U	Fe	V	Rb	Mo	Tl	K	Ni
	1	0.96	0.92	0.91	0.87	0.86	0.82	0.81	0.64	0.63	-0.54	-0.53	0.40	-0.38	-0.35	-0.25	0.20	-0.15	0.13	-0.11	-0.09	0.07	0.06
Tl	Tl	Ni	V	U	Zr	Ti	Zn	Fe	Th	Mg	Cr	K	Co	Mo	Sr	As	Ca	P	Mn	Al	Cs	Rb	Cu
	1	0.98	0.68	0.62	-0.46	-0.39	-0.38	-0.36	-0.33	-0.31	0.25	0.23	-0.21	-0.20	-0.18	-0.13	-0.12	-0.11	-0.09	-0.09	-0.09	0.06	-0.04
As	As	P	Mn	Ca	Al	Th	Cs	Zr	Rb	Cr	K	Ti	V	Mg	Cu	Zn	Fe	Sr	Ni	U	Tl	Mo	Co
	1	0.98	0.94	0.92	-0.68	-0.57	-0.54	-0.54	-0.49	-0.48	-0.45	-0.45	0.43	-0.38	-0.36	-0.32	0.29	0.25	-0.19	0.13	-0.13	-0.10	0.10
Fe	Fe	K	Rb	Co	Zn	Zr	U	Ti	Cr	Tl	Mg	As	Mn	Ni	Mo	Sr	Ca	Cs	P	Th	Cu	V	Al
	1	-0.91	-0.77	0.55	0.51	0.49	-0.45	0.43	0.42	-0.36	0.30	0.29	0.28	-0.26	-0.26	-0.23	0.21	0.20	0.16	0.05	0.05	-0.01	0.00
Mn	Mn	Ca	As	P	Al	V	Th	Zr	Sr	Cs	Cr	Ti	K	Rb	Co	Fe	Cu	Mg	Zn	U	Ni	Tl	Mo
	1	0.99	0.94	0.90	-0.54	0.50	-0.48	-0.47	0.39	-0.38	-0.38	-0.37	-0.35	-0.34	0.29	0.28	-0.28	-0.24	-0.22	0.13	-0.11	-0.09	-0.02
Cu	Cu	Mg	Cs	Th	Zn	Tl	Al	Cr	Sr	Co	As	Zr	P	U	Mn	Ca	Rb	K	Ni	Fe	Tl	Mo	V
	1	0.89	0.87	0.82	0.82	0.82	0.82	0.70	0.58	0.57	-0.36	0.34	-0.32	-0.28	-0.28	-0.22	0.17	0.11	0.06	0.05	-0.04	-0.03	0.00
Mo	Mo	Rb	V	U	Th	Cr	K	Fe	Co	Tl	Ni	Cs	P	Al	As	Zr	Mg	Ti	Sr	Ca	Cu	Zn	Mn
	1	0.60	-0.37	-0.32	0.29	-0.28	0.26	-0.26	0.20	-0.20	-0.17	-0.11	-0.11	0.10	-0.10	-0.10	-0.08	-0.07	0.06	-0.05	-0.03	-0.03	-0.02
Rb	Rb	K	Fe	Mo	As	P	Mn	Th	Sr	Al	Ca	V	Cr	Cu	Co	Cs	Zn	Mg	Tl	Ni	Ti	Zr	U
	1	0.81	-0.77	0.60	-0.49	-0.41	-0.34	0.31	0.30	0.29	-0.29	-0.24	-0.19	0.17	-0.14	0.13	-0.10	0.08	0.06	0.06	-0.04	-0.03	0.03

Table 15. Pearson Correlation for Oxidized Sandstone in the George Ver and Loco Lee Deposits

Zn	Zn	Ti	Th	U	Co	Zr	As	Mg	Cs	Fe	Cr	Al
	1	0.91	0.91	0.84	0.83	0.83	0.81	0.78	0.78	0.77	0.71	0.65
Al	Al	Cr	Cs	Ti	Mg	Zr	Th	Zn	Tl	Fe	Ni	U
	1	0.94	0.92	0.82	0.81	0.71	0.68	0.65	-0.65	0.58	-0.52	0.50
Cr	Cr	Cs	Mg	Al	Ti	Zr	Th	Zn	Tl	Mn	P	Fe
	1	0.97	0.95	0.94	0.92	0.88	0.84	0.71	-0.65	0.64	0.53	0.52
Ni	Ni	Mo	Tl	Sr	Cu	K	Co	Al	Rb	V	As	Cs
	1	0.90	0.87	-0.77	0.69	-0.59	0.54	-0.52	-0.47	-0.43	0.40	-0.40
Co	Co	U	As	Fe	Zn	Mo	Sr	Ti	Th	Ni	Tl	Zr
	1	0.96	0.96	0.89	0.83	0.78	-0.63	0.62	0.60	0.54	0.46	0.43
Mg	Mg	Zr	Cs	Th	Cr	Ti	Al	Zn	Mn	P	Ca	Tl
	1	0.98	0.97	0.95	0.95	0.95	0.81	0.78	0.78	0.69	0.65	-0.59
K	K	Rb	Cu	Ni	Ca	P	Al	Mn	Th	Mo	Zr	Tl
	1	0.98	-0.93	-0.59	-0.48	-0.47	0.44	-0.44	-0.34	-0.32	-0.31	-0.29
Ca	Ca	P	Mn	Sr	Zr	Mg	Tl	Th	Cu	Cs	Cr	Mo
	1	1.00	0.98	0.75	0.66	0.65	-0.61	0.53	0.53	0.50	0.49	-0.48
P	P	Ca	Mn	Sr	Zr	Mg	Tl	Th	Cs	Cr	Cu	Mo
	1	1.00	0.99	0.76	0.70	0.69	-0.64	0.57	0.55	0.53	0.52	-0.49
Ti	Ti	Th	Mg	Zr	Cs	Cr	Zn	Al	U	Fe	As	Co
	1	0.97	0.95	0.94	0.93	0.92	0.91	0.82	0.70	0.70	0.68	0.62
Zr	Zr	Mg	Th	Ti	Cs	Cr	Zn	Mn	Al	P	Ca	Cu
	1	0.98	0.98	0.94	0.92	0.88	0.83	0.78	0.71	0.70	0.66	0.50
Sr	Sr	Tl	Mo	Ni	P	Ca	Mn	Co	As	U	Cs	Cr
	1	-0.96	-0.93	-0.77	0.76	0.75	0.70	-0.63	-0.55	-0.52	0.51	0.50
V	V	Ni	Mn	Ca	Cu	P	Mo	Cr	Ti	Mg	Th	Zr
	1	-0.43	-0.40	-0.37	-0.37	-0.33	-0.21	-0.17	-0.16	-0.15	-0.14	-0.13
Th	Th	Zr	Ti	Mg	Zn	Cs	Cr	Mn	Al	U	Co	As
	1	0.98	0.97	0.95	0.91	0.88	0.84	0.68	0.68	0.62	0.60	0.59
U	U	As	Fe	Co	Zn	Ti	Mo	Th	Sr	Al	Cr	Zr
	1	1.00	0.98	0.96	0.84	0.70	0.66	0.62	-0.52	0.50	0.47	0.47
Cs	Cs	Cr	Mg	Ti	Zr	Al	Th	Zn	Tl	Mn	P	Sr
	1	0.97	0.97	0.93	0.92	0.92	0.88	0.78	-0.67	0.64	0.55	0.51
Tl	Tl	Sr	Mo	Ni	Cs	Cr	Al	P	Ca	Mn	Mg	Zr
	1	-0.96	0.90	0.87	-0.67	-0.65	-0.65	-0.64	-0.61	-0.61	-0.59	-0.49
As	As	U	Fe	Co	Zn	Mo	Ti	Th	Sr	Al	Cr	Zr
	1	1.00	0.98	0.96	0.81	0.69	0.68	0.59	-0.55	0.47	0.44	0.43
Fe	Fe	As	U	Co	Zn	Ti	Mo	Al	Th	Cr	Cs	Sr
	1	0.98	0.98	0.89	0.77	0.70	0.60	0.58	0.57	0.52	0.47	-0.47
Mn	Mn	P	Ca	Zr	Mg	Sr	Th	Cs	Cr	Tl	Ti	Cu
	1	0.99	0.98	0.78	0.78	0.70	0.68	0.64	0.64	-0.61	0.58	0.55
Cu	Cu	K	Rb	Ni	Mn	Th	Ca	P	Zr	Mo	Zn	Co
	1	-0.93	-0.88	0.69	0.55	0.55	0.53	0.52	0.50	0.45	0.40	0.40
Mo	Mo	Sr	Tl	Ni	Co	As	U	Fe	P	Ca	Cu	Mn
	1	-0.93	0.90	0.90	0.78	0.69	0.66	0.60	-0.49	-0.48	0.45	-0.39
Rb	Rb	K	Cu	P	Ca	Ni	Mn	Th	Zr	Al	Zn	Mo
	1	0.98	-0.88	-0.47	-0.47	-0.47	-0.44	-0.39	-0.38	0.36	-0.31	-0.25

Cu	Mo	Mn	Rb	K	P	Ca	Ni	V	Sr	Tl
0.40	0.33	0.32	-0.31	-0.22	0.20	0.15	0.13	0.12	-0.09	-0.09
As	K	Sr	Mn	Rb	Mo	Co	P	Cu	Ca	V
0.47	0.44	0.43	0.37	0.36	-0.30	0.29	0.27	-0.23	0.22	0.02
Sr	Ca	U	As	Ni	Co	Mo	V	K	Rb	Cu
0.50	0.49	0.47	0.44	-0.37	0.30	-0.26	-0.17	0.17	0.10	0.08
U	Cr	Fe	Mg	P	Ca	Mn	Zn	Zr	Th	Ti
0.37	-0.37	0.29	-0.22	-0.20	-0.17	-0.13	0.13	-0.09	0.06	-0.03
Cu	Mg	Cs	Cr	Al	Ca	P	Rb	K	Mn	V
0.40	0.35	0.34	0.30	0.29	-0.29	-0.26	-0.23	-0.21	-0.13	0.03
Sr	U	Fe	As	Cu	Co	Rb	Ni	Mo	K	V
0.49	0.44	0.43	0.40	0.36	0.35	-0.22	-0.22	-0.20	-0.15	-0.15
Zn	Co	Fe	Cr	Mg	Sr	Ti	V	Cs	As	U
-0.22	-0.21	0.20	0.17	-0.15	0.11	-0.10	0.10	0.06	0.04	0.03
K	Rb	Ti	V	As	Fe	U	Co	Al	Ni	Zn
-0.48	-0.47	0.41	-0.37	-0.33	-0.33	-0.30	-0.29	0.22	-0.17	0.15
Rb	K	Ti	V	As	Fe	Al	U	Co	Zn	Ni
-0.47	-0.47	0.45	-0.33	-0.30	-0.29	0.27	-0.27	-0.26	0.20	-0.20
Mn	P	Ca	Cu	Tl	Sr	V	Rb	K	Mo	Ni
0.58	0.45	0.41	0.36	-0.35	0.20	-0.16	-0.16	-0.10	0.09	-0.03
Tl	U	As	Co	Fe	Sr	Rb	K	V	Mo	Ni
-0.49	0.47	0.43	0.43	0.43	0.41	-0.38	-0.31	-0.13	-0.09	-0.09
Mg	Fe	Al	Zr	Th	Ti	Cu	K	Zn	Rb	V
0.49	-0.47	0.43	0.41	0.22	0.20	-0.15	0.11	-0.09	0.05	0.01
Zn	Fe	Tl	K	Rb	As	Co	U	Al	Cs	Sr
0.12	-0.12	-0.12	0.10	-0.08	-0.07	0.03	-0.03	0.02	0.01	0.01
P	Fe	Cu	Ca	Rb	K	Tl	Sr	V	Mo	Ni
0.57	0.57	0.55	0.53	-0.39	-0.34	-0.32	0.22	-0.14	0.10	0.06
Cs	Mg	Ni	Tl	Ca	P	Cu	Mn	K	V	Rb
0.46	0.44	0.37	0.31	-0.30	-0.27	0.21	-0.12	0.03	-0.03	0.01
Ca	Fe	U	As	Ni	Co	Mo	Cu	K	Rb	V
0.50	0.47	0.46	0.42	-0.40	0.34	-0.28	0.13	0.06	-0.04	0.01
Co	Ti	As	Th	U	Cu	K	Fe	Rb	V	Zn
0.46	-0.35	0.35	-0.32	0.31	0.29	-0.29	0.25	-0.19	-0.12	-0.09
Cs	Ni	Mg	Tl	Ca	P	Cu	Mn	V	K	Rb
0.42	0.40	0.40	0.35	-0.33	-0.30	0.21	-0.14	-0.07	0.04	0.03
Mg	Zr	Ca	P	Ni	Tl	K	Rb	Mn	V	Cu
0.43	0.43	-0.33	-0.29	0.29	0.25	0.20	0.19	-0.13	-0.12	0.09
Rb	K	V	Mo	Al	Zn	As	Ni	Fe	Co	U
-0.44	-0.44	-0.40	-0.39	0.37	0.32	-0.14	-0.13	-0.13	-0.13	-0.12
V	Ti	Mg	Tl	Al	U	As	Sr	Cs	Fe	Cr
-0.37	0.36	0.36	0.29	-0.23	0.21	0.21	-0.15	0.13	0.09	0.08
Zn	K	Al	Cs	Cr	Rb	V	Mg	Th	Zr	Ti
0.33	-0.32	-0.30	-0.28	-0.26	-0.25	-0.21	-0.20	0.10	-0.09	0.09
Co	Mg	Tl	Fe	Ti	Cr	V	Sr	Cs	As	U
-0.23	-0.22	-0.19	0.19	-0.16	0.10	-0.08	0.05	-0.04	0.03	0.01

Table 16. Pearson Correlation for the Limb Sandstone in the George Ver and Loco Lee Deposits

Zn	Zn	Mg	Co	U	Cs	V	Ti	Cu	Sr	Rb	Ni	Cr	Zr	Fe	K	Ca	P	Tl	Th	Mo	Mn	Al	As
	1	1.00	1.00	0.99	0.97	-0.96	0.96	0.94	0.94	0.93	0.90	0.89	0.88	0.82	0.77	0.73	0.70	-0.68	0.64	0.61	0.56	-0.18	-0.11
Al	Al	Th	As	Mo	Cr	Ca	P	Ti	Sr	Ni	Fe	Cu	Mn	Cs	Mg	K	V	Co	Zr	Zn	Rb	U	Tl
	1	-0.76	0.72	0.67	-0.61	-0.55	-0.48	-0.45	-0.44	-0.42	0.41	-0.41	0.35	-0.27	-0.24	0.21	0.20	-0.19	0.18	-0.18	0.09	-0.04	0.00
Cr	Cr	Ti	Cu	Sr	Ni	Cs	Mg	Co	Zn	Ca	V	Th	U	P	Rb	Zr	Al	Tl	K	Fe	As	Mn	Mo
	1	0.98	0.96	0.95	0.93	0.92	0.92	0.90	0.89	0.86	-0.86	0.86	0.81	0.77	0.72	0.61	-0.61	-0.58	0.55	0.47	-0.45	0.26	0.18
Ni	Ni	Cu	Cs	Ca	Cr	Co	Ti	Mg	Zn	Rb	Sr	Tl	U	K	V	Th	Zr	Fe	As	P	Al	Mo	Mn
	1	0.99	0.97	0.96	0.93	0.92	0.92	0.92	0.90	0.85	0.84	-0.84	0.83	0.78	-0.77	0.61	0.58	0.54	-0.54	0.51	-0.42	0.30	0.13
Co	Co	Mg	Zn	Cs	U	Cu	Ti	Rb	V	Ni	Sr	Cr	Zr	K	Fe	Ca	Tl	P	Th	Mo	Mn	Al	As
	1	1.00	1.00	0.99	0.98	0.96	0.96	0.95	-0.94	0.92	0.92	0.90	0.84	0.80	0.80	0.77	-0.73	0.66	0.62	0.59	0.49	-0.19	-0.18
Mg	Mg	Zn	Co	Cs	U	Ti	Cu	V	Sr	Rb	Ni	Cr	Zr	Fe	Ca	K	P	Tl	Th	Mo	Mn	Al	As
	1	1.00	1.00	0.98	0.98	0.97	0.96	-0.95	0.95	0.92	0.92	0.92	0.85	0.78	0.77	0.76	0.71	-0.69	0.67	0.55	0.51	-0.24	-0.17
K	K	Tl	Rb	Cs	Co	Ni	U	Fe	Zn	Mg	Cu	Mo	Ca	Zr	Ti	V	Cr	Sr	Mn	Al	As	P	Th
	1	-0.95	0.94	0.82	0.80	0.78	0.78	0.78	0.77	0.76	0.76	0.70	0.69	0.63	0.62	-0.59	0.55	0.51	0.23	0.21	-0.20	0.09	0.06
Ca	Ca	Ni	Cu	Cr	Cs	Tl	Ti	Co	Mg	As	Zn	Rb	K	Sr	U	V	Al	Th	P	Zr	Fe	Mn	Mo
	1	0.96	0.91	0.86	0.86	-0.83	0.80	0.77	0.77	-0.76	0.73	0.70	0.69	0.68	0.63	-0.57	-0.55	0.54	0.34	0.31	0.30	-0.16	0.05
P	P	Th	Sr	V	Ti	Cr	Mg	Zn	Zr	U	Co	Mn	Cu	Cs	Ni	Al	Fe	Rb	Ca	Mo	K	As	Tl
	1	0.93	0.89	-0.86	0.79	0.77	0.71	0.70	0.69	0.68	0.66	0.65	0.61	0.60	0.51	-0.48	0.44	0.41	0.34	0.21	0.09	0.09	0.00
Ti	Ti	Sr	Cr	Mg	Cu	Zn	Co	Cs	V	Ni	U	Th	Rb	Ca	P	Zr	Fe	K	Tl	Al	Mn	Mo	As
	1	0.98	0.98	0.97	0.97	0.96	0.96	0.96	-0.94	0.92	0.91	0.82	0.81	0.80	0.79	0.75	0.62	0.62	-0.60	-0.45	0.42	0.36	-0.29
Zr	Zr	Fe	U	V	Zn	Mn	Mg	Co	Mo	Rb	Sr	Cs	Ti	P	Cu	K	Cr	Ni	Th	Tl	As	Ca	Al
	1	0.95	0.94	-0.92	0.88	0.87	0.85	0.84	0.84	0.83	0.80	0.76	0.75	0.69	0.67	0.63	0.61	0.58	0.46	-0.41	0.38	0.31	0.18
Sr	Sr	Ti	V	Cr	Mg	Zn	Co	Cu	U	Cs	P	Th	Ni	Zr	Rb	Ca	Fe	Mn	K	Tl	Al	Mo	As
	1	0.98	-0.97	0.95	0.95	0.94	0.92	0.90	0.90	0.90	0.89	0.87	0.84	0.80	0.75	0.68	0.63	0.54	0.51	-0.45	-0.44	0.38	-0.15
V	V	Sr	U	Zn	Mg	Ti	Co	Zr	Cs	Cr	P	Cu	Rb	Fe	Ni	Th	Mn	Mo	K	Ca	Tl	Al	As
	1	-0.97	-0.96	-0.96	-0.95	-0.94	-0.94	-0.92	-0.89	-0.86	-0.86	-0.85	-0.82	-0.80	-0.77	-0.75	-0.71	-0.59	-0.59	-0.57	0.46	0.20	-0.06
Th	Th	P	Sr	Cr	Ti	Al	V	Cu	Mg	Zn	Co	Cs	Ni	U	Ca	Zr	Rb	Mn	As	Fe	Mo	Tl	K
	1	0.93	0.87	0.86	0.82	-0.76	-0.75	0.68	0.67	0.64	0.62	0.62	0.61	0.57	0.54	0.46	0.33	0.33	-0.27	0.19	-0.09	-0.08	0.06
U	U	Zn	Co	Mg	V	Rb	Zr	Cs	Ti	Sr	Fe	Cu	Ni	Cr	K	Mo	P	Mn	Tl	Ca	Th	Al	As
	1	0.99	0.98	0.98	-0.96	0.94	0.94	0.94	0.91	0.90	0.89	0.88	0.83	0.81	0.78	0.72	0.68	0.66	-0.65	0.63	0.57	-0.04	0.03
Cs	Cs	Cu	Co	Mg	Zn	Ni	Ti	U	Rb	Cr	Sr	V	Ca	K	Tl	Zr	Fe	Th	P	Mo	Mn	As	Al
	1	0.99	0.99	0.98	0.97	0.97	0.96	0.94	0.93	0.92	0.90	-0.89	0.86	0.82	-0.80	0.76	0.72	0.62	0.60	0.49	0.36	-0.32	-0.27
Tl	Tl	K	Rb	Ni	Ca	Cs	Cu	Co	Mg	Zn	U	Ti	Cr	Fe	As	V	Sr	Mo	Zr	Th	Mn	P	Al
	1	-0.95	-0.85	-0.84	-0.83	-0.80	-0.78	-0.73	-0.69	-0.68	-0.65	-0.60	-0.58	-0.55	0.49	0.46	-0.45	-0.44	-0.41	-0.08	0.07	0.00	0.00
As	As	Ca	Mn	Al	Mo	Ni	Tl	Cr	Cu	Fe	Zr	Cs	Ti	Th	K	Co	Mg	Sr	Zn	Rb	P	V	U
	1	-0.76	0.74	0.72	0.56	-0.54	0.49	-0.45	-0.44	0.39	0.38	-0.32	-0.29	-0.27	-0.20	-0.18	-0.17	-0.15	-0.11	-0.09	0.09	-0.06	0.03
Fe	Fe	Mo	Zr	U	Rb	Zn	V	Co	Mn	Mg	K	Cs	Sr	Ti	Cu	Tl	Ni	Cr	P	Al	As	Ca	Th
	1	0.95	0.95	0.89	0.88	0.82	-0.80	0.80	0.79	0.78	0.78	0.72	0.63	0.62	0.61	-0.55	0.54	0.47	0.44	0.41	0.39	0.30	0.19
Mn	Mn	Zr	Fe	Mo	As	V	U	P	Zn	Sr	Mg	Co	Rb	Ti	Cs	Al	Th	Cr	Cu	K	Ca	Ni	Tl
	1	0.87	0.79	0.77	0.74	-0.71	0.66	0.65	0.56	0.54	0.51	0.49	0.47	0.42	0.36	0.35	0.33	0.26	0.26	0.23	-0.16	0.13	0.07
Cu	Cu	Ni	Cs	Ti	Mg	Co	Cr	Zn	Ca	Sr	U	Rb	V	Tl	K	Th	Zr	P	Fe	As	Al	Mo	Mn
	1	0.99	0.99	0.97	0.96	0.96	0.96	0.94	0.91	0.90	0.88	0.87	-0.85	-0.78	0.76	0.68	0.67	0.61	0.61	-0.44	-0.41	0.36	0.26
Mo	Mo	Fe	Zr	Mn	Rb	U	K	Al	Zn	V	Co	As	Mg	Cs	Tl	Sr	Ti	Cu	Ni	P	Cr	Th	Ca
	1	0.95	0.84	0.77	0.75	0.72	0.70	0.67	0.61	-0.59	0.59	0.56	0.55	0.49	-0.44	0.38	0.36	0.36	0.30	0.21	0.18	-0.09	0.05
Rb	Rb	Co	U	K	Zn	Cs	Mg	Fe	Cu	Ni	Tl	Zr	V	Ti	Sr	Mo	Cr	Ca	Mn	P	Th	Al	As
	1	0.95	0.94	0.94	0.93	0.93	0.92	0.88	0.87	0.85	-0.85	0.83	-0.82	0.81	0.75	0.75	0.72	0.70	0.47	0.41	0.33	0.09	-0.09

Table 17. Pearson Correlation for Reduced Sandstone in the George Ver and Loco Lee Deposits

Zn	Zn	As	Co	Ni	V	Mg	Fe	Mn	Ti	Cr	P	Cu	Th	Al	Zr	Rb	Cs	K	Sr	Mo	U	Tl	Ca
	1	1.00	1.00	0.99	0.97	0.96	0.93	0.93	0.89	0.88	0.88	0.87	0.85	0.80	-0.79	0.70	0.61	-0.60	0.55	0.37	0.33	0.23	0.07
Al	Al	Th	Cu	Rb	Cs	Ti	V	Sr	P	Ni	Zn	Cr	Fe	Co	As	Mo	Tl	Mg	U	Mn	Ca	Zr	K
	1	1.00	0.99	0.97	0.96	0.92	0.91	0.88	0.85	0.83	0.80	0.80	0.80	0.79	0.78	0.73	0.71	0.70	0.69	0.53	-0.47	-0.44	-0.43
Cr	Cr	Fe	Ti	Mg	Ni	V	Co	Zn	K	Th	As	Cu	Rb	Al	Mn	Sr	Cs	P	Zr	Mo	Tl	Ca	U
	1	0.99	0.97	0.94	0.92	0.92	0.91	0.88	-0.87	0.85	0.85	0.81	0.80	0.80	0.78	0.77	0.67	0.62	-0.41	0.18	0.16	0.13	0.12
Ni	Ni	Co	Zn	V	As	Mg	Fe	Ti	Cr	Mn	Cu	Th	P	Al	Rb	Zr	K	Cs	Sr	Mo	U	Tl	Ca
	1	1.00	0.99	0.99	0.99	0.97	0.96	0.93	0.92	0.91	0.89	0.88	0.85	0.83	0.75	-0.72	-0.66	0.65	0.63	0.36	0.32	0.24	0.06
Co	Co	Ni	Zn	As	Mg	V	Fe	Mn	Cr	Ti	Cu	Th	P	Al	Zr	Rb	K	Cs	Sr	Mo	U	Tl	Ca
	1	1.00	1.00	0.99	0.98	0.97	0.96	0.94	0.91	0.90	0.85	0.83	0.83	0.79	-0.75	0.69	-0.67	0.59	0.57	0.30	0.26	0.17	0.13
Mg	Mg	Co	Fe	Ni	Zn	As	Mn	Cr	V	Ti	K	Th	Cu	Al	P	Zr	Rb	Sr	Cs	Ca	Mo	U	Tl
	1	0.98	0.98	0.97	0.96	0.95	0.94	0.94	0.92	0.89	-0.80	0.76	0.76	0.70	0.70	-0.65	0.63	0.55	0.50	0.29	0.12	0.07	0.01
K	K	Cr	Fe	Mg	Ti	Co	Ni	Mn	V	Zn	Sr	As	Th	Rb	Ca	Al	Cu	U	Cs	Mo	Tl	P	Zr
	1	-0.87	-0.83	-0.80	-0.75	-0.67	-0.66	-0.63	-0.61	-0.60	-0.57	-0.56	-0.50	-0.49	-0.49	-0.43	-0.42	0.36	-0.32	0.30	0.27	-0.17	0.09
Ca	Ca	Tl	U	Mo	Cs	Rb	K	Al	Sr	Mn	Cu	Th	P	Mg	Fe	Cr	Co	Ti	Zr	V	As	Zn	Ni
	1	-0.95	-0.89	-0.88	-0.64	-0.49	-0.49	-0.47	-0.44	0.41	-0.40	-0.39	-0.35	0.29	0.15	0.13	0.13	-0.11	-0.10	-0.10	0.08	0.07	0.06
P	P	Cu	As	V	Zn	Al	Ni	Th	Co	Zr	Mo	Ti	U	Rb	Mn	Cs	Mg	Fe	Cr	Tl	Sr	Ca	K
	1	0.91	0.89	0.88	0.88	0.85	0.85	0.85	0.83	-0.83	0.74	0.73	0.72	0.71	0.71	0.70	0.70	0.69	0.62	0.59	0.50	-0.35	-0.17
Ti	Ti	Cr	Fe	V	Th	Ni	Cu	Al	Rb	Co	Mg	Zn	Sr	As	Cs	K	P	Mn	Zr	Mo	Tl	U	Ca
	1	0.97	0.96	0.96	0.95	0.93	0.92	0.92	0.91	0.90	0.89	0.89	0.86	0.85	0.82	-0.75	0.73	0.71	-0.43	0.40	0.38	0.35	-0.11
Zr	Zr	Mn	P	As	Zn	Co	Ni	V	Mg	Cu	Fe	Th	Al	Ti	Cr	U	Mo	Rb	Cs	Tl	Ca	K	Sr
	1	-0.83	-0.83	-0.83	-0.79	-0.75	-0.72	-0.67	-0.65	-0.57	-0.53	-0.47	-0.44	-0.43	-0.41	-0.36	-0.36	-0.23	-0.20	-0.11	-0.10	0.09	0.00
Sr	Sr	Rb	Cs	Al	Th	Ti	Cu	Cr	V	Fe	Ni	Tl	K	Co	Zn	Mg	Mo	P	As	U	Ca	Mn	Zr
	1	0.97	0.94	0.88	0.88	0.86	0.81	0.77	0.72	0.71	0.63	0.62	-0.57	0.57	0.55	0.55	0.52	0.50	0.50	0.46	-0.44	0.26	0.00
V	V	Ni	Zn	Co	As	Ti	Cu	Fe	Th	Mg	Cr	Al	P	Rb	Mn	Cs	Sr	Zr	K	Mo	U	Tl	Ca
	1	0.99	0.97	0.97	0.96	0.96	0.95	0.95	0.94	0.92	0.92	0.91	0.88	0.84	0.83	0.77	0.72	-0.67	-0.61	0.49	0.44	0.39	-0.10
Th	Th	Al	Cu	Rb	Ti	V	Cs	Sr	Ni	Cr	Fe	Zn	P	Co	As	Mg	Mo	Tl	U	Mn	K	Zr	Ca
	1	1.00	0.99	0.97	0.95	0.94	0.94	0.88	0.88	0.85	0.85	0.85	0.85	0.83	0.82	0.76	0.67	0.64	0.62	0.59	-0.50	-0.47	-0.39
U	U	Mo	Tl	Ca	Cs	P	Al	Cu	Th	Rb	Sr	V	K	Zr	Ti	As	Zn	Ni	Co	Fe	Cr	Mg	Mn
	1	1.00	0.95	-0.89	0.73	0.72	0.69	0.67	0.62	0.61	0.46	0.44	0.36	-0.36	0.35	0.34	0.33	0.32	0.26	0.14	0.12	0.07	0.02
Cs	Cs	Rb	Al	Sr	Th	Cu	Ti	Tl	Mo	V	U	P	Cr	Ni	Ca	Fe	Zn	Co	As	Mg	K	Mn	Zr
	1	0.98	0.96	0.94	0.94	0.91	0.82	0.82	0.78	0.77	0.73	0.70	0.67	0.65	-0.64	0.64	0.61	0.59	0.57	0.50	-0.32	0.27	-0.20
Tl	Tl	Mo	U	Ca	Cs	Al	Rb	Cu	Th	Sr	P	V	Ti	K	Ni	Zn	As	Co	Cr	Fe	Mn	Zr	Mg
	1	0.96	0.95	-0.95	0.82	0.71	0.70	0.66	0.64	0.62	0.59	0.39	0.38	0.27	0.24	0.23	0.22	0.17	0.16	0.14	-0.13	-0.11	0.01
As	As	Zn	Co	Ni	V	Mg	Mn	Fe	P	Cu	Ti	Cr	Zr	Th	Al	Rb	Cs	K	Sr	Mo	U	Tl	Ca
	1	1.00	0.99	0.99	0.96	0.95	0.94	0.91	0.89	0.86	0.85	0.85	-0.83	0.82	0.78	0.66	0.57	-0.56	0.50	0.37	0.34	0.22	0.08
Fe	Fe	Cr	Mg	Ni	Ti	Co	V	Zn	As	Mn	Th	K	Cu	Al	Rb	Sr	P	Cs	Zr	Mo	Ca	U	Tl
	1	0.99	0.98	0.96	0.96	0.96	0.95	0.93	0.91	0.85	0.85	-0.83	0.83	0.80	0.77	0.71	0.69	0.64	-0.53	0.20	0.15	0.14	0.14
Mn	Mn	Mg	As	Co	Zn	Ni	Fe	Zr	V	Cr	Ti	P	Cu	K	Th	Al	Ca	Rb	Cs	Sr	Tl	Mo	U
	1	0.94	0.94	0.94	0.93	0.91	0.85	-0.83	0.83	0.78	0.71	0.71	0.63	-0.63	0.59	0.53	0.41	0.40	0.27	0.26	-0.13	0.05	0.02
Cu	Cu	Th	Al	V	Rb	Ti	P	Cs	Ni	Zn	As	Co	Fe	Sr	Cr	Mg	Mo	U	Tl	Mn	Zr	K	Ca
	1	0.99	0.99	0.95	0.93	0.92	0.91	0.91	0.89	0.87	0.86	0.85	0.83	0.81	0.81	0.76	0.71	0.67	0.66	0.63	-0.57	-0.42	-0.40
Mo	Mo	U	Tl	Ca	Cs	P	Al	Cu	Th	Rb	Sr	V	Ti	As	Zn	Ni	Zr	Co	K	Fe	Cr	Mg	Mn
	1	1.00	0.96	-0.88	0.78	0.74	0.73	0.71	0.67	0.66	0.52	0.49	0.40	0.37	0.37	0.36	-0.36	0.30	0.30	0.20	0.18	0.12	0.05
Rb	Rb	Cs	Al	Th	Sr	Cu	Ti	V	Cr	Fe	Ni	P	Tl	Zn	Co	Mo	As	Mg	U	K	Ca	Mn	Zr
	1	0.98	0.97	0.97	0.97	0.93	0.91	0.84	0.80	0.77	0.75	0.71	0.70	0.70	0.69	0.66	0.66	0.63	0.61	-0.49	-0.49	0.40	-0.23

A)

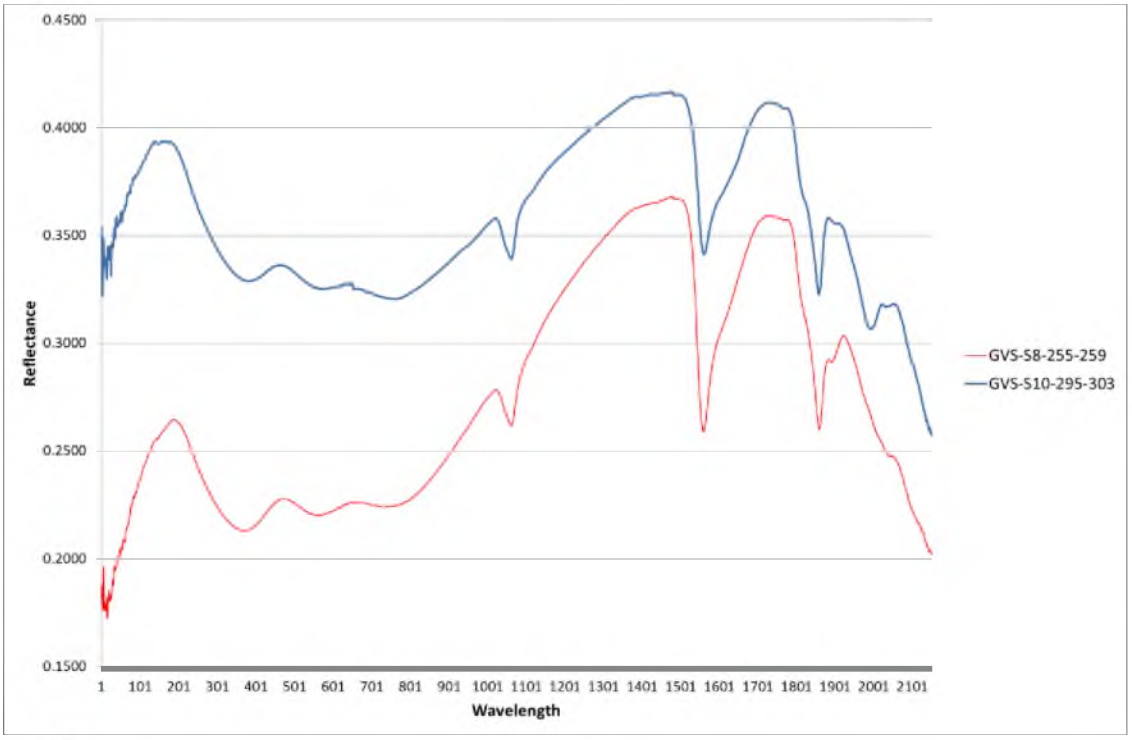

B)

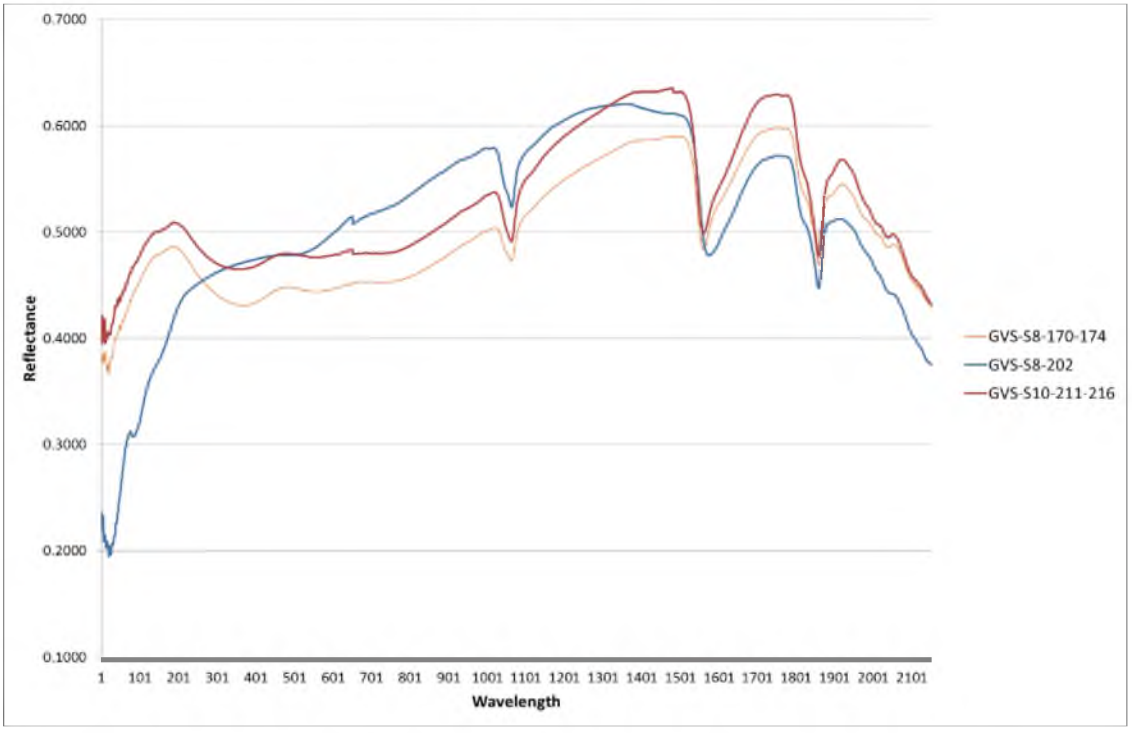

Fig. 29. Spectra of samples with QEMSCAN analysis. A) VNIR spectra for reduced sandstone samples. B) Spectra for oxidized sandstone samples.

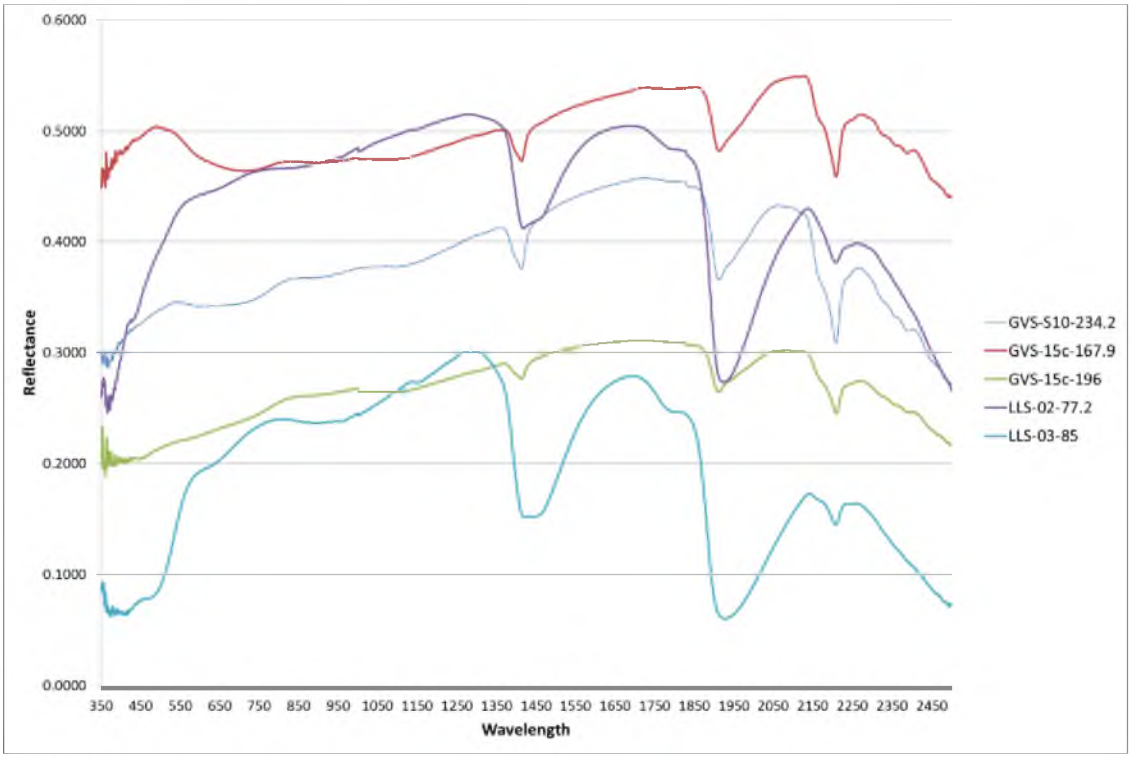

A)

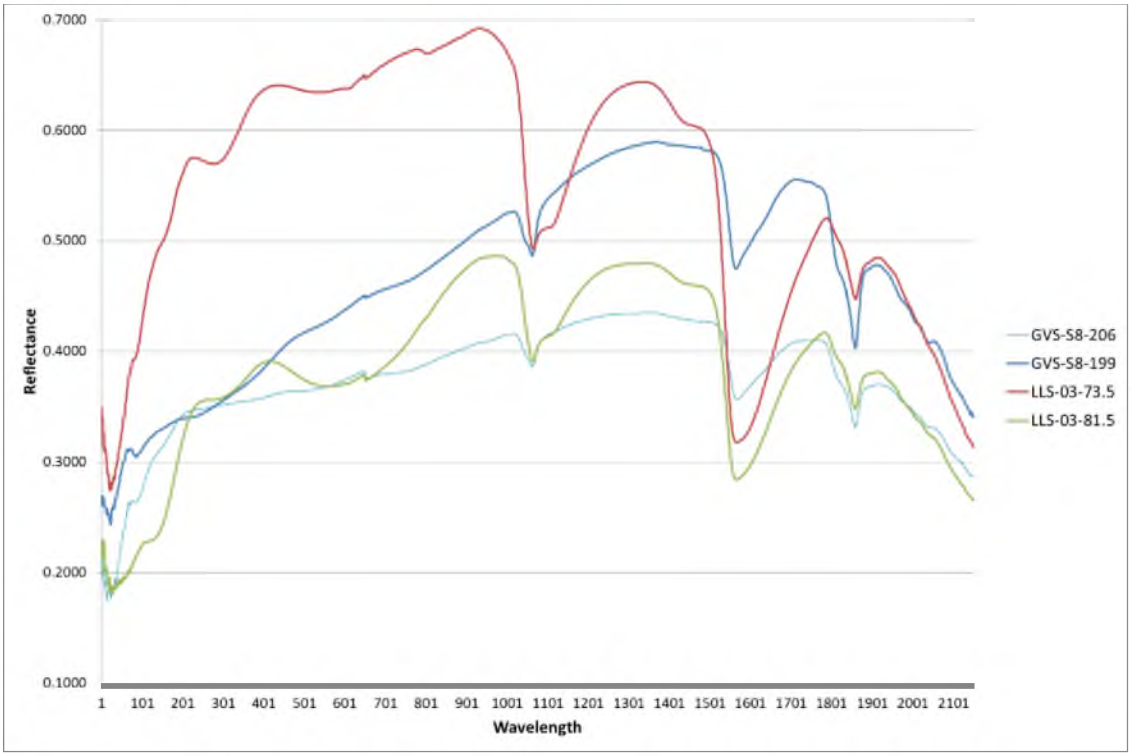

B)

Fig. 30. Spectra of samples with QEMSCAN analysis. A) VNIR spectra for mineralized sandstone samples. B) Spectra for limb sandstone samples.

REFERENCES

Armstrong, F.C., 1970, Geologic Factors Controlling Uranium Resources in the Gas Hills District, Wyoming. Wyoming Geological Association Guidebook 22nd Annual Field Conference, p. 31-44.

Austin, R.S. and King, J.W., 1966, Some Characteristics of Roll-Type Uranium deposits at Gas Hills, Wyoming. Society of Mining Engineering, p. 73-80.

Bailey, R.V., 1965, Applied Geology in the Shirley Basin Uranium District, Wyoming. Wyoming University, Contributions to Geology, v. 4, p. 27-35.

Clark, R.N., Swayze, G.A., Wise, R., Livo, E., Hoefen, T., Kokaly, R., Sutley, S.J., 2007, USGS digital spectral library splib06a: U.S. Geological Survey, Digital Data Series 231.

Dahlkamp, F.J., 1991, Uranium Ore Deposits. New York: Springer-Verlag, p. 250-305.

Davis, J.F., 1969, Uranium Deposits of the Powder River Basin, in Wyoming uranium: Wyoming University, Contributions to Geology, v. 8, no. 2, pt. 1, p. 131-141.

Files, F.G., 1970, Geology and Alteration Associated with Wyoming Uranium Deposits. University of California, Berkeley, PhD dissertation, 113 p.

Garrels, R.M., 1984, Montmorillonite/Illite Stabilty Diagrams. Clays and Clay Minerals, v. 32, p.239-240.

Granger, H.C. and Warren C.G., 1969, Unstable Sulfur Compounds and the Origin of Roll Type Uranium Deposits. Economic Geology, v. 64, p. 160-171.

Granger, H.C. and Warren C.G., 1978, Some Speculations on the Genetic Geochemistry and
Hydrology of Roll-Type Uranium Deposits. Thirtieth Annual Field Conference – 1978 Wyoming Geological Association Guidebook, p. 349-361.

Harshman, E.N. and Adams, S.S., 1980, Geology and Recognition Criteria for Roll-Type Uranium

Deposits in Continental Sandstones. U.S. Department of Energy and Bendix Field Engineering Corporation, p. 1-185.

Harshman, E. N., 1962, Alteration as a Guide to Uranium Ore, Shirley Basin, Wyoming. In Short papers in geology, hydrology, and topography: U.S. Geological Survey Professional Paper 450-D, p. D8-D10.
Harshman, E. N., 1966, Genetic Implications of some Elements Associated with Uranium Deposits, Shirley Basin, Wyoming, in Geological Survey Research 1966: U.S. Geological Survey Professional Paper 550-C, p. C167-C173.

Harshman, E. N., 1970, Uranium Ore Rolls in the United States. In Uranium Exploration Geology: International Atomic Energy Agency, Vienna, p. 219-232.

Harshman, E.N., 1974, Distribution of Elements in Some Roll Type Uranium Deposits. In Formation of Uranium Ore Deposits, International Atomic Energy Agency, Vienna, p. 169-183.

Ludwig, K.R., 1979, Age of Uranium Mineralization in the Gas Hills and Crooks Gap Districts, Wyoming, as Indicated by U-Pb Isotope Apparent Ages. Economic Geology, v. 74, p. 1654-1668.

Melin, R.E., 1969, Uranium Deposits in Shirley Basin, Wyoming, in Wyoming Uranium: Wyoming Univ. Contr. Geology, v. 8, no. 2, pt. 1, p. 143-149.

Miller, D.R., 2009, Strathmore Minerals Corp., www.strathmoreminerals.com/i/pdf/Strathmore-Rodman-Sept-2009.pdf

Min, M., 2005, Mineral Paragenesis and Textures Associated with Sandstone-Hosted Roll-Front Uranium Deposits, NW China. Ore Geology Review, v. 26, p. 51-69

Olives, J. and Amouric, M., 2000, Mixed Layerig of Illite-Smectite: Results From High-Resolution Transmission Electron Microscopy and Lattice-Energy Calculations. Clays and Clay Minerals, v. 48, no.2, p. 282-289.

Petrelli, M., Poli, G., Perugini, D., Peccerillo, A., Petrograph: a New Software to Visualize, Model, and Present Geochemical Data in Igneous Petrology. Gechemical, Geophysical, Geosystems. v.6, Q07011, P0110.1029/2005GC000932, 2005

Robb, L., 2005, Introduction to Ore-Forming Processes. Blackwell Publishing, p. 209-238.

Rosholt, J.N., Zartman, RE., Nkomo, IT., 1973, Lead Isotope Systematics and Uranium Depletion in the Granite Mountains, Wyoming, Geological Society of America Bulletin, v. 84, p. 989-1002.

Rubin, B., 1970, Uranium Roll Front Zonation in the Southern Powder River Basin, Wyoming. December WGA Earth Science Bulletin, p. 5-12.

Seeland, D., 1978, Sedimentology and Stratigraphy of the Lower Eocence Wind River Formation, Central Wyoming. Thirtieth Annual Field Conference, 1978, Wyoming Geological Association Guidebook, p. 181-198.

Shebl, M.A., and Surdam, R.C., 1996, Redox Reactions in Hydrocarbon Clastic Reservoirs: Experimental Validation of This Mechanism for Porosity Enhancement. Chemical Geology, v. 132, p. 103-117.

Silva, E.F., 2009, Mineralogy and Geochemistry of Trace Metals and REE in Volcanic Massive Sulfide Host Rocks, Stream Sediments, Stream Waters, and Acid Mine Drainage from the Lousal Mine Area (Iberian Pyrite Belt, Portugal). Applied Geochemistry no. 24, p. 383-401.

Snow, C.D., 1978, Gas Hills Uranium District, Wyoming – A review of History and Production.
Thirtieth Annual Field Conference – 1978 Wyoming Geological Association Guidebook, p. 329-
334.

Stewart, C.L., 2002, The Mineralogy of Uranium Roll Front Deposits and it's Significance to In-Situ Carbonate Leach Mining. University of Wyoming, Thesis, 248 p.

Sun, S.S. and McDonough, W.F., 1989, Chemical and Isotopic Systematics of Oceanic Basalts: Implications for Mantle Composition and Processes. Geological Society of London Special Publication, no. 42, p. 313-345.

Zeller, H.D., 1957, The Gas Hills Uranium District and Some Probable Controls for Ore Deposition. Twelfth Annual Field Conference – 1957 Wyoming Geological Association Guidebook, p. 156-160.

Zielinkski, R.A., 1980, Uranium in Secondary Silica: a Possible Exploration Guide, Econ Geol, v. 75, p. 592-602.